

Spring 5-3-2024

## **Full Annual Cycle Analysis of American Woodcock (*Scolopax minor*) Distribution, Habitat Use, and Migration Ecology**

Liam A. Berigan

*University of Maine*, [liam.berigan@maine.edu](mailto:liam.berigan@maine.edu)

Follow this and additional works at: <https://digitalcommons.library.umaine.edu/etd>



Part of the [Ornithology Commons](#)

---

### **Recommended Citation**

Berigan, Liam A., "Full Annual Cycle Analysis of American Woodcock (*Scolopax minor*) Distribution, Habitat Use, and Migration Ecology" (2024). *Electronic Theses and Dissertations*. 3941.  
<https://digitalcommons.library.umaine.edu/etd/3941>

This Open-Access Dissertation is brought to you for free and open access by DigitalCommons@UMaine. It has been accepted for inclusion in Electronic Theses and Dissertations by an authorized administrator of DigitalCommons@UMaine. For more information, please contact [um.library.technical.services@maine.edu](mailto:um.library.technical.services@maine.edu).

**FULL ANNUAL CYCLE ANALYSIS OF AMERICAN WOODCOCK (SCOLOPAX MINOR)**  
**DISTRIBUTION, HABITAT USE, AND MIGRATION ECOLOGY**

By

Liam A. Berigan

B.S. Cornell University, 2017

M.S. Kansas State University, 2019

**A DISSERTATION**

Submitted in Partial Fulfillment of the  
Requirements for the Degree of  
Doctor of Philosophy  
(in Wildlife Ecology)

The Graduate School

The University of Maine

May 2024

**Advisory Committee:**

Erik Blomberg, Assoc. Professor, Dept. of Wildlife, Fisheries, and Conservation Biology

Amber Roth, Assoc. Professor, Dept. of Wildlife, Fisheries, and Conservation Biology and  
School of Forest Resources

Joseph Zydlowski, Professor, Dept. of Wildlife, Fisheries, and Conservation Biology

Parinaz Rahimzadeh-Bajgiran, Assoc. Professor, School of Forest Resources

Sabrina Morano, Assist. Professor, Dept. of Wildlife, Fisheries, and Conservation Biology

**FULL ANNUAL CYCLE ANALYSIS OF AMERICAN WOODCOCK (SCOLOPAX  
MINOR) DISTRIBUTION, HABITAT USE, AND MIGRATION ECOLOGY**

By Liam Berigan

Dissertation Advisors:  
Dr. Erik Blomberg & Dr. Amber Roth

An Abstract of the Dissertation Presented in  
Partial Fulfillment of the Requirements for the  
Degree of Doctor of Philosophy  
(in Wildlife Ecology)  
May 2024

The widespread availability of satellite tracking devices has made it possible to track individual migratory birds throughout the full annual cycle, examining how distribution and habitat use change between seasons and regions while also describing the characteristics of migratory movements. We used these devices to examine the full annual cycle ecology of American Woodcock (*Scolopax minor*; hereinafter woodcock), an early successional habitat specialist whose populations are declining throughout their range in eastern North America. We used these data to develop a multi-season distribution model for woodcock management in Pennsylvania, demonstrating the importance of considering habitat use across multiple seasons for migratory bird conservation. We also used woodcock migratory movements to demonstrate improved methods for classifying animal locations into migratory states, allowing inferences into migratory behavior despite sparse and incomplete data. We examined changes in woodcock habitat selection among seasons, finding that woodcock likely undergo a functional response in their habitat selection to changes in habitat availability throughout the full annual cycle. Finally, we described woodcock flight altitudes

and their corresponding vulnerability to various airspace obstacles, finding that low altitude flights are likely a contributing factor to woodcocks' disproportionate collisions with buildings. Stabilizing woodcock populations will likely require better understanding of woodcock ecology throughout the full annual cycle, as well as the threats they face at each stage. We hope that our comprehensive analysis of woodcock distribution, habitat use, and migration ecology throughout the full annual cycle will improve conservation of this iconic upland bird species.

## **DEDICATION**

To my family: my parents, Michael Berigan and Karen Akerlof, and my brothers, Cormac and Kieran Berigan. I would not have made it this far without their support.

## **ACKNOWLEDGEMENTS**

One of the joys of working on a massive, collaborative research project such as the Eastern Woodcock Migration Research Cooperative is getting to work with an incredible array of wildlife biologists and enthusiasts who were willing to sacrifice their evenings, nights, and early mornings to our nocturnal mist netting and trapping efforts. I would like to thank the 43 collaborating organizations which have joined us in the field, funded satellite tags, or deployed their own transmitters since this project began in 2017, a full list of whom is available at [www.woodcockmigration.org/partners.html](http://www.woodcockmigration.org/partners.html). Special thanks to those partners who joined me when I traveled for fieldwork in 2020–2022, including U.S. Fish and Wildlife Service staff at Silvio O. Conte and Missisquoi National Wildlife Refuges, Vermont Fish and Wildlife, Audubon Vermont, The Nature Conservancy in Vermont, USDA Forest Service, Florida Fish and Wildlife Conservation Commission, South Carolina Department of Natural Resources, and Environment and Climate Change Canada. The Pennsylvania Game Commission funded the first year of my dissertation, and their staff (including but not limited to Ken Duren, Lisa Williams, Scott Bearer, Kevin Wenner, and Phillip Kasper) played a formative role in the development of the Woodcock Priority Area Siting Tool described in Chapter 1. Subsequent years were funded by the University of Maine’s Canadian-American Center, Susan J. Hunter Presidential Teaching Assistantship, and the Maine Agricultural and Forest Experiment Station; I greatly appreciate their support. I would also like to thank my advisors, Erik Blomberg and Amber Roth, for their endless support over the last 4 years, especially when fieldwork, modeling, or life in general were not going as intended. Both are fantastic scientists and mentors who I feel privileged to have learned from. My graduate committee, including Joseph Zydlewski, Parinaz Rahimzadeh-Bajgiran, and Sabrina Morano, have been an incredible resource during this process, and I appreciate their time and willingness to help me troubleshoot research ideas and analytical issues. The administrative staff in the department, Molly Jean Langlais Parker,

Katherine Goodine, and Rena Carey, were all critical to the success of this project. Molly went above and beyond to help after FedEx lost some of our genetic samples in transit, and I greatly appreciate her efforts to get those samples returned. I would like to thank Alex Fish, who was the graduate student preceding me on the project, for building a strong framework for the project to continue after the conclusion of his fieldwork, and for many nights in the field teaching me to catch woodcock. I would also like to thank Rachel Darling, the student who took over the project at the conclusion of my fieldwork, for doing such an incredible job sustaining the project while expanding the cooperative into new regions and addressing novel questions. Sarah Clements played a substantial role in the analyses used in Chapters 3 and 4 and is largely responsible for teaching me to use the programming language JAGS. I am deeply indebted to her for her patience and her time throughout this process, as well as her friendship (and willingness to let me spend time with her horse, Maya). I would like to thank the denizens of Nutting 232A, including Annie Stupik, Emily Filiberti, Luke Douglas, Kurt Ongman, and Rachel Darling for their friendship and support over the past few years, and their reminders that there is a place for work life balance in graduate school. My roommates, including Carl Pohlman, Kory Whittum, Drajad Seto, and the Mensingers (Matt, Sarah, and Auggie) have all been fantastic friends and top-notch Wingspan players. I would especially like to thank Meredith Lewis for her support and for all the adventures we have been on in the last three years. I am lucky to have a partner who is not just a great person but a fantastic ornithologist, and many of the anecdotes and inter-species comparisons included in the following chapters are the product of our conversations about migratory bird ecology. Finally, I would like to thank the many graduate students and postdocs in the department for welcoming me to Maine, and helping this place feel like home.

## TABLE OF CONTENTS

DEDICATION .....	ii
ACKNOWLEDGEMENTS .....	iii
LIST OF TABLES .....	viii
LIST OF FIGURES.....	x
LIST OF EQUATIONS .....	xiii
1 CHAPTER 1: MULTI-SEASONAL SPECIES DISTRIBUTION MODELS BETTER	
FACILITATE HABITAT CONSERVATION FOR A MIGRATORY BIRD ..... 1	
1.1 Introduction.....	2
1.2 Methods.....	6
1.2.1 Study Area .....	6
1.2.2 Breeding and migratory season data .....	7
1.2.3 Species distribution modeling.....	8
1.2.4 Analysis of covariate relationships and comparative distribution of seasonal	
habitat.....	11
1.2.5 Spatial decision support system .....	12
1.3 Results.....	14
1.4 Discussion .....	22
2 CHAPTER 2: ADAPTING HIDDEN MARKOV MODELS FOR TRACKING	
MIGRATORY BIRDS USING DATA FROM SMALL GPS TRANSMITTERS ..... 26	
2.1 Introduction.....	27
2.2 Methods.....	32
2.2.1 Collecting data via GPS transmitters .....	32
2.2.2 Delineating spring and fall migration .....	33

2.2.3	Delineating spring and fall migration .....	39
2.2.4	Data and code availability.....	42
2.3	Results.....	43
2.3.1	HMM error rates .....	43
2.3.2	Variable importance.....	45
2.3.3	Migratory characteristics .....	47
2.3.4	Long-distance movements and non-migratory individuals.....	50
2.4	Discussion .....	52
3	<b>CHAPTER 3: FUNCTIONAL RESPONSES IN AMERICAN WOODCOCK HABITAT SELECTION THROUGHOUT THE FULL ANNUAL CYCLE .....</b>	<b>56</b>
3.1	Introduction.....	57
3.2	Methods.....	61
3.2.1	Data collection and preprocessing .....	61
3.2.2	Delineating levels of habitat selection .....	63
3.2.3	Delineating availability .....	63
3.2.4	Extracting habitat covariates.....	64
3.2.5	Scale of habitat selection .....	65
3.2.6	Habitat selection.....	67
3.3	Results.....	69
3.3.1	Scale of habitat selection .....	69
3.3.2	Habitat selection coefficients .....	73
3.3.3	Individual variation in habitat selection.....	77
3.4	Discussion .....	79

4	CHAPTER 4: LOW MIGRATORY FLIGHT ALTITUDES EXPLAIN INCREASED COLLISION RISK FOR AMERICAN WOODCOCK .....	83
4.1	Introduction.....	84
4.2	Methods.....	87
4.2.1	Data collection and preprocessing .....	87
4.2.2	Modeling altitude distributions .....	88
4.2.3	Comparison of flight altitudes to other metrics .....	90
4.3	Results.....	90
4.4	Discussion .....	98
5	BIBLIOGRAPHY .....	101
6	APPENDICES .....	115
A.	Appendix A .....	115
B.	Appendix B .....	116
7	BIOGRAPHY OF THE AUTHOR.....	128

## LIST OF TABLES

Table 1.1. Explanatory variables used to model woodcock distributions in Pennsylvania, USA. Suites indicate conceptual grouping of variables into classes relevant to woodcock occurrence.....	9
Table 1.2. Variables selected via backwards variable selection using the R package VSURF (Genuer et al. 2022) for the migratory and breeding season models.....	16
Table 2.1. Covariates used to delineate movement states in hidden Markov Models (HMMs), and the type of distribution fit to each covariate in the HMMs.....	36
Table 2.2. Definitions of long-distance movement states manually delineated for American Woodcock.....	42
Table 2.3. Migratory characteristics of full and base models for each seasonal hidden Markov model, in addition to detection rates for long-distance movements outside of spring and fall migration.....	48
Table 3.1. Hypotheses regarding factors that may affect the scale of habitat selection and habitat selection coefficients for American Woodcock ( <i>Scolopax minor</i> ).....	60
Table 4.1. Characteristics of American Woodcock ( <i>Scolopax minor</i> ) altitudes above ground level during migratory flights, measured using a base model (bold) as well as season and age models.....	92
Table 4.2. Proportion of American Woodcock ( <i>Scolopax minor</i> ) migratory flight altitudes within height intervals related to weather radar and airspace obstacles.....	93
Table A.1. Area-under-the-curve (AUC; Fielding and Bell 1997) scores for three different modeling techniques evaluated for use in creating species distribution models. ....	115
Table B.1. Individual exceptions to the full model ruleset made in hidden Markov Model delineation to improve seasonal model fits for individual birds. ....	117

Table B.2. 50% threshold values for 4 land cover types, demonstrating the distance (m) from the centroid within which at least half of GPS points fall when a GPS transmitter is taking locations while stationary.....	125
---	-----

## LIST OF FIGURES

Figure 1.1. Seasonal ranges and hypothetical migration routes of American woodcock in eastern North America. Seasonal ranges were delineated by eBird's Status and Trends project (Fink et al. 2022) using citizen science data.....	5
Figure 1.2. Conceptual diagram of user decision options in the Woodcock Priority Area Siting Tool (W-PAST). .....	14
Figure 1.3. Comparison of relationships between landscape variables and habitat suitability for breeding and migratory season models of American Woodcock in Pennsylvania, USA.....	17
Figure 1.4. Breeding and migratory predictive habitat suitability layers suggest that woodcock select habitat at finer scales during the migratory season. ....	19
Figure 1.5. Breeding and migratory season habitat suitability for woodcock (5A) by EPA level 3 ecoregion (5B) in Pennsylvania (Omernik and Griffith 2014).....	21
Figure 2.1. Range delineation (Linscott et al. 2022) and step-threshold (Burnside et al. 2017) methods of delineating migratory tracks. ....	29
Figure 2.2. Complete and incomplete tracks of a theoretical migratory bird. ....	30
Figure 2.3. Movement state transition diagram for each hidden Markov Model (HMM). .....	39
Figure 2.4. Error rates for movement state assignments by hidden Markov models (HMMs) for fall, spring (male), and spring (female) migrations, as measured through the model validation process.....	44
Figure 2.5. Reduction in accuracy from the full model due to removal of individual data streams, as well as the base model which included none of these 6 data streams.....	46
Figure 2.6. Spatial and temporal distribution of summer migrations, dispersals, and foray loops of American Woodcock marked with GPS transmitters in eastern North America.....	51

Figure 3.1. Map of Bird Conservation Regions (BCRs; Sauer et al. 2003) in eastern North America .....	62
Figure 3.2. Scales at which American Woodcock ( <i>Scolopax minor</i> ) selected habitat covariates throughout their full annual cycle, derived from GPS locations collected throughout eastern North America .....	70
Figure 3.3. Scales of American Woodcock ( <i>Scolopax minor</i> ) habitat selection among seasons and habitat covariates, derived from GPS locations collected throughout eastern North America .....	71
Figure 3.4. Scales at which American Woodcock ( <i>Scolopax minor</i> ) select habitat covariates among age-sex classes, derived from GPS locations collected throughout eastern North America .....	72
Figure 3.5. Mean habitat selection coefficients for covariates from the age-sex suite of habitat selection models. ....	74
Figure 3.6. Mean habitat selection coefficients for covariates from the Bird Conservation Region (BCR) suite of habitat selection models. ....	75
Figure 3.7. Selection preferences of American Woodcock ( <i>Scolopax minor</i> ) for needleleaf forests, wetland, and urban areas among seasons, derived from GPS locations collected throughout eastern North America .....	76
Figure 3.8. Individual variation in habitat selection (standard deviation of $\delta$ in Equation 3.2), summed by covariate, season, Bird Conservation Region (BCR), and age-sex class. ....	78
Figure 4.1. Means and standard deviations of American Woodcock ( <i>Scolopax minor</i> ) flight altitudes above ground level during fall and spring migration.....	95
Figure 4.2. Means and standard deviations of American Woodcock ( <i>Scolopax minor</i> ) flight altitudes above ground level for adult and juvenile individuals .....	96

Figure 4.3. Distribution of woodcock flight altitudes above ground level compared to the heights of low-rise buildings (red; 47m), land-based wind turbines (orange; 32–164m), and large communications towers (yellow; 244m). ....	97
Figure B.1. Movement state transition diagram for the hidden Markov Model used to identify potential mortalities among tagged American Woodcock ( <i>Scolopax minor</i> ). ....	124
Figure B.2. Movement state transition diagram for each hidden Markov Model (HMM), and corresponding classes uploaded to the Movebank repository. ....	127

## **LIST OF EQUATIONS**

Equation 1.1.....	12
Equation 3.1.....	65
Equation 3.2.....	65
Equation 3.3.....	67
Equation 4.1.....	88
Equation 4.2.....	89

## **CHAPTER 1: MULTI-SEASONAL SPECIES DISTRIBUTION MODELS BETTER FACILITATE HABITAT CONSERVATION FOR A MIGRATORY BIRD**

Species distribution models have issues with cross-seasonal transferability when data collected during a single season do not reflect habitat relationships across other seasons. This issue can be addressed using spatial decision support systems, which allow users to incorporate multiple season-specific distribution models into a single tool to facilitate conservation decisions. We applied this framework to an analysis of multi-season habitat use for a migratory bird, the American woodcock (*Scolopax minor*). We modeled woodcock breeding and migratory habitat distributions in Pennsylvania, USA, using random forest classifiers, and integrated the predictions of both models into a single decision support system using a Shiny application. The Shiny application accepts user input through breeding and migratory season weights, allowing users to customize the tool based on area-specific management priorities. We found low cross-seasonal transferability between seasonal models, with Pearson correlations of 0.15 at a pixel-scale and 0.39 at a local management area scale, indicating that conservation of breeding habitat alone is unlikely to result in efficient conservation of woodcock migratory habitat. Woodcock breeding and migratory habitat is also unevenly distributed at a regional scale, with three Pennsylvania ecoregions having low breeding suitability but high migratory suitability. Creating a multi-season distribution model for woodcock management highlighted important migratory areas that may otherwise be overlooked due to a lack of breeding season occupancy, such as urban greenspaces. Flexibility in data sources and ability to compensate for low cross-seasonal transferability in distribution models make multi-season distribution modeling ideal for the study of birds and other migratory taxa.

## 1.1 Introduction

Species distribution models are frequently used to assist conservation decision-making (Miller 2010), however, they are known to have issues with transferability. For example, models developed in one area may not be reflective of animal distributions in other parts of their range (spatial transferability; *sensu* Randin et al. 2006), or may fail to project species distributions into the future due to changing conditions (temporal transferability; *sensu* Dobrowski et al. 2011). We posit that an additional subcategory of spatiotemporal transferability exists, which we call cross-seasonal transferability, for situations where species habitat associations differ among seasons or life stages, resulting in animals using fundamentally different space throughout the year. For example, wildlife science has a long history of bias towards studying animals during the breeding season, which may neglect the value of non-breeding habitat for survival and ignore carry-over effects into the breeding season (Norris and Marra 2007). By building species distribution models which focus solely on occurrence data collected during breeding, we may disregard portions of a species' distribution that are essential to persistence.

Spatial decision support systems (SDSS; Hopkins and Armstrong 1985) may provide a useful mechanism to circumvent issues of cross-seasonal transferability by combining distribution models from multiple seasons of the full annual cycle during the decision-making process. SDSS utilize user-friendly, interactive toolsets to guide users through making a set of spatial prioritization decisions (Sugumaran and Degroote 2010). SDSS frequently come as extensions of existing geographic information systems (McConnell and Burger 2011), but the learning curve and costs associated with professional geographic information systems can often be an impediment to reaching the intended user base (Harper 2006). The widespread adoption of interactive online mapping tools, such as *leaflet* (Agafonkin 2022) and ArcGIS Online (ESRI 2023a), has greatly expanded the capacity to custom build SDSS that are accessible via a web browser and can be easily used by decision makers with little additional training (Sugumaran and Sugumaran 2007). SDSS provide an interface which allows

users to interact with multiple spatial data layers, such as species distribution models. In circumstances where species distribution models have low cross-seasonal transferability, SDSS can compensate by incorporating multiple season-specific species distribution models into the decision-making process.

Migratory birds are clearly sensitive to issues of cross-seasonal transferability through use of different geographic areas throughout their annual cycle, coarsely divided into breeding, wintering, and migratory seasons (Marra et al. 2015). Resource requirements frequently differ among these three seasons, often resulting in bird use of fundamentally different habitat types (Rice et al. 1980, Allen et al. 2020, Stanley et al. 2021). However, there are circumstances in which breeding, wintering, and migratory habitat may occur within the same region, especially for short-distance migrants, which are generally defined as those migrating less than 2,000 km (Rappole 2013). Examples of short-distance migrants include wintering waterfowl, such as common eider (*Somateria mollissima*), where more northern breeding populations overwinter in the same regions that more southern populations breed (Goudie et al. 2020), and nomadic finch species such as pine siskin (*Spinus pinus*), which migrate, breed, and overwinter in the same regions despite differential resource requirements among seasons (Dawson 2020). An SDSS approach that combines season-specific species distribution models into a single predictive layer could be particularly useful to avoid issues of cross-seasonal transferability when managing such species.

We developed a SDSS framework to spatially-prioritize habitat management while integrating data from multiple seasons of a migratory bird's full annual cycle. Our case study is focused on American woodcock (*Scolopax minor*; hereinafter "woodcock") in Pennsylvania, USA. Woodcock are short distance migrants with considerable overlap among migratory, breeding, and wintering ranges (Myatt and Krementz 2007, Fig. 1.1), but fundamentally different habitat requirements among seasons (Allen et al. 2020). We aimed to develop a SSDS tool to aid conservation practitioners

considering trade-offs between managing for breeding and migratory season habitat in Pennsylvania. Our specific objectives for the SDSS were to 1) maximize predictive accuracy of breeding and migratory season distribution models, 2) combine seasonal distribution models into a single prioritization layer using user-specified weights, and 3) evaluate relative suitability of local management areas using a multi-season framework.

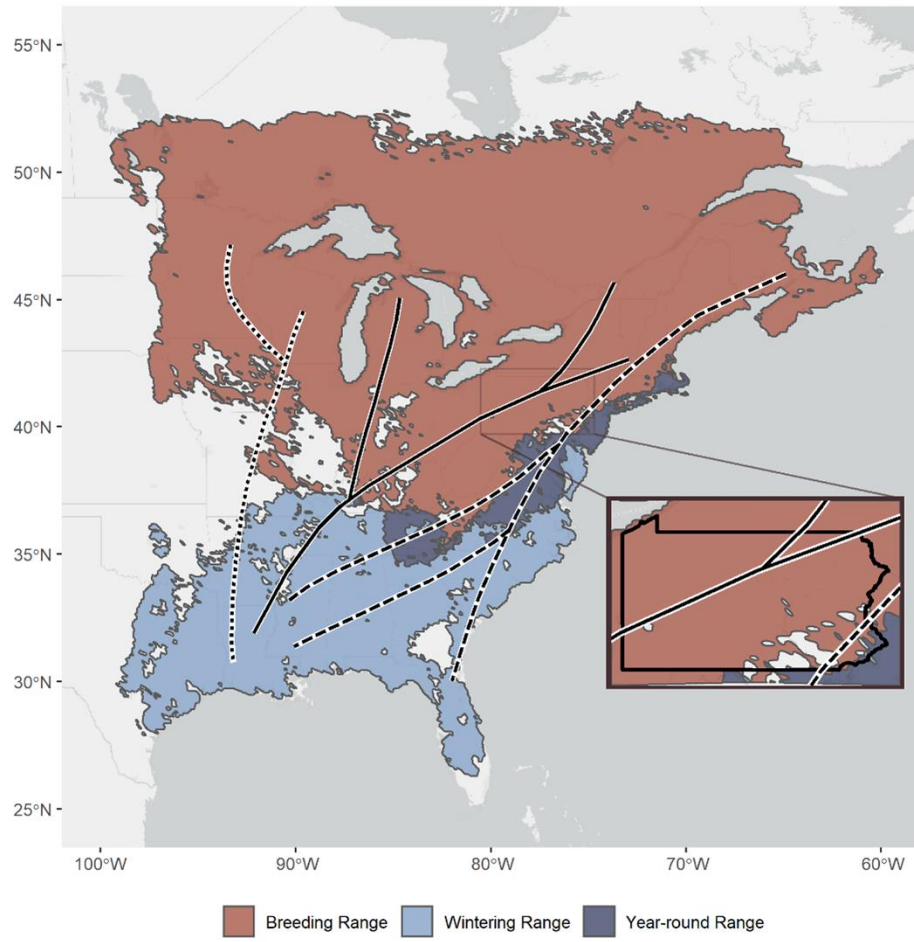


Figure 1.1. Seasonal ranges and hypothetical migration routes of American woodcock in eastern North America. Seasonal ranges were delineated by eBird's Status and Trends project (Fink et al. 2022) using citizen science data. Migration routes illustrate potential connections among eastern (dashed line), central (solid line), and western (dotted line) population segments. Migration routes were originally proposed by Glasgow (1958) and later reproduced by Moore et al. (2019). Inset illustrates multiple migration routes intersecting with the breeding range in the state of Pennsylvania.

## **1.2 Methods**

### *1.2.1 Study Area*

We modeled woodcock habitat distribution throughout the state of Pennsylvania, which provides breeding habitat for an estimated 2.3% of the global woodcock population (52,400 birds). The state also provides stopover habitat during spring and fall migration for woodcock breeding throughout the northeastern United States and eastern Canada, which accounts for nearly 1/3rd of the global woodcock population (30.5% of global woodcock, 684,500 birds; Kelley et al. 2008). Pennsylvania also contains some wintering habitat for woodcock, which is negligible compared to breeding and stopover habitat (Fig. 1.1). Pennsylvania is composed of 11 U.S. Environmental Protection Agency (EPA) level 3 Ecoregions (Omernik and Griffith 2014), which reflect the topological gradient from Pennsylvania's ridge-and-valleys in the central portion of the state to the coastal lowlands along the edge of Lake Erie. Less mountainous areas in Pennsylvania tend to be heavily agricultural (e.g., Northern Piedmont Ecoregion, 38% agricultural; Jin et al. 2019), with development primarily concentrated around the two largest cities, Philadelphia (pop. 1,600,000) and Pittsburgh (pop. 300,000; U.S. Census Bureau 2021). Mountainous areas, such as the North Central Appalachians ecoregion, remain in mostly contiguous forest cover (84% forest; Jin et al. 2019).

Woodcock in Pennsylvania are managed by the Pennsylvania Game Commission, a state wildlife management agency, which regulates hunting and manages habitat for wildlife. The Pennsylvania Game Commission owns more than 600,000 hectares of land, referred to hereinafter as state gamelands, which are managed primarily for wildlife and to provide hunting and trapping opportunities for the public (Pennsylvania Game Commission 2023). Managing woodcock habitat for both breeding and migratory seasons are priorities for the Pennsylvania Game Commission, which requires tools to prioritize management projects on state gamelands.

### *1.2.2 Breeding and migratory season data*

To model woodcock habitat distribution during the breeding and migratory seasons, we used separate data sources that described woodcock occupancy during each of those time periods. For the breeding season (March–May), we used survey data collected as part of the federally-coordinated American Woodcock Singing Ground Survey (Seamans and Rau 2020) and additional state-level monitoring conducted by the Pennsylvania Game Commission. Both state and federal surveys consisted of 5.76 km routes with 10 evenly spaced points, where observers listened for woodcock songs during their crepuscular breeding display. Observers recorded counts of all males singing during 2-minute intervals shortly after dusk. We used survey data collected from 2016–2020, and distilled records to presence or likely absence at each point based on detection of at least one male during the 5-year period. Male woodcock are often assumed to display near female nesting habitat, and so male displays are likely an indicator of male and female presence at the scale of application (McAuley et al. 2020).

We delineated woodcock occurrence during the migratory season using GPS-tracking data from the Eastern Woodcock Migration Research Cooperative, a collaboration of 42 federal, state, provincial, non-profit, and university partners throughout the United States and Canada ([www.woodcockmigration.org](http://www.woodcockmigration.org)). We captured woodcock at 34 sites in Quebec, Ontario, Nova Scotia, Maine, Vermont, New York, Rhode Island, Pennsylvania, Maryland, West Virginia, Virginia, North Carolina, South Carolina, Georgia, Alabama, and Florida using mist nets during mornings and evening flights (Sheldon 1960), or using spotlights and dip nets at night (Rieffenberger and Kletzly 1966, McAuley et al. 1993). We attached 4g, 5g, or 6.3g PinPoint GPS Argos transmitters (Lotek Wireless Inc., Newmarket, Ontario, CA) to captured woodcock. Transmitters recorded GPS locations at 12–60m accuracy and were programmed to record diurnal locations every 1–3 days. Transmitters, bands, and attachment materials never exceeded 4% of a bird’s body weight, and all capture and

handling were conducted with methods approved by the University of Maine Institutional Animal Care and Use Committee (Protocol # A2020-07-01).

We used woodcock location data to identify stopover locations, defined as any place where a migrant bird can land and survive until the next migratory flight (Mehlman et al. 2005). We consider woodcock to be migrating after they have made their first >16.1 km movement in fall or spring, and to complete their migration after they have made their last >16.1 km movement in the respective season. The >16.1 km threshold was chosen as it roughly divides the bimodal distribution of log-standardized step lengths, presumably distinguishing between local- and long-distance movements (Blomberg et al. 2023). Because woodcock migrate at night, we considered all diurnal locations between migratory initiation and termination to be stopovers. We grouped successive locations within 3 km into a single stopover site, based on our observations that movements <3 km tended to be recursive rather than directional, and removed all but one location from each stopover from the analysis to reduce pseudoreplication and spatial autocorrelation of closely clustered locations. We also generated 10,000 locations randomly distributed throughout Pennsylvania, which we considered pseudoabsence locations.

#### *1.2.3 Species distribution modeling*

We constructed separate species distribution models for migratory and breeding seasons to accommodate differences in habitat associations and data sources. Each model used explanatory variables with demonstrated relevance to woodcock habitat associations (McAuley et al. 2020), with suites of variables including land use/land cover, forest successional class, topography, region, and soil moisture (Table 1.1). We additionally calculated landscape metrics from the *landscapemetrics* package (Hesselbarth et al. 2019) in program R (R Core Team 2024), which represented landscape composition and configuration. To generate composition metrics, we resampled the National Land

Cover Dataset to a 90m pixel resolution, and then calculated the percent of each cover type within 500m, 1km, 5km, and 10km radii for each pixel. For configuration metrics, we used the National Land Cover Dataset to create a binary forest/non-forest layer, which we resampled to 90m resolution, and then calculated each configuration metric within 500m, 1km, 5km, and 10km radii of each pixel.

Table 1.1. Explanatory variables used to model woodcock distributions in Pennsylvania, USA. Suites indicate conceptual grouping of variables into classes relevant to woodcock occurrence.

<b>Suite</b>	<b>Covariate</b>	<b>Source</b>
Land use/land cover	Land use/land cover	National Land Cover Dataset (Jin et al. 2019)
Forest successional class	Forest successional class	LANDFIRE (USGS and USDA 2020)
Topography	Elevation	(USGS 2000)
	Slope	Derived from elevation
Region	EPA level 3 ecoregions	Omernik and Griffith (2014)
Soil moisture	Soil drainage	Web soil survey (NRCS 2021)
	Topographic wetness index	Derived from elevation (Fink 2013)
Landscape composition (0.5, 1, 5, and 10km scales)	% Forest	Derived from National Land Cover Dataset using landscapemetrics
	% Agricultural	(Hesselbarth et al. 2019)
	% Developed	
Landscape configuration (0.5, 1, 5, and 10km scales)	Aggregation index	Derived from National Land Cover Dataset using landscapemetrics
	Cohesion	
	Edge density	(Hesselbarth et al. 2019)

We conducted a pilot evaluation of several potential modeling techniques fit to a subset of woodcock occurrence data, including using MaxEnt (Phillips et al. 2006), random forest classification (Breiman 2001), and boosted regression trees (Elith et al. 2008). All models were fit using the R package SDMtune (Vignali et al. 2020). We compared model outputs using area-under-the-curve (AUC), a common metric of predictive accuracy for classification models (Fielding and

Bell 1997). The random forest classifier had the highest AUC among modeling approaches, and we therefore used random forest techniques for all subsequent models (Table A.1).

For the breeding season model, we used a random forest classifier designed for clustered data (Wang and Chen 2016), and applied survey route as a clustering variable to compensate for spatial autocorrelation among points on the same survey route. As federal survey routes were randomly distributed (Clark 1970) and state surveys were distributed opportunistically, we included survey type (state vs federal) as an explanatory variable to accommodate differences in route distribution. For the migratory season, we used a traditional random forest classification model, written using the randomForest package in R (Liaw and Wiener 2002). We assessed the accuracy of all models using a k-fold cross validation approach, where separate training and testing datasets were randomly sampled for each fold. We sampled folds at a survey route level for the breeding season model to accommodate autocorrelation within survey routes and prevent data leakage between the training and testing datasets. We used 10 folds for the breeding season model (90% training, 10% testing), but only 5 folds for the migratory season model (80% training, 20% testing) to accommodate the smaller sample size of the stopover dataset. We averaged AUCs for each of the folds to produce a mean AUC for each model and created predictive layers at 90m resolution that averaged predictions across folds.

To avoid overwhelming final predictive models with highly correlated or uninformative variables, we used the R package VSURF (Genuer et al. 2022) to implement a three-step backwards variable-selection approach, where each step produced a more parsimonious model. The first step eliminated irrelevant variables with lower variable importance than a defined threshold value (determined based on guidelines in Genuer et al. 2015). The second step retained only variables with the smallest out-of-bag error rates when training the model, effectively eliminating variables with some relevance but not critical for prediction. The third step used a stepwise process to test whether each included variable led to an out-of-bag error decrease that was larger than a defined threshold

value, effectively removing redundant variables from consideration (Genuer et al. 2015). We compared predictive accuracy of models created from each step using AUC, and retained the model from the step that produced the highest AUC to create a final predictive layer for each season.

We normalized the predictive layer for each season on a percentile scale, indicating whether a given pixel had a greater likelihood of woodcock occupancy than the corresponding percentage of other pixels in the state; for example, a value of 0.65 indicates that the pixel contains habitat that is more suitable than 65% of other pixels statewide. We termed these habitat suitability layers, with habitat suitability defined as a bounded, continuous index representing the degree to which a given site possesses the habitat components required for species occupancy (U.S. Fish and Wildlife Service 1996). We occasionally refer to these habitat suitability layers as representing habitat distribution, which we define as the geographic distribution of habitat on the landscape, or as a representation of where areas of greater suitability occur or are absent.

#### *1.2.4 Analysis of covariate relationships and comparative distribution of seasonal habitat*

Random forest techniques do not provide easily interpretable covariate relationships, leaving the user to determine how covariates might influence the outcomes of the model (Breiman 2001). While we were not interested in exploring woodcock-habitat relationships per se, we nevertheless wanted to understand how environmental variables contributed to model predictions. We also sought to highlight regional differences in the distribution of breeding and migratory habitat among ecoregions. To depict these differences, we sampled covariate values, ecoregion type, and model-predicted suitability at 10,000 randomly distributed points throughout Pennsylvania. We used hex plots to visualize trends between covariates and predictions for each season, and visualized variation among each EPA level 3 ecoregion in Pennsylvania using box-and-whisker plots.

We used two metrics to evaluate cross-seasonal transferability between breeding and migratory season species distribution models, to better understand the utility of a multi-season modeling approach. The first was a Pearson correlation coefficient between the breeding and migratory season layers, calculated using the R package terra (Cohen et al. 2009, Hijmans 2023), which measured the correlation between breeding and migratory suitability on the scale of individual pixels (90 m). The second metric measured the Pearson correlation between the total breeding habitat and the total migratory habitat provided by each gameland (described below in section 1.2.5), illustrating the co-occurrence of breeding and migratory habitat at the scale of the average state gameland (1992 ha).

### *1.2.5 Spatial decision support system*

We created a SDSS in the Shiny ecosystem (Chang et al. 2022), named the Woodcock Priority Area Siting Tool (W-PAST), to facilitate local woodcock management planning. The SDSS allowed users to assign weights to each seasonal habitat suitability layer in 10% increments (ex. 20% migratory and 80% breeding season), and then combined seasonal predictions into a single multi-season layer (Fig. 1.2). The weighting was conducted on a pixel-by-pixel basis as a simple weighted average where  $p_w$  indicates the value of the weighted pixel value,  $w_m$  the weight of importance for migratory habitat,  $w_b$  the breeding season weight,  $p_m$  the migratory pixel value, and  $p_b$  the breeding season pixel value.

#### **Equation 1.1**

$$p_w = (w_m \times p_m) + (w_b \times p_b)$$

$$w_m = 1 - w_b$$

Practitioners often benefit from SSDS features customized to their management applications. In the case of the Pennsylvania Game Commission, a primary goal was to increase availability of woodcock habitat on state-managed gamelands, requiring functionality within the tool to compare

habitat suitability among gamelands. We built four comparison metrics into the SDSS that were calculated using the weighted averages of the breeding and migratory season predictive layers: average pixel value, total habitat, % high quality, and % medium quality. Average pixel value was the arithmetic mean of all pixels within a state gameland, which tended to favor small gamelands predominantly composed of woodcock habitat and was intended to demonstrate where a small amount of habitat management could increase local woodcock populations. Total habitat was average pixel value multiplied by the acreage of the gameland, which favored larger gamelands that contained relatively large amounts of woodcock habitat in aggregate by virtue of their size. Total habitat could be used to determine which gamelands would provide the most habitat in aggregate if they were managed for woodcock. Percent high quality habitat was the percentage of cells within a gameland that had values greater than the 33rd percentile of all pixel values in the state, and percent medium quality was the percentage of cells falling between the 66th and 33rd percentile. These percentile-based metrics allowed users to quantify the proportion of a gameland which might be suitable for woodcock management. By multiplying the percent high or medium quality by the gameland acreage (also provided in the tool), the user could also derive the acreage in each gameland that could be managed for woodcock effectively. Further instructions for using these metrics in management are included in a user manual, publicly available with the SDSS at [www.woodcock.shinyapps.io/W-PAST](http://www.woodcock.shinyapps.io/W-PAST).

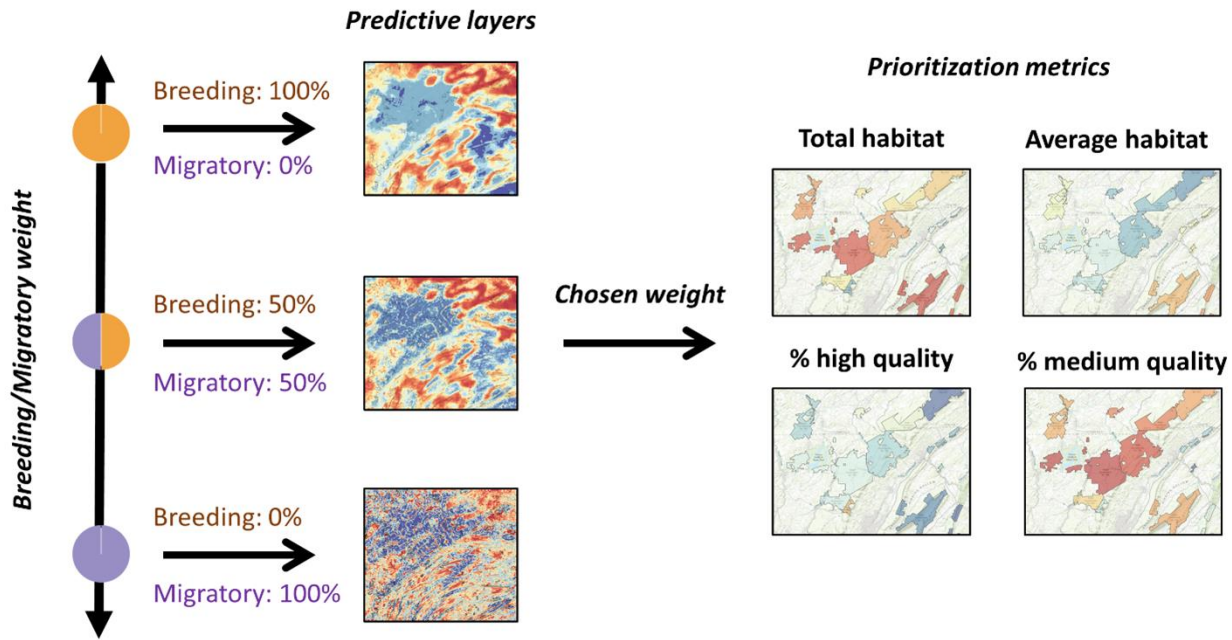


Figure 1.2. Conceptual diagram of user decision options in the Woodcock Priority Area Siting Tool (W-PAST). Users can choose the weighting of migratory and breeding season habitat at 10% increments based on management priorities. The resulting weights are used to generate a statewide predictive layer and gameland prioritization metrics, which allow the user to compare the suitability of gamelands for woodcock management.

### 1.3 Results

We collected data from 328 migrant woodcock marked with GPS transmitters throughout the eastern portion of the woodcock's range between fall 2017 and spring 2021. Eighty-two individuals (25%) recorded GPS locations at 113 stopovers in Pennsylvania. Breeding season survey data were available for 770 locations along 77 federal American Woodcock Singing-Ground Survey routes and 800 locations along 80 Pennsylvania Game Commission state survey routes. The most predictive breeding season model ( $AUC = 0.83$ ) was the result of the second variable selection step, in which all variables with low predictive capacity were removed. This model was heavily informed by landscape variables at 5 and 10 km scales (Table 1.2), and no variables at the finest spatial scale (0.5 km) or in the suite

of soil moisture characteristics were included in the most informative model. Graphs of habitat suitability for each covariate showed strong, non-linear relationships (Fig. 1.3). Suitability was highest for landscapes with 0–25% developed land area, 0–50% agricultural land area, and aggregation index values of 80–100, all at the 10km scale. At the 5km scale, the breeding season model also showed high suitability in landscapes with 30–100% forest cover (Fig. 1.3).

Table 1.2. Variables selected via backwards variable selection using the R package VSURF (Genuer et al. 2022) for the migratory and breeding season models. The migratory model employs the full set of variables, while the breeding season model uses a subset of variables inclined towards coarse resolution landscape variables.

Suite	Migratory	Breeding
Landscape (500m)	Aggregation Index, Cohesion, Edge Density, % Forest, % Agricultural, % Developed	
Landscape (1km)	Aggregation Index, Cohesion, Edge Density, % Forest, % Agricultural, % Developed	% Agricultural
Landscape (5km)	Aggregation Index, Cohesion, Edge Density, % Forest, % Agricultural, % Developed	Cohesion, % Forest, % Agricultural, % Developed
Landscape (10km)	Aggregation Index, Cohesion, Edge Density, % Forest, % Agricultural, % Developed	Aggregation Index, Cohesion, % Agricultural, % Developed
Land Cover	Forest, Successional Class	
Geography	Elevation, Slope, Ecoregions	Elevation, Ecoregions
Soil Moisture	Drainage, Topographic Wetness Index	

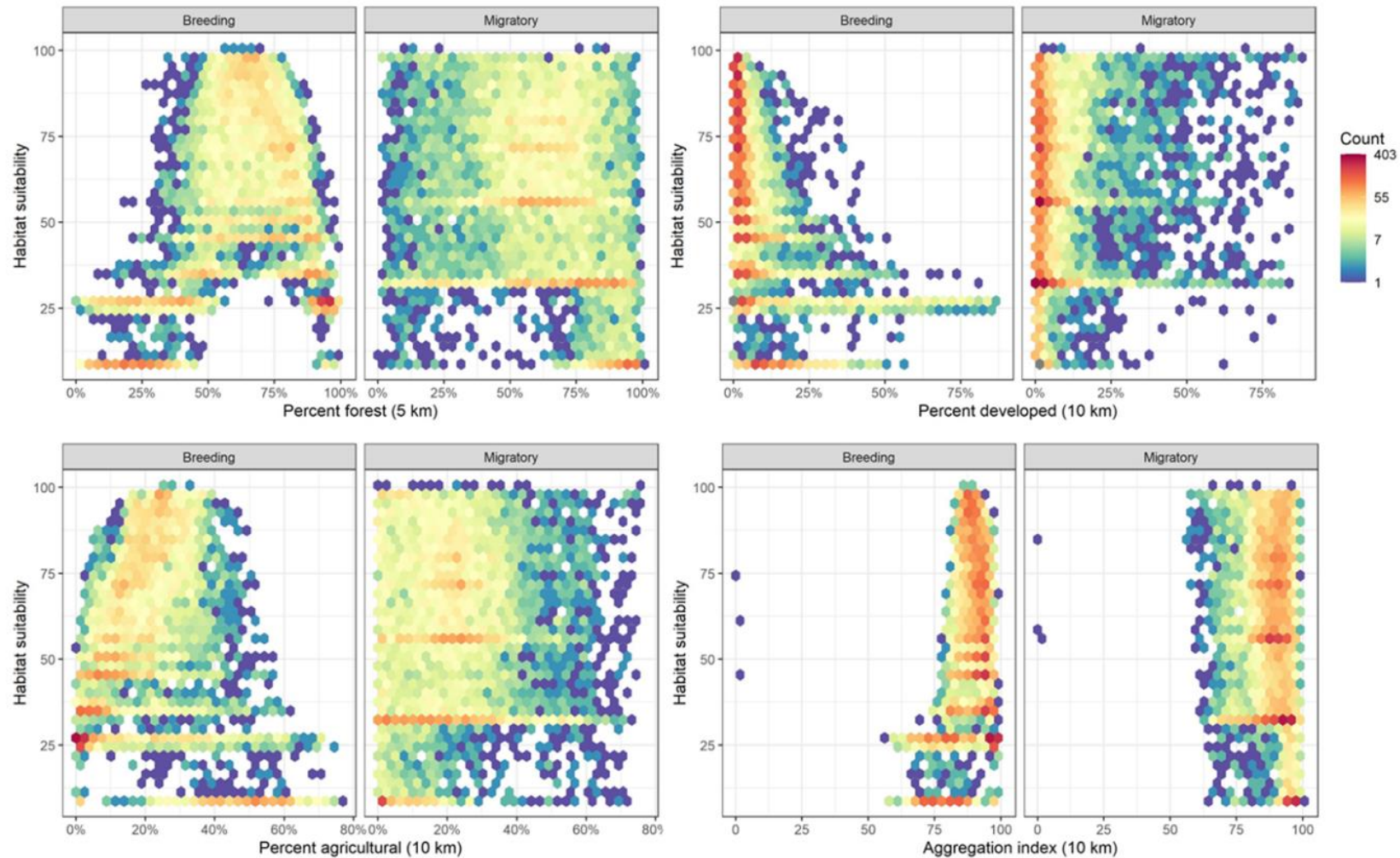


Figure 1.3. Comparison of relationships between landscape variables and habitat suitability for breeding and migratory season models of American woodcock in Pennsylvania, USA. Habitat suitability is displayed on a percentile scale, indicating whether a certain pixel was more suitable for woodcock occupancy than the corresponding percentage of other pixels in the state.

The most predictive migratory model (AUC=0.78) was the full model, including all landscape, land cover, geographic, and soil moisture covariates (Table 1.2). Likely due to the wide array of covariates influencing the model, individual covariate graphs do not show clear visual patterns between migratory habitat suitability and any one covariate. However, the migratory model illustrated greater tolerance of migrant woodcock for developed and dis-aggregated landscapes at a 10 km scale than the breeding season model (Fig. 1.3). The two models were also distinguished by the scale at which covariates influenced habitat suitability; the most informative breeding season model was not influenced by any landscape covariates at the 500 m scale, and only 1 landscape covariate at the 1 km scale, whereas the most informative migratory model included all available small-scale landscape covariates. Because of the influence of covariates at 500 m and 1 km scales, the migratory model predicted much more spatial variation in habitat distribution than the breeding season model, despite identical pixel resolutions (Fig. 1.4).

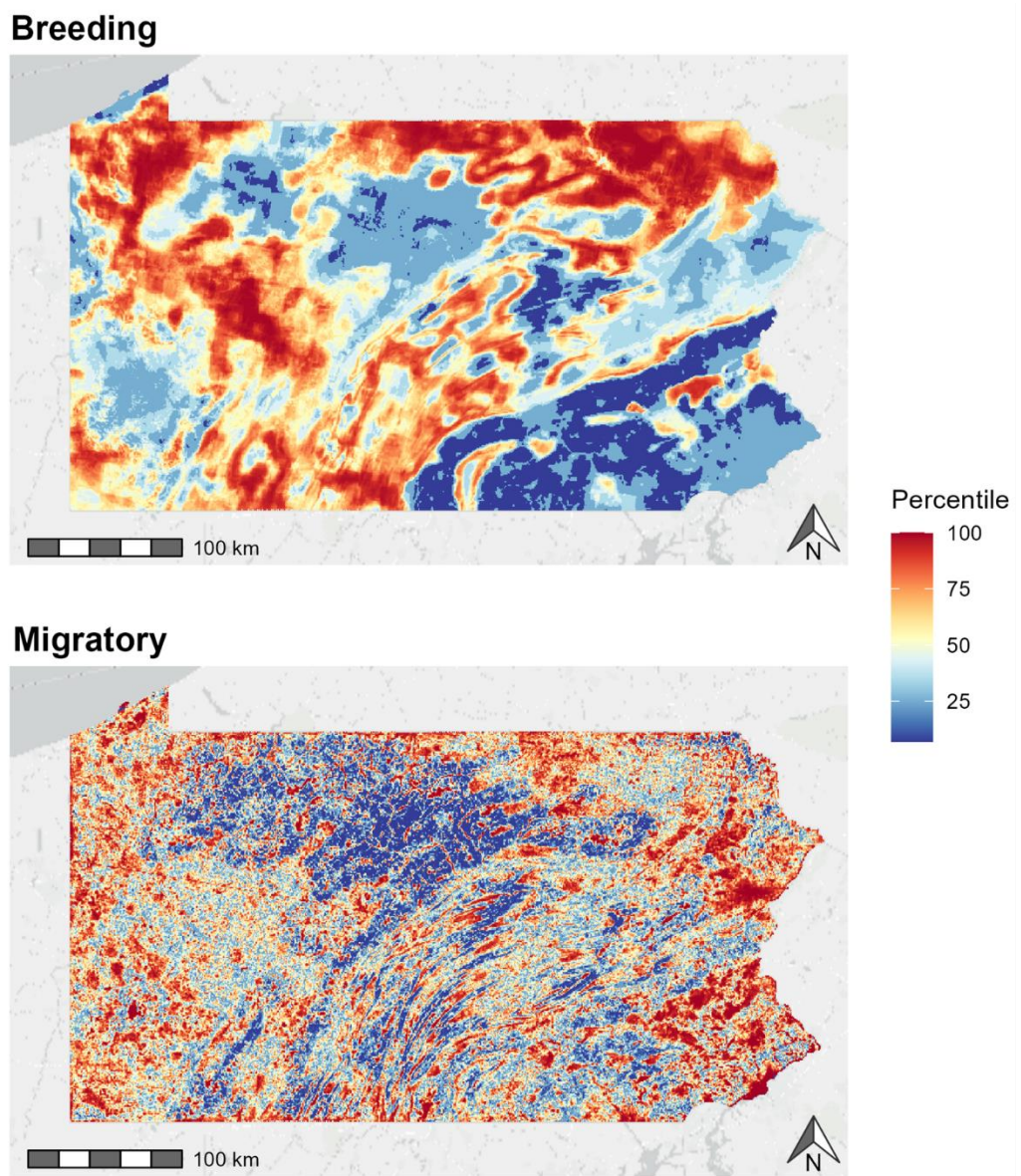


Figure 1.4. Breeding and migratory predictive habitat suitability layers suggest that woodcock select habitat at finer scales during the migratory season. Certain areas which are not appropriate for breeding season habitat management, such as southeastern Pennsylvania, may be appropriate for migratory habitat management. Percentile indicates whether a certain pixel was more suitable for woodcock occupancy than the corresponding percentage of other pixels in the state; for example, a value of 0.65 indicates that the pixel contains habitat that is more suitable than 65% of other pixels statewide.

Breeding season habitat was not evenly distributed among ecoregions (Fig. 1.5A), with mean habitat suitability values ranging from 22.9–86.0%. Migratory habitat was more evenly distributed among ecoregions, with mean habitat suitability values ranging from 46.5–87.5%. Most of the difference between the distribution of migratory and breeding season habitat was in the Northern Piedmont, Middle Atlantic Coastal Plain, and Central Appalachians ecoregions, which had mean breeding season habitat suitability values of <30% and mean migratory season habitat suitability values of >60% (Fig. 1.5B). Breeding and migratory habitat rarely co-occurred at a pixel level, with a Pearson correlation coefficient of 0.15 between the breeding and migratory season predictive layers. Breeding and migratory habitat were slightly more likely to co-occur on gamelands, with a Pearson correlation coefficient of 0.39 between the total breeding habitat and total migratory habitat provided by gamelands.

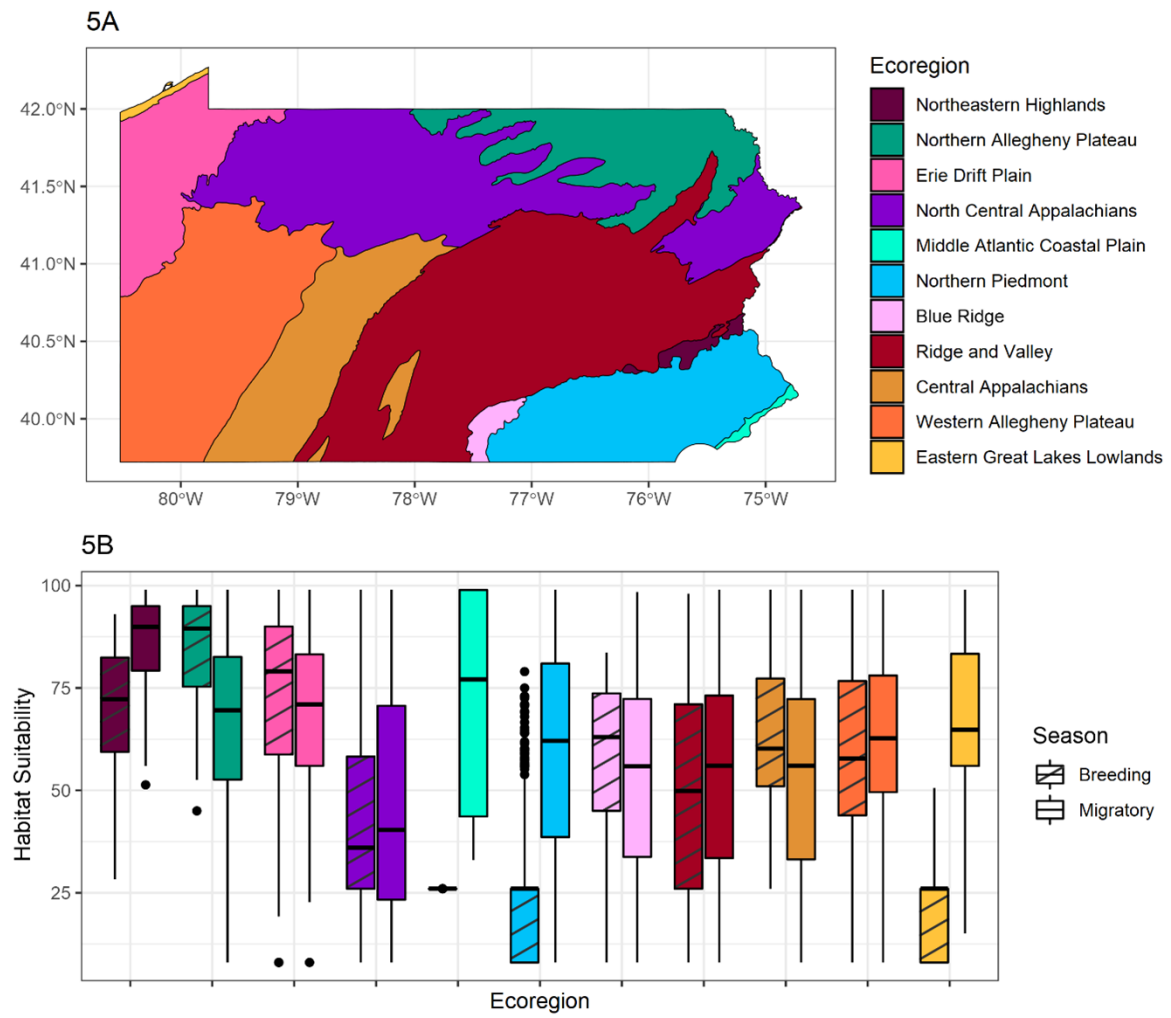


Figure 1.5. Breeding and migratory season habitat suitability for woodcock (5A) by EPA level 3 ecoregion (5B) in Pennsylvania (Omernik and Griffith 2014). Three ecoregions, Northern Piedmont, Middle Atlantic Coastal Plain, and Eastern Great Lakes Lowlands, had mean breeding season habitat suitability values of <30% and mean migratory season habitat suitability values of >60%. Habitat suitability is calculated based on randomly sampled locations within each ecoregion and uses a percentile scale, indicating whether a certain pixel was more suitable for woodcock occupancy than the corresponding percentage of other pixels in the state. Box plots, arranged in the same order as the figure legend, indicate the median and interquartile range while whiskers extend to the largest/smallest value within 1.5 times the interquartile range.

## **1.4 Discussion**

We found that models of woodcock habitat distribution exhibited poor cross-seasonal transferability between distribution models, with low correlation between breeding and migratory habitat models at multiple spatial scales (Pearson correlation at pixel-level: 0.15, gameland-level: 0.39). As such, management focused on breeding habitat alone is unlikely to maximize conservation of migratory habitat for this species. We demonstrated a potential solution to increase cross-seasonal transferability through the integration of multi-season species distribution models into a single SDSS tool. The SDSS emphasizes the importance of user input by allowing choice in the weighting of breeding and migratory habitat to meet local management objectives and encourages users to make informed decisions regarding the importance of habitat during these stages.

Regional differences between the breeding and migratory models underscore the importance of multi-season distribution models in delineating regional priorities for migratory bird management. For the woodcock model, we found relatively low breeding season suitability within the Northern Piedmont, Middle Atlantic Coastal Plain, and the Eastern Great Lakes Lowlands ecoregions, despite high migratory suitability. User-weighted prioritization of seasonal habitat might allow managers in regions in which woodcock breeding habitat is scarce to instead prioritize migratory habitat management. On the other hand, a manager of an area that provides breeding habitat in a region where breeding habitat is scarce might decide that their most effective decision would be to prioritize breeding habitat as much as possible. We posit that there might be several effective management strategies based on the information provided in multi-season distribution models, and the incorporation of user-specified weights empowers users to customize the tool to suit their own management objectives.

We showed that American Woodcock occurred in distinctly different habitat during the breeding and migratory seasons in Pennsylvania and were associated with different spatial scales

between seasons. During the breeding season, woodcock habitat suitability was dependent primarily on covariates at 5- and 10-km scales, while during the migratory season habitat suitability was additionally dependent on covariates at 500-m and 1-km scales. This pattern supports past observations that migratory birds select habitat at a finer scale during migration (Stanley et al. 2021). Due to these differences in the scale, managers may need to adjust management to match the scale of the season of interest (Fattorini et al. 2020). For example, woodcock management for breeding season habitat in Pennsylvania might focus on conserving broad swaths of habitat on large public lands, such as Pennsylvania state gamelands. As the predictive layer is fairly uniform across even large state gamelands, performing habitat management at that scale would likely be effective. However, the migratory model had a much finer spatial resolution, and was much more likely to predict smaller pockets of habitat in areas not traditionally targeted by wildlife management agencies, such as urban areas or landscapes more heavily dominated by agriculture and privately-owned lands (McCance et al. 2017). Differences in the spatial scale of habitat associations among seasons demonstrate the necessity of modeling occupancy for each season separately and to ensure that management supports the habitat requirements at appropriate scales for animals throughout the full annual cycle.

Multi-season distribution modeling may also highlight areas of potential for conservation that are not traditionally managed for wildlife habitat due to a lack of breeding season occupancy. Woodcock were more tolerant of developed land cover during the migratory season than the breeding season, and the migratory season model predicted use of highly developed areas such as suburban Philadelphia and Pittsburgh. This corresponds with findings of Buler and Dawson (2014), who found that migratory birds heavily used urban greenspaces during stopover, perhaps due to attraction to high levels of artificial light at night (McLaren et al. 2018) and lack of other stopover options. One implication is that, in addition to management for woodcock at smaller spatial scales, practitioners may need to consider management of urban greenspaces for migratory birds. Opportunities for urban

habitat conservation might come through partnerships with public and private landowners, such as park authorities and utility companies, to conserve migratory habitat in urban greenspaces (Cerra 2017). Another opportunity for urban habitat conservation might be the Urban National Wildlife Refuge program (USFWS 2023), which has dual roles in preserving wildlife habitat and expanding access to natural areas for historically excluded communities. Pennsylvania is host to one Urban National Wildlife Refuge, John Heinz National Wildlife Refuge at Tinicum, located in the Philadelphia suburbs. Our model predicted high migratory habitat suitability for woodcock within this refuge, demonstrating how urban wildlife refuges may provide crucial stopover habitat in heavily urbanized areas.

A multi-season distribution model framework is particularly well suited to migratory bird management due to its flexibility in application of multiple data sources, which is particularly useful for species that are studied using separate techniques and surveys during each season. While there are several surveys for examining bird distribution during the breeding and wintering seasons (e.g. Robbins et al. 1986, Bonter and Greig 2021), examining bird habitat use during the migratory period continues to be a challenge. Individually-marked birds with GPS transmitters are the gold standard for this type of analysis, as stopover locations can be separated from breeding and wintering locations for each tagged bird. However, GPS transmitters are still too large to attach to many small migratory birds, and the low number of stopovers attained per individual (mean = 1.4, sd = 0.6 in this study) combined with the considerable price of these transmitters may make attaining a large sample size a financial difficulty for most study species. The use of citizen science data collected during migration, such as the eBird data collection platform (Sullivan et al. 2009), may provide a more generalizable way to collect stopover location data, but certain assumptions must be made to distinguish true migratory locations from early breeding/wintering season arrivals. Decisions on seasonal management priorities can also be informed by other data sources and models, such as multi-season

survival models to determine whether breeding or migratory habitat has a greater role in limiting survival or migratory corridor models to identify high densities of migrants (Cohen et al. 2022). SDSS provide a framework for blending these multi-season datasets and models to improve management and conservation decision making for migratory birds.

Non-avian taxa are also likely to find benefits from the application of multi-season distribution models. Seasonally differing habitat use within a region is common among altitudinal migrants, including ungulates (Boyce 1991, Mauer 1998), and partial migrants ranging from large mammals to insects (Chapman et al. 2011). Cross-seasonal transferability issues which arise from these habitat differences can be addressed through a multi-season distribution modeling framework, allowing flexibility in data sources and facilitating user choice in seasonal prioritization.

## **CHAPTER 2: ADAPTING HIDDEN MARKOV MODELS FOR TRACKING MIGRATORY BIRDS USING DATA FROM SMALL GPS TRANSMITTERS**

Recent technological advances resulting in the widespread collection of tracking data from migratory birds necessitates tools for the effective processing and classification of that data. Tools such as hidden Markov models provide opportunities to classify movement states from high-resolution Global Positioning System (GPS) data collected at frequent, regular intervals. However, small-bodied migratory birds cannot carry large enough tags to collect GPS data frequently. Use of additional data streams may assist with assigning cryptic movement states to sparse and irregular GPS data. Here we apply a correlated random walk model and additional data streams to fit hidden Markov models to GPS data from American Woodcock (*Scolopax minor*; hereinafter “woodcock”). Our objectives were to determine if the use of additional data streams resulted in an improved capacity to predict migratory states and characterize woodcock migratory distance, duration, phenology, and the presence of long-distance movements outside of fall and spring migration. We found that individual data streams only marginally improved model performance, but collectively data streams decreased model error rates by a median value of 5.93%. Migratory characteristics measured using the full model (all additional data streams) were similar to the base model (only step length and turn angle) for all birds during fall and for males during spring, although the full model was 2.12 times more likely to identify a migratory endpoint than the base model for females during spring. The mean duration and distance of migration was also underestimated by 7 days and 278 kilometers for the base model as opposed to the full model for females during spring. Long-distance movements outside of fall and spring migration, such as dispersals and foray loops, were less frequently identified with the base model (3 dispersals, 15 foray loops) as opposed to the full model (4 dispersals, 18 foray loops). Using additional data streams may be beneficial for birds with overlapping seasonal distributions and

prolonged stopovers, demonstrating the benefits that new or repurposed movement models may have for understanding avian migratory ecology.

## 2.1 Introduction

The amount of tracking data collected from small birds has exploded in the 21<sup>st</sup> century (Iverson et al. 2023b), providing opportunities to address facets of bird migration that have long eluded ornithologists, such as migration phenology (Wright et al. 2021), habitat use (Moskát et al. 2019, Iverson et al. 2023a), survival (Klaassen et al. 2014), and connectivity (Combreaud et al. 2011). In particular, tracking devices that record GPS locations can provide data at a high temporal resolution with near global coverage. GPS transmitters have traditionally required large batteries or solar panels which limit their use to larger birds. However, recent innovations in these technologies have allowed GPS technology to become available for a much larger group of bird species than has historically been the case (Bridge et al. 2011, Flack et al. 2022).

In order to answer questions about bird migration, GPS data are often classified into movement states that delineate periods of pre-migration, migration, and post-migration, under one of several simple frameworks. The range delineation method (Fig. 2.1A; Linscott et al. 2022) is based on the known breeding and wintering ranges, where a bird is considered to have begun migration when it leaves the breeding range, and completed migration when it enters the wintering range, and vice versa. The range delineation method has the advantage of being robust to incomplete tracks; if a bird dies or transmitter failure occurs during the bird's migration, the bird's final state is still apparent. However, the range delineation method requires constrained breeding and wintering ranges that have little overlap with the migratory range (e.g., Bar-tailed Godwit, *Limosa lapponica*; Battley et al. 2012). The step-length or distance threshold (Burnside et al. 2017) method defines the start of migration by the first step longer than a defined distance threshold, and migration ends with the last

step longer than the distance threshold (Fig. 2.1B). The step-threshold method relaxes the assumption that breeding and wintering ranges do not overlap with the migratory range, making this method applicable to birds with widespread breeding and wintering ranges (ex. Pine Siskin, *Spinus pinus*; Dawson 2020). However, the step-threshold method does not handle incomplete tracks well; if a bird dies or its transmitter fails during migration, it is impossible to determine whether the bird has made its final migratory step (Fig. 2.2). Quantifying the terminal migration state is particularly important for survival and connectivity analyses, but also has relevance for phenology and habitat analyses for which accurate migratory delineation is important.

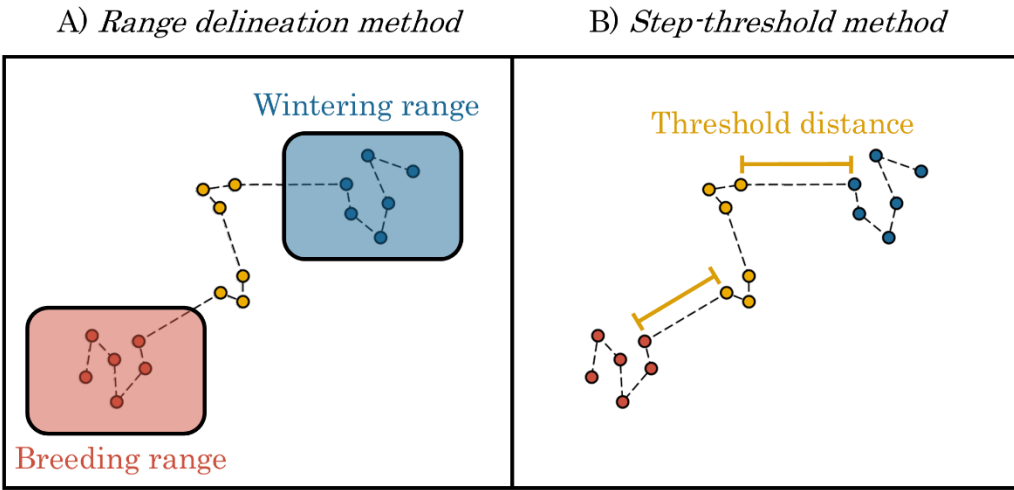


Figure 2.1. Range delineation (Linscott et al. 2022) and step-threshold (Burnside et al. 2017) methods of delineating migratory tracks. Using the range delineation method (Panel A), migratory locations can be defined as all locations outside both the breeding and the wintering range. Using the step-threshold method (Panel B), migratory locations can be categorized as all locations occurring after the first migratory step (determined using a threshold step length) and prior to the final migratory step.

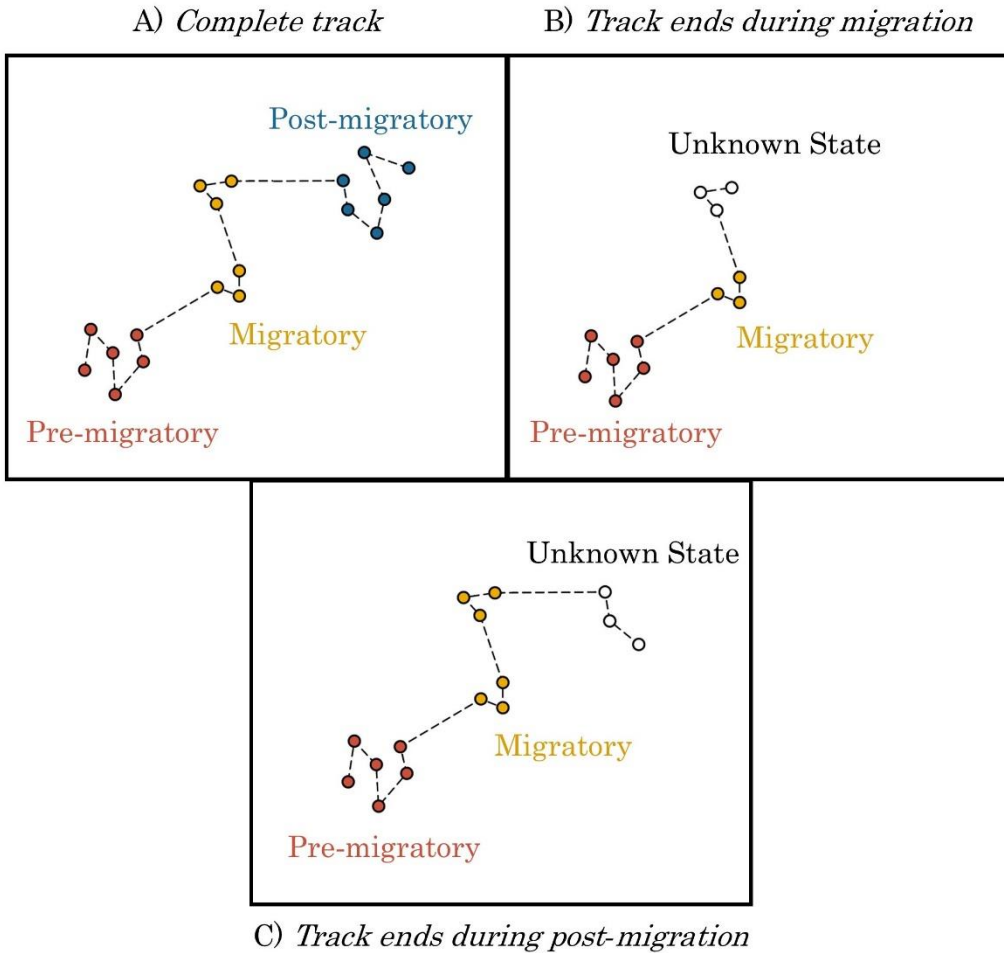


Figure 2.2. Complete and incomplete tracks of a theoretical migratory bird. For birds with complete tracks (Panel A; encompassing the entire temporal period of migration), the pre-migratory, migratory, and post-migratory stages of the track are apparent, and can be identified using the range delineation or step-length threshold methods. For birds with incomplete tracks (Panels B and C) the final state of the bird cannot be determined using a step-length threshold. If points cannot otherwise be delineated using breeding and wintering ranges, incomplete tracks end in an uncertain state that could be either migratory or post-migratory.

Hidden Markov models (HMMs) use observed distributions of outcome variables to assign movement states to animal tracking data and could potentially overcome limitations of rule-based assignments, particularly for the final movement state of incomplete movement tracks (Langrock et al. 2012, Zucchini et al. 2017). Step length and turn angle are the two most common data streams used by hidden Markov models in movement analyses, although additional data streams (such as acceleration, depth/altitude, and immersion in water) can be used to improve the model's predictive capabilities (Dean et al. 2013). Hidden Markov models have delineated foraging, dispersal, and migratory behaviors for a variety of bird taxa including shorebirds, sage-grouse, prairie grouse, and seabirds (Blomberg et al. 2023, Berigan et al. 2024, Dean et al. 2013, Picardi et al. 2022, Mander et al. 2022, Zhang et al. 2019). These taxa can carry large transmitters (often with solar panels) that provide high frequency, regular location data over long periods of time, which assists with fitting hidden Markov models. However, the small size and forest dwelling habits (i.e., no direct sunlight for solar panels) of smaller birds may preclude high frequency data collection for GPS transmitters attached to them and complicate fitting those data using traditional hidden Markov model approaches.

We illustrate the fitting of HMMs to low-frequency GPS data using American woodcock (*Scolopax minor*; hereinafter woodcock). Woodcock are widely distributed throughout eastern North America, typically breeding in the northern United States and southern Canada and wintering in the southern United States. They are frequently among the latest migrants to leave the breeding range as frost encroaches in the fall and the earliest to arrive as snow melts in the spring (Moore et al. 2021). Woodcock are particularly flexible in their migratory and reproductive timing; females regularly nest in the migratory and wintering ranges and have been observed migrating among nesting attempts (Slezak et al. 2024a). Woodcock are of appropriate size to carry small GPS transmitters, which are often constrained by limited battery life (woodcock mass: 116–279 g, transmitter mass: 4–6 g; McAuley et al. 2020).

Here we present a modified approach combining step-threshold and hidden Markov models to classify large-scale movement behaviors, such as migration, using sparse and irregular GPS data. We suggest a three-stage process: 1) interpolation of data at a regular interval using a correlated random walk model (Kareiva and Shigesada 1983), 2) delineating known movement states using the step-threshold method, and 3) estimating unknown movement states using a hidden Markov model with additional data streams that describe the time, location, and movement characteristics of each GPS point. We demonstrate this approach on data collected from American Woodcock during a range-wide study of migratory phenology, habitat use, and survival. Our objectives were to determine whether use of additional data streams facilitated estimation of terminal movement states from incomplete GPS tracks and improved our ability to quantify of woodcock migratory distance, duration, phenology, and long-distance movements outside of fall and spring migration.

## 2.2 Methods

### 2.2.1 *Collecting data via GPS transmitters*

We used GPS-tracking data from 2017–2022 collected by the Eastern Woodcock Migration Research Cooperative, a collaboration of 43 agency, non-profit, and academic organizations in eastern North America (Blomberg et al. 2023, Clements et al. 2024, Fish et al. 2024). We captured woodcock at 78 sites throughout Quebec, Ontario, Nova Scotia, Maine, Vermont, New Jersey, New York, Rhode Island, Pennsylvania, Maryland, West Virginia, Virginia, North Carolina, South Carolina, Georgia, Alabama, Louisiana, and Florida. We used mist nets to capture woodcock during morning and evening flights (Sheldon 1960) and using spotlights and dip nets on night roosts (Rieffenberger and Kletzly 1966, McAuley et al. 1993). We attached 4g, 5g, or 6.3g PinPoint GPS Argos transmitters (Lotek Wireless Inc., Newmarket, Ontario, CA) to captured woodcock. Transmitters, bands, and harness materials never exceeded 4% of a bird's body mass, and all capture and handling were

conducted with methods approved by the University of Maine Institutional Animal Care and Use Committee (Protocol # A2017-05-02 and A2020-07-01).

GPS transmitters were programmed with one of several schedules, each of which collected data at a slightly different pace to optimize battery life according to specific project objectives. The most frequent schedules recorded locations daily, while infrequent schedules recorded locations every 2–3 days during migratory time periods and every 3–7 days outside of migration. Certain schedules were programmed to switch between frequent and infrequent modes, and transmitters were occasionally set to go dormant for periods of 1–3 months during summer and fall to preserve battery life for separate study objectives. Transmitters were predicted to collect a maximum of 75–150 GPS locations, depending on transmitter size and schedule, at 12–60m accuracy. Transmitters relayed GPS locations to the ARGOS satellite network after every 3<sup>rd</sup> location; however, transmitters occasionally failed to relay data, sometimes resulting in missing programmed locations.

## 2.2.2 *Delineating spring and fall migration*

### 2.2.2.1 *Track interpolation and application of the step-threshold method*

We delineated woodcock movements during periods of fall (Aug. 1<sup>st</sup>–Feb. 25<sup>th</sup>) and spring (Jan. 5<sup>th</sup>–Jun. 30<sup>th</sup>) migration. However, for a small subset of birds ( $n = 14$ ; 3%) we extended these date ranges due to migratory movements that occurred outside these periods (Appendix B.1). To ensure that fall and spring migratory movements were delineated separately, we modeled spring migrations first for each woodcock, and shortened the end of the default fall migration timeframe (Aug. 1–Feb. 25) to 1 day before the subsequent spring migration began for that individual.

We interpolated daily locations within each track prior to fitting HMMs, as infrequent and missing locations can impede the ability of the HMMs to detect recursive movements (defined as repeated visitations to the same locations in a systematic manner, *sensu* Berger-Tal and Bar-David

2015) which could be indicative of stopovers and post-migratory settlement. We used a correlated random walk model implemented in the R package *crawl* (Johnson and London 2018, R Core Team 2024), which interpolated locations based on prior and subsequent location, speed, and direction. We predicted that interpolated locations would improve the capacity of the HMM to detect recursive movements more accurately during stationary periods, however, during initial model fitting, we observed that they did not accurately reflect the distribution of known migratory movements. To address this tendency, we only used the correlated random walk model to interpolate locations between points that were <16.1 km apart (i.e., when the bird was either at a stopover or not migrating). Due to the directional consistency inherent in correlated random walks, models occasionally produced erroneous loops of interpolated points when birds made recursive movements during non-migratory periods. These interpolated loops were often lengthy and could artificially create step lengths  $\geq$ 16.1 km. To ensure that HMMs did not incorrectly assign these loops as migratory movements, we removed all loops of interpolated points for which the total length of the loop exceeded 10 times the distance between observed points and replaced the loops with predicted locations spaced evenly between the observed points.

Following point interpolation, we applied the threshold method (Burnside et al. 2017) to define migration for each season on an individual basis, beginning after the first movement  $\geq$ 16.1 km and ending after the final  $\geq$ 16.1 km movement. We chose a 16.1 km threshold as it roughly bisects the bimodal distribution of log-transformed step lengths in the dataset (Blomberg et al. 2023). We then used HMMs to refine movement state classifications and assign ending states to incomplete migration tracks.

#### *2.2.2.2 Use of additional data streams to inform HMMs*

We measured a subset of variables as additional data streams, which we believed would allow models to better differentiate between stopovers and post-migratory locations (Table 2.1). Log mean distance to the nearest 7 points measured whether the nearest 7 bird locations (meant to approximate space use over the period of 1 week) reflected intensive use of the same area, and presumably resource utilization, or spread-out movement throughout the area, possibly reflecting exploration. Residence time measured the time difference between the first and last day that the bird was located within a 10 km radius of a focal location. This reflected the difference between the amount of time that woodcock spent occupying stopover sites as opposed to their post-migratory sites. Ordinal day captured woodcocks' annual phenology of migration. Latitude reflected latitudinal differences in the breeding, migratory, and wintering ranges of woodcock. Distance from start measured whether a bird had moved  $\geq 16.1$  km from its position at the beginning of the season, indicating it had departed its initial site to begin migration. Breeding range reflected whether the bird was currently within the woodcock breeding range, as delineated using the eBird 2021 Status and Trends abundance maps (Fink et al. 2022).

We created two versions of each seasonal HMM, described as base and full models, with different suites of data streams used to inform each. The base model included only step length, turn angle, and step length threshold data streams, while the full model included all 6 additional data streams (Table 2.1). We estimated error rates, migratory characteristics, and long-distance movements separately for each base and full model (described further below) to allow us to infer how additional data streams changed the model's predictive capacity and ability to make inferences into migratory ecology.

Table 2.1. Covariates used to delineate movement states in hidden Markov Models (HMMs), and the type of distribution fit to each covariate in the HMMs. Data streams are categorized by their appearance in the base and full models, with the base model using only the 3 core data streams and the full model using all 9 data streams. Point-specific attributes (latitude, ordinal day, distance from start, breeding range, log(distance to nearest points), residence time) are based on the woodcock's location at the beginning of the step.

Covariate	Distribution	Description
<i>Base &amp; Full Model</i>		
Step length	Gamma	Length of the current step
Turn angle	Wrapped Cauchy (Kent and Tyler 1988)	Angle between the current and previous step
Step length threshold	Bernoulli	Binomial indicating if the current step length is $\geq 16.1$ km. Implemented with a fixed distribution so that all steps $\geq 16.1$ km are migratory.
<i>Full model</i>		
Log(distance to nearest points)	Normal	Natural logarithm of the mean distance to the nearest 7 points.
Residence time	Normal	Number of days that the bird has spent/will spend within a 10km radius.
Ordinal day	Normal	Days since the beginning of the migratory season
Latitude	Normal	Latitude at the beginning of the step
Distance from start threshold	Bernoulli	Binomial indicating if the bird moved $>16.1$ km from its location at the beginning of the migratory season
Breeding range	Bernoulli	Binomial indicating if the step begins in the American Woodcock breeding range (Fink et al. 2022).

### 2.2.2.3 Seasonal HMM design

We implemented HMMs in the R package `momentuHMM` (McClintock and Michelot 2018). We conducted separate HMMs for fall and spring migration, and further subset spring migration by sex due to different breeding motivations during spring migration (Blomberg et al. 2023, Slezak et al. 2024a) which we assumed *a priori* would result in fundamentally different movement characteristics. We constructed a multi-state model for each HMM to identify transitions occurring between movement states (Fig. 2.3). Models for spring migration by females, and all woodcock during fall, featured 4 states: pre-migration, migration, stopover, and post-migration. Birds began the season in a pre-migration state and transitioned to migration following the first movement  $\geq 16.1$  km, which was the only state in which movements  $\geq 16.1$  km were permitted. From the migration state, birds could remain in migration or enter either a stopover state or a post-migration state. Once entering the stopover state, birds could remain in stopover or transition back to the migration state. The post-migration state could only be reached from the migration state and did not allow for any further state transitions. These state assignments were generally enforced using the fixed transition framework in the `momentuHMM` package, but occasional errors occurred when improbable state assignments caused the framework to fail to enforce state transition rules. These errors and their fixes are detailed in Appendix B.2.

While most models had a single post-migration state, the spring male model included two post-migration states, post-migration (frequent) and post-migration (infrequent), which males could enter in spring at the conclusion of migration. The inclusion of these two states fixed an artifact in the dataset caused by male-specific transmission schedules switching to less-frequent transmission late in the spring migratory season. Infrequent locations caused the correlated random walk model to infer a greater proportion of steps during the late migratory period, producing a much narrower turn angle distribution than observed earlier in the season. The inclusion of two post-migratory states with

separate turn angle distributions, which birds could transition between freely, allowed the model to better account for this source of variation in turn angles when delineating post-migratory movements.

We excluded any birds that did not have at least 1 step  $\geq 16.1$  km, or which collected fewer than 3 points, from migratory delineation in the respective season. We assigned a fixed pre-migration state for the initial step of most birds captured during breeding or wintering, and a fixed migration state if the first step was  $\geq 16.1$  km. Because birds captured in Virginia, New Jersey, and Maryland were sometimes captured during migration, we allowed the HMM to estimate the initial state of the model for birds captured in these locations. We fixed final steps to the post-migratory state for any fall woodcock that were also known to initiate a subsequent spring migration.

We visually inspected all HMM state assignments, which sometimes identified circumstances where birds did not fit model predictions due to extra-seasonal movements (6% of tracks), early initiation or late termination of migration (3%) or transmitter error (1%). There were also additional issues with initial state designations that were encountered only by the base model (3% of tracks). In these cases, we manually reclassified state assignments (Appendix B.1). Woodcock that died during migration occasionally continued to transmit and caused the HMM to falsely classify dead birds as post-migratory. We have included methods used in delineating GPS mortalities and removing them from the dataset in Appendix B.3.

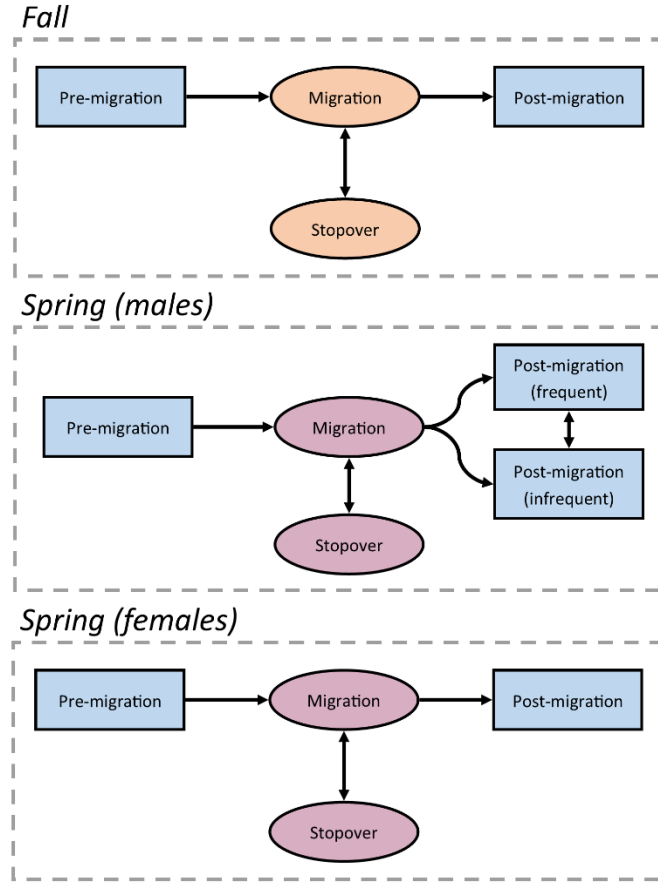


Figure 2.3. Movement state transition diagram for each hidden Markov Model (HMM). Blue boxes represent pre- and post-migratory states, while yellow and red circles represent states during fall and spring migrations, respectively. The spring male model includes two post-migration states to compensate for less frequent GPS locations collected from males in late spring.

### 2.2.3 Delineating spring and fall migration

#### 2.2.3.1 HMM error rates and variable importance

We assessed the accuracy of HMM state assignments using a leave-one-out validation based on individuals with known terminal states. For individuals with transmitters that functioned past the end of each migration period, we truncated the movement track by removing one week of points, simulating a scenario where data transmission was lost prior to the end of migration. We then refitted

the HMM to the truncated data, and evaluated whether the model correctly assigned the known final movement state. We repeated this process by truncating an additional week of data from each track to evaluate the capacity of models to correctly assign latent states throughout the period of migration (fall: Oct. 1st–Jan 15th, spring: Mar. 15th–Jun. 15th). We repeated the validation process for 50 individuals, with replacement, for each model set. We measured the accuracy of final state assignment based on Type I and Type II errors, where a Type I error occurred when a known post-migratory state was falsely classified as migratory, and a Type II error occurred when a known migratory state was falsely classified as post-migratory.

To determine which additional data streams had the greatest impact on model error rates, we repeated the leave-one-out validation but omitted one of the additional data streams from the full model (Table 2.1) and measured how Type I and Type II error changed compared to the full and base models. We inferred variable importance based on the relative change in Type I and II errors following removal.

#### *2.2.3.2 Migratory characteristics*

We calculated several migration metrics that described the duration, distance, and timing of each movement state. Duration was the sum of the number of days between the first movement in each state and the initial location of the subsequent movement state (e.g., the start and end of migration). Distance was the sum of the total step distance in each movement state. For birds undergoing fall or spring migration, total distance excluded movements designated as stopovers, i.e. steps <16.1 km, and only reflected the summed distance of migratory steps. Timing was the ordinal date of the transition point between movement states. We used medians and ranges to report the population-level timing of migratory initiation and termination, as medians are well suited to accommodating outliers that were common in the initiation and termination dates. We compared all migration metrics

between full and base models to evaluate improvements in inference resulting from the more complex full model.

#### *2.2.3.3 Long-distance movements and non-migratory individuals*

Woodcock occasionally underwent long-distance movements outside of the spring and fall migratory periods. To determine if the full and base models affected our ability to detect these long-distance movements, we manually classified 3 potential movement states: foray loops, dispersals, and summer migrations (Table 2.2). Foray loops and dispersals were both presumably exploratory movements, where dispersals resulted in displacement from the original site while foray loops did not. We counted the frequency of dispersals and foray loops based for all birds with locations spanning at least 1 month, which was long enough to correctly classify movement classes. Summer migrations were movements of similar distance and direction to fall migration, but occurred prior to August 1, well before the normal onset of fall migration. We counted the frequency of summer migrations based on all birds tracked between May 1<sup>st</sup>–Sep. 1<sup>st</sup>.

To determine if the use of the full and base models impacted our detection of non-migratory individuals, we calculated the percentage of individuals that did not migrate using the pool of all individuals tracked between the nominal start of the migratory season (Fall: Oct. 15, Spring: Feb. 15) and the date by which most birds had initiated migration (95<sup>th</sup> quantile of the departure dates for that season). Any individuals that had at least one location before, during, and after this period, but did not enter a corresponding migratory state, were designated as non-migratory for that season. We used the same time periods to determine whether a bird migrated during the season before or after its non-migratory season.

Table 2.2. Definitions of long-distance movement states manually delineated for American Woodcock.

<b>Class</b>	<b>Definition</b>
Summer Migratory	Post-breeding, southerly movements initiated before Aug 1 that preclude fall migratory movements.
Foray loops	Circular or out-and-back movements with steps $\geq 16.1$ km that result in $< 16.1$ km of net displacement between the first and last point. Foray loops can occur during any season, provided they are temporally distinct from a bird's migratory movements.
Dispersals	Movements that include step lengths $\geq 16.1$ km and result in $\geq 16.1$ km of net displacement between the first and last point. Dispersal movements follow directions which are not typical of co-occurring seasonal migrations. Note that this differs from dispersal defined in an evolutionary context, <i>sensu</i> Ronce (2007).

#### 2.2.4 Data and code availability

To make data available for use in future research, we uploaded all woodcock GPS locations and their movement state assignments to a Movebank repository (reference ID 351564596). The process of refining these designations for use in Movebank is detailed in Appendix B.4. All code used in this study is publicly available at <https://github.com/EWMRC/fac-classification>.

## 2.3 Results

### 2.3.1 HMM error rates

We analyzed 522 seasonal movement tracks from 401 tagged woodcock, of which 45 tracks (9%) in the full model and 56 tracks (11%) in the base model required modifications to the methods described above to correctly fit the seasonal HMMs (detailed in Appendix B.1). The full model improved classification accuracy for all three seasonal HMMs compared to the base model (Fig. 2.4). Type I error rates were similar for full (median 6.0%, range 0–24.2%) and base models (median 6.0%, range 0–24.2%) during fall migration, but Type II error rates were lower for the full model (median 0%, range 0–4.3%) compared to the base model (median 10.6%, range 0–28.3%). The spring male full model exhibited lower rates of Type I (median 8.3%, range 0–15.6%) error than the base model (median 15.6%, range 0–61.1%), and comparable rates of Type II error (full: median 4.3%, range 0–11.4%; base: median 4.3%, range 0–13.6%). The spring female full model exhibited greater Type I errors (median 6.8%, range 0–18.8%) during some time periods than the base model (median 2.1%, range 0–4.2%), but also exhibited reduced Type II error rates (median 6.3%, range 2.0%–11.4%) compared with the base model (median 52.1%, range 10.0–77.6%).

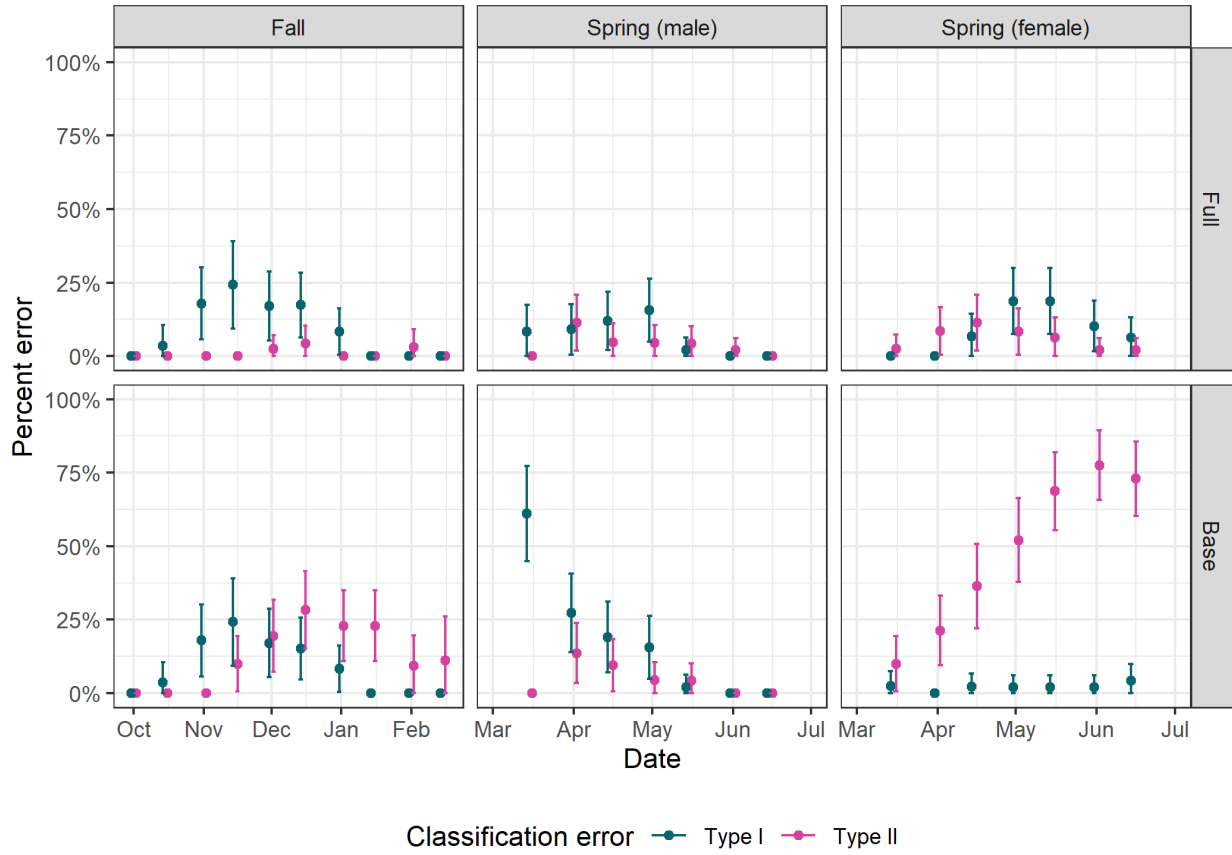


Figure 2.4. Error rates for movement state assignments by hidden Markov models (HMMs) for fall, spring (male), and spring (female) migrations, as measured through the model validation process. The horizontal axis reflects the cutoff date for each model that was used to simulate an incomplete track ending on that date. HMMs were grouped into full and base models, where full models included all possible data streams and base models including only step length and turn angle. Type 1 errors reflected false classification as post-migratory while the true state was migratory, whereas Type 2 errors reflected false classification as migratory while the true state was post-migratory. Bars show the 95% confidence interval of the mean.

### 2.3.2 *Variable importance*

Individual removal of variables from the full model had low overall impact (median -0.31%, range -17.17–2.70%) on Type I and Type II error rates of the seasonal models (Fig. 2.5). The importance of a withheld variable often differed by season, with the removal of some variables (e.g., ordinal day) leading to reduced error in one season and increased error in another. Residence time produced the greatest reduction in error rates, with a 2.81–17.17% drop in Type II error rates for all 3 seasonal models. The full model caused a 0.71–42.55% reduction in Type II error rates for those 3 models, suggesting that these variables have a more appreciable impact on error rates when used in aggregate.

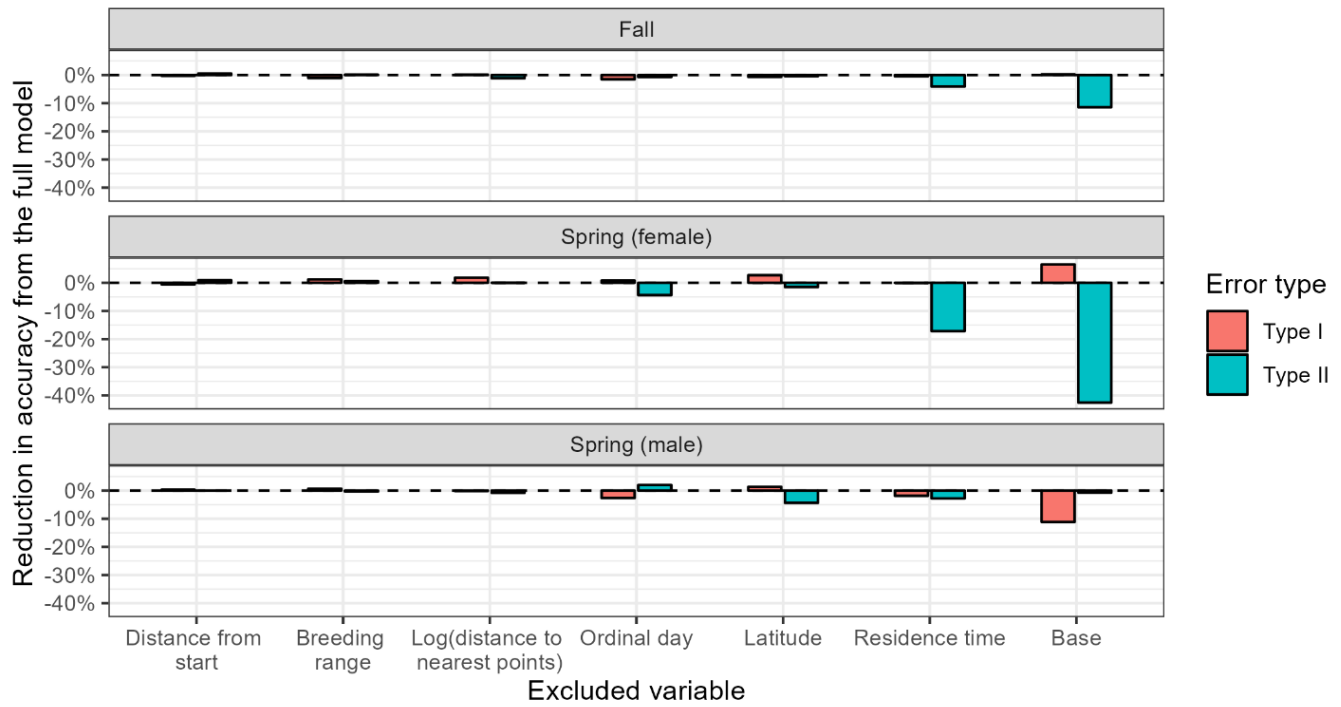


Figure 2.5. Reduction in accuracy from the full model due to removal of individual data streams, as well as the base model which included none of these 6 data streams. Type I errors occurred when the ending state was falsely classified as migratory, and Type II errors occurred when the ending state was falsely classified as post-migratory. Negative values indicate reductions in accuracy, while positive values indicate that accuracy improved when the variable was excluded from the model.

### *2.3.3 Migratory characteristics*

Among all seasons, the measured characteristics of woodcock migratory movements, such as distance, duration, phenology, and the percentage of individuals completing migration, changed least between the fall full and base models (Table 2.3). The full spring male model was 1.15 times more likely to identify a migratory endpoint than the base model. There was no difference in mean migratory duration between the two models, although the base model underestimated mean migratory distance by 45 km compared to the full. The spring male base model estimated that the median migratory initiation and termination dates were two days earlier than the full model. The spring female model exhibited more drastic differences between the base and full models, with the full model 2.12 times more likely to identify a migratory endpoint than the base model. The mean duration and distance of spring female migration was underestimated by 7 days and 278 km for the base model as compared to the full model, while the median initiation date of the base model was 4 days earlier and the median termination date was 12 days earlier than that of the full model.

Table 2.3. Migratory characteristics of full and base models for each seasonal hidden Markov model, in addition to detection rates for long-distance movements outside of spring and fall migration.

<b>Season</b>	<b>Metric</b>	<b>Full model</b>	<b>Base model</b>
Fall migration	Percent completed migration <sup>1</sup>	56%	55%
	Duration <sup>2</sup>	32 days ( $\pm$ 26, 1–134 days)	32 days ( $\pm$ 26, 1–134 days)
	Distance <sup>3</sup>	1353 km ( $\pm$ 647, 20–3210 km)	1344 km ( $\pm$ 645, 20–3210 km)
	Initiation date <sup>4</sup>	Nov. 7 <sup>th</sup> (Aug. 29 <sup>th</sup> –Jan. 11 <sup>th</sup> )	Nov. 7 <sup>th</sup> (Aug. 29 <sup>th</sup> –Jan. 11 <sup>th</sup> )
	Termination date <sup>5</sup>	Dec. 6 <sup>th</sup> (Oct. 28 <sup>th</sup> –Feb. 4 <sup>th</sup> )	Dec. 5 <sup>th</sup> (Oct. 28 <sup>th</sup> –Feb. 4 <sup>th</sup> )
	Percent completed migration <sup>1</sup>	75%	86%
	Duration <sup>2</sup>	39 days ( $\pm$ 24, 4–95 days)	39 days ( $\pm$ 25, 4–95 days)
	Distance <sup>3</sup>	1554 km ( $\pm$ 644, 296–3337 km)	1509 km ( $\pm$ 649, 262–3337 km)
	Initiation date <sup>4</sup>	Feb. 29 <sup>th</sup> (Jan. 6 <sup>th</sup> –Apr. 14 <sup>th</sup> )	Feb. 27 <sup>th</sup> (Jan. 6 <sup>th</sup> –Apr. 17 <sup>th</sup> )
	Termination date <sup>5</sup>	Apr. 6 <sup>th</sup> (Jan. 20 <sup>th</sup> –Jun. 7 <sup>th</sup> )	Apr. 4 <sup>th</sup> (Jan. 20 <sup>th</sup> –Jun. 7 <sup>th</sup> )
Spring migration (male)	Percent completed migration <sup>1</sup>	55%	26%
	Duration <sup>2</sup>	49 days ( $\pm$ 29, 2–128 days)	42 days ( $\pm$ 28, 2–101 days)
	Distance <sup>3</sup>	1671 km ( $\pm$ 626, 455–3424 km)	1393 km ( $\pm$ 698, 248–3424 km)
	Initiation date <sup>4</sup>	Mar. 5 <sup>th</sup> (Jan 14 <sup>th</sup> –Apr. 26 <sup>th</sup> )	Mar. 1 <sup>st</sup> (Jan 14 <sup>th</sup> –Apr. 23 <sup>rd</sup> )
	Termination date <sup>5</sup>	Apr. 25 <sup>th</sup> (Mar. 10 <sup>th</sup> –Jun. 28 <sup>th</sup> )	Apr. 13 <sup>th</sup> (Mar. 2 <sup>nd</sup> –May. 25 <sup>th</sup> )
Long-distance movements	Dispersals <sup>6</sup>	3 detected (0.7%; 2 M, 1 F)	2 detected (0.4%; 2 M, 1 F)
	Foray loops <sup>7</sup>	18 detected (4%; 8 M, 10 F)	15 detected (3%; 7 M, 8 F)
	Summer mig. <sup>8</sup>	3 detected (5%; 2 M, 1 F)	3 detected (5%; 2 M, 1 F)

Table 2.3 Continued.

<sup>1</sup> Percent of birds which completed their migration prior to the end of their track.

<sup>2</sup> Mean duration of migration, with standard deviation and range.

<sup>3</sup> Mean distance of migration, with standard deviation and range.

<sup>4</sup> Median and range of migratory initiation dates.

<sup>5</sup> Median and range of migratory termination dates.

<sup>6</sup> Number of individuals which underwent a dispersal among all birds tracked for at least one month ( $n = 456$ ), including the percentage of birds which underwent a dispersal and the number of dispersals associated with males and females. Note that one bird underwent two dispersals, bringing the total number of dispersal movements detected to 4 for the full model and 3 for the base model.

<sup>7</sup> Number of individuals which underwent a foray loop among all birds tracked for at least one month ( $n = 456$ ), including the percentage of birds which underwent a foray loop and the number of foray loops associated with males and females.

<sup>8</sup> Number of individuals which underwent a summer migration among all birds tracked throughout May 1st–Sep. 1<sup>st</sup> ( $n = 65$ ), including the percentage of birds which underwent a summer migration and the number of summer migrations associated with males and females.

#### *2.3.4 Long-distance movements and non-migratory individuals*

Long distance movements outside of spring and fall migration were less frequently detected using the base model than the full model, with the full model detecting 3 more foray loops and 1 more dispersal than the base model (Table 2.3). Using the long-distance movements detected by the full model, we found that dispersal movements had a mean duration of 6 days (1–10 days) and the mean distance traveled was 129 km (30–263 km). Foray loops had a mean duration of 20 days (2–95 days) and a mean total distance traveled of 221 km (34–951 km). The number of summer migrations detected was not impacted by use of the full or base model, with 3 of 65 birds (5%; 2 males, 1 female) tracked throughout May 1<sup>st</sup>–Sep. 1<sup>st</sup> migrating south during the summer. These summer migratory movements initiated around May 27<sup>th</sup>, Jun. 20<sup>th</sup>, and Jul. 13<sup>th</sup> and terminated around Jul. 8<sup>th</sup>, Jul. 25<sup>th</sup>, and Aug. 22<sup>nd</sup> (Fig. 2.6). Summer migrations had a mean duration of 39 days (35–42 days) and a mean distance traveled of 756 km (523–1106 km).

Non-migrants were detected by both the full and base models, with some differences in detection rates. The full model detected 6 non-migrants in the fall (3% of individuals tracked between Oct. 15th–Dec. 5th; 3 males, 3 females) and spring (3% of individuals tracked between Feb. 15<sup>th</sup>–Mar. 29<sup>th</sup>; 1 male, 5 females). The base model detected one fewer non-migrant in fall (3% of individuals tracked between Oct. 15th–Dec. 8<sup>th</sup>; 2 males, 3 females) and the same number of non-migrants in spring (3% of individuals tracked between Feb. 15<sup>th</sup>–Mar. 28<sup>th</sup>; 1 male, 5 females). The fall non-migrants detected using the full model overwintered in Rhode Island (3), Pennsylvania (1), Connecticut (1), and Virginia (1), while the spring non-migrants summered in Virginia (2), Maryland (1), Florida (1), Georgia (1), and Alabama (1). Individuals that abstained from migration during one season were observed migrating in prior or subsequent seasons when data were available (5 of 5 birds detected in the full model).

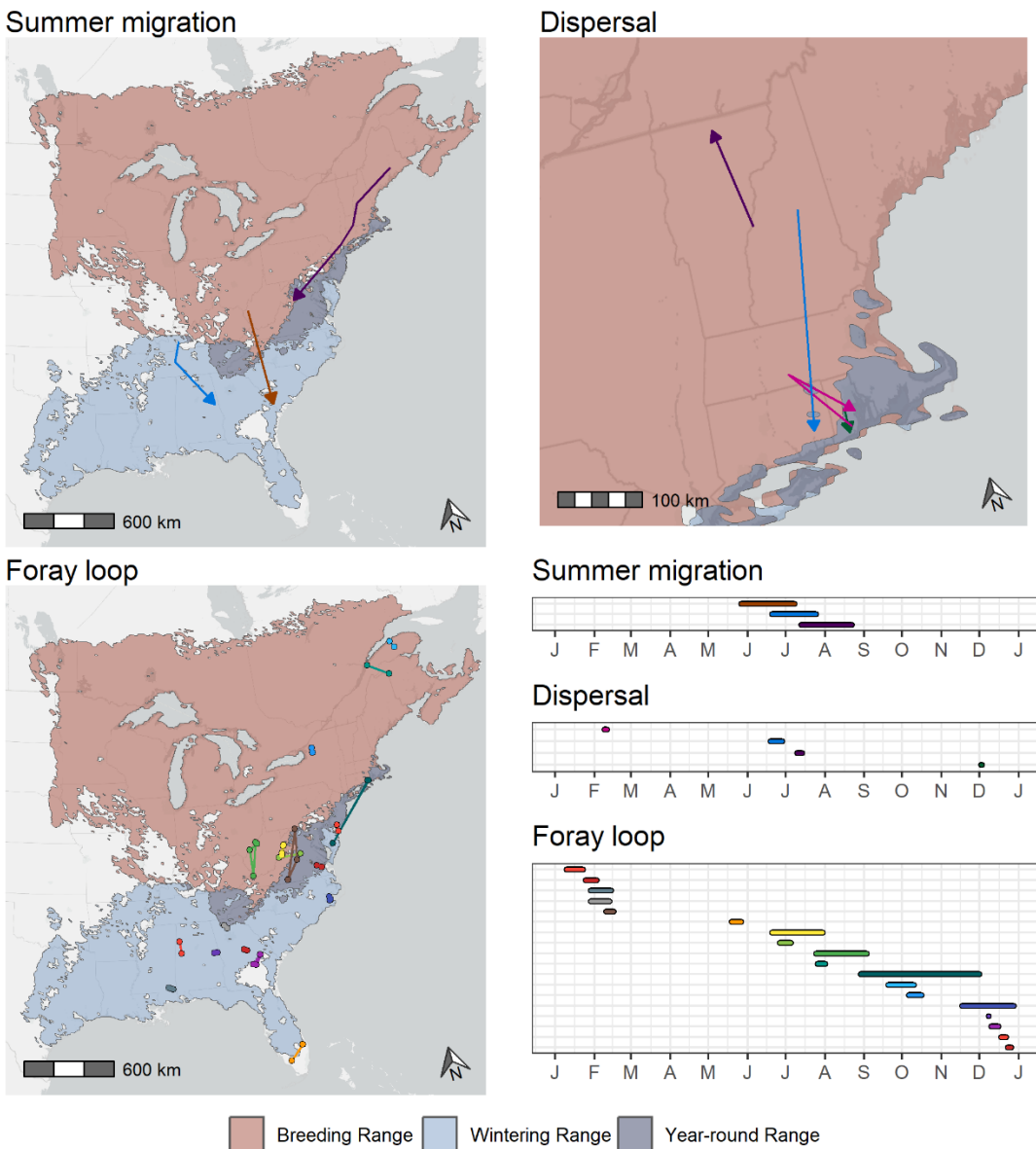


Figure 2.6. Spatial and temporal distribution of summer migrations, dispersals, and foray loops of American Woodcock marked with GPS transmitters in eastern North America. Maps are superimposed over the breeding, wintering, and year-round range of the American Woodcock as delineated by the eBird Status and Trends dataset (Fink et al. 2022). Timelines depict the duration of each movement by month, and each movement is matched from the map to the timeline by color. These long-distance movements are derived from the full model, which includes all possible data streams for informing delineations of woodcock migratory movements.

## 2.4 Discussion

Combining the step-threshold method with a set of hidden Markov models resulted in a technique that could be used to estimate the migratory state of American Woodcock with a quantifiable level of accuracy. We found that the use of additional data streams allowed HMMs to fit the migratory movements of woodcock with lower error rates for several seasonal models. The most substantial improvement was among Type II errors for spring females (full: median 6.3%, range 2.0%–11.4%; base: median 52.1%, range 10.0–77.6%), although spring males also had some improvements in Type I error rates early in the season (full: median 8.3%, range 0–15.6%; base: median 15.6%, range 0–61.1%). These differences were mirrored by our migratory characteristics results, which found that spring females had the most substantial differences between the full and base models, with less pronounced differences for spring males and few differences for fall birds (Table 3). Individual variable results suggest that the improved error rates and classification of migratory characteristics seems to be due to several added data streams working in aggregate, with each individual variable having a reduced influence when used in isolation (Fig. 5). The three most important of these variables, ordinal day, latitude, and residence time, demonstrate how spatial and temporal variables can assist in delineating migratory and post-migratory states even for a species that has considerable overlap in seasonal ranges and migratory/non-migratory periods (Chp. 1, Fish et al. 2024).

Our results demonstrate that certain seasons, in particular spring female migration, are more difficult to accurately characterize using only step length and turn angle. The difficulties encountered with spring females are likely due to female woodcocks' tendency to nest during spring migration, with continued migration following nest failure (Slezak et al. 2024a). Under this reproductive system, movement patterns of female woodcock during stopover may be very similar to those post-migration, which may lead to difficulties in discriminating among movement states based only on step length and turn angle. The addition of data streams, especially residence time, ordinal day, and latitude,

increased the accuracy of the spring female model (Fig. 5), likely distinguishing among early, southerly nesting attempts that are prone to failure and resumption of migration and later nesting attempts which are less likely to have a subsequent migratory movement. While woodcock have an uncommon breeding system (Slezak et al. 2024a), this technique for refining HMMs may be useful for any migratory bird with lengthy stopovers and spatial overlap in their seasonal ranges. For example, Sora (*Porzana carolina*) use the Chesapeake Bay in Virginia, Maryland, and Delaware, USA, as both a breeding and a staging area during spring migration, and an HMM technique like ours could be used to differentiate between breeding and staging states based on movement characteristics (Duerr and Watts 2012). This technique may be widely applicable to shorebirds and waterbirds, for which extended stopover and staging behaviors are common (Colwell 2010, Stafford et al. 2014), as well as facultative migrants (e.g. American Robin, *Turdus migratorius*) which encounter substantial overlap in their migratory, breeding, and wintering ranges (Vanderhoff et al. 2020).

We found that the increased classification accuracy of the full model allowed us to identify more long-distance movements outside of fall and spring migration. These movements were relatively uncommon (dispersals: 0.7% of individuals in the full model; foray loops: 4%; summer migrations: 5%), and motivations may range from avoiding negative environmental conditions in the winter (e.g., movements from Rhode Island to Maryland and back) to foraging and exploratory behaviors. Dispersal movements and foray loops have been observed among a variety of songbird, grouse, and shorebirds, most frequently occurring after the breeding season (Earl et al. 2016, Cooper and Marra 2020, Hoepfner 2023). During our study we observed dispersal movements and foray loops throughout the year, including dispersal movements during summer and winter and foray loops during every season except for the peak of spring migration. Cooper and Marra (2020) suggest that the prevalence of dispersals and foray loops is underestimated due to the difficulty of tracking small birds at fine spatial scales, and this may be exacerbated due to the prevalence of single-season

movement studies (Marra et al. 2015). Dispersals can in some cases allow population exchange and gene flow among subpopulations, and identifying these movements is important for understanding avian life history and population dynamics (Bohonak 1999, Morales et al. 2010). Robust frameworks for differentiating these movements from fall and spring migrations, such as we present here, could improve our ability to document these movements in future studies.

Onboard data collected by the transmitter, such as acceleration, altitude, or depth, have traditionally been used as data streams to inform animal movement HMMs (Dean et al. 2013), but these data are frequently unavailable for small transmitters. Our results demonstrate that external data streams, such as spatial and temporal variables derived from the movement track, can have a similar benefit for predicting migratory states. Extensions of HMMs which incorporate feedback when calculating transition probabilities, such as an increased likelihood of switching from a foraging state to a transit state after spending time feeding, may also be well suited to explaining the temporal patterns that distinguish migratory stopover behavior from post-migratory resource utilization (Zucchini et al. 2008).

Modeling migratory bird movements presents several challenges that differ from other classes of animal movement. As we demonstrate, small transmitters carried by migratory birds collect sparse and irregular data that can cause difficulty in fitting movement models. Migratory birds also undergo rapid shifts between slow, recursive movements at stopover sites and fast, direct movements during migratory flights, which may impede models that assume consistency in movement modes (e.g., correlated random walk models, Kareiva and Shigesada 1983; see section 2.2.1 of this manuscript for issues encountered). Other studies have demonstrated these issues can be overcome by incorporating new or repurposed statistical models or supplementing GPS data with seasonal abundance data (Nichols et al. 2018, Nicol et al. 2023, Fuentes et al. 2023). Further research on these techniques may

allow us to extend movement modeling techniques to a much greater array of avian species and give us greater insight into the ecology and habits of migratory birds.

## **CHAPTER 3: FUNCTIONAL RESPONSES IN AMERICAN WOODCOCK HABITAT**

### **SELECTION THROUGHOUT THE FULL ANNUAL CYCLE**

Migratory birds shift their habitat selection throughout the year, due in part to functional responses to shifts in habitat availability among their breeding, migratory, and wintering ranges. However, these changes in habitat selection among seasons and regions are infrequently quantified due to the difficulty associated with following individual migratory birds throughout their full annual cycle. We examine how American Woodcock (*Scolopax minor*) habitat selection, including the scale of selection and individual variability, shifts in response to seasonal, demographic, and regional factors which might cause a functional response to habitat availability. In 2017–2023, we deployed satellite GPS transmitters on 572 woodcock throughout the eastern portion of their range. We used 1,015,886 GPS locations from 530 of these woodcock fit to step selection functions to examine selection of 10 landcover covariates derived from the North American Land Change Monitoring System at multiple spatial scales. We found that woodcock select habitat at smaller scales (50–100m) during migration than they do throughout the rest of the year (200–1000m), potentially due to differing mechanisms used to select stopover, breeding, and wintering habitat. We found that selection for several covariates (needleleaf forest, wetland, urban) became less pronounced outside of the post-migratory breeding season, presumably due to decreased energetic demands allowing more generalist habitat selection. Habitat selection coefficients varied extensively among seasons and regions, but less so among age-sex classes. Seasonal and regional variation in habitat selection could be due in part to niche partitioning, ecological differences in cover types between regions, differing resource requirements by season, or functional responses to habitat availability. Further research may allow us to determine the importance of these factors in explaining shifts in the habitat selection of migratory birds throughout the full annual cycle.

### **3.1 Introduction**

Migratory birds frequently undergo changes in their habitat selection throughout the full annual cycle. Passerine species, such as the Kirtland's Warbler (*Setophaga kirtlandii*), which are closely associated with specific cover types during the breeding season often shift to an unrelated cover type while wintering (Botecetti et al. 2020). Shorebird species, such as the Short-Billed Dowitcher (*Limnodromus griseus*), which use exclusively freshwater muskegs and bogs for breeding may instead associate with saltwater habitats during the migratory and wintering seasons (Jehl Jr. et al. 2020). While several potential factors, such as niche partitioning and breeding season-specific resource requirements, could be potential causes for these shifts in habitat selection, one prominent factor is functional responses to changing availability of resources (Mysterud and Ims 1998). Functional responses can result in animals selecting less strongly for a resource as its availability increases on the landscape (specialist response), selecting for a resource more strongly as availability increases on the landscape (increasing use), or moderating their selection against a resource as it becomes more available (relaxed avoidance, Holbrook et al. 2019). This theory has been widely applied to non-migratory organisms and given that migration entails movement between two areas with different resource availability (Dingle 2014) functional responses are likely a leading cause of shifts in habitat selection throughout the full annual cycle.

In addition to differing habitat selection among seasons and regions throughout the full annual cycle, birds may also adjust the scale of their habitat selection. Multi-scalar relationships are common in avian habitat selection, with selection often differing, and sometimes being undetectable, outside of certain spatial scales (Pribil and Picman 1997, Buler et al. 2007). Shifts in the scale of selection between seasons may indicate changes in the mechanism of habitat selection between seasons, with implications for the strength of seasonal habitat relationships (Chernetsov 2006). Individual variability may also change in respect to season and region. Individual variation in habitat selection

has been well documented, and quantifying individual variation in selection preferences is a common element of modern habitat selection analyses (Leclerc et al. 2016, Muff et al. 2020). Differing individual variability between seasons and regions might indicate a shift in available niche space, presenting a possible opportunity for a functional response (Newsome et al. 2015).

These factors, including habitat selection, scale of selection, and individual variability may also shift in response to age and sex class. Variation in habitat use among age-sex classes for birds may arise from several different causes. Competitive exclusion may result in the exclusion of subordinate age-sex classes from high quality habitat, frequently resulting in negative consequences for body condition (Marra et al. 1993, Mettke-Hofmann et al. 2015). Differing reproductive roles, resulting in differing resource needs between sexes, may result in differential habitat selection during the breeding season but not the rest of the year (Phillips et al. 2004). Niche divergence, resulting from circumstances where sexes are physiologically distinct enough that they occupy differing ecological niches, may result in differential habitat selection throughout the full year (Orgeret et al. 2021). Age-sex classes may modify the impacts of a functional response in circumstances when these classes select habitat differently, making their measurement important to determining the extent of a functional response (Mysterud and Ims 1998).

Changes in habitat selection throughout the full annual cycle are infrequently studied due to the difficulty associated with tracking individual birds during or after migratory movements. Technological advances have made this possible due to the advent of small GPS transmitters, which can be attached to an increasing proportion of migratory birds with near global satellite coverage (Bridge et al. 2011). One species that has been a recent focus of GPS transmitter studies (Moore et al. 2019, 2021) is the American Woodcock (*Scolopax minor*; hereinafter woodcock). Woodcock are an early successional forest habitat specialist which primarily eats earthworms and are associated more closely with upland habitats than most other North American shorebirds (McAuley et al. 2020).

Woodcock have been noted to associate with wetlands and deciduous or mixed forests (Massee et al. 2014), although they frequently utilize night roost habitat in fields, presumably to avoid predation (Krementz et al. 1995). In spring, male woodcock display in forest openings (often created through logging activity), usually near second-growth hardwood stands that serve as nesting and brooding habitat (Kelley et al. 2008). Woodcock have a unique itinerant breeding system in which females may make several nesting attempts during their migration, and continue migrating after nest or brood failure (Slezak et al. 2024a). This breeding system has led to reports of nesting throughout much of the woodcock's wintering and migratory range (McAuley et al. 2020). Woodcock habitat selection differs based on sex and season, with woodcock often displaying more tolerance for urban and heavily agricultural areas during migration (Allen et al. 2020, Slezak et al. 2024b, Chp. 1).

Here we examine how woodcock habitat selection, including the scale of selection and individual variability, shifts in response to seasonal, demographic, and regional factors which might cause a functional response to habitat availability. Our hypotheses (Table 3.1) are derived from our main objectives, 1) to determine how multi-scalar habitat selection differs among seasons, age-sex classes, and regions, and 2) to measure the extent to which habitat selection remains consistent between seasons at a population and individual level.

Table 3.1. Hypotheses regarding factors that may affect the scale of habitat selection and habitat selection coefficients for American Woodcock (*Scolopax minor*).

Hypotheses	Predictions	References
<i>The scale of habitat selection will differ by...</i>		
... season	Woodcock will select habitat at smaller scales outside of the post-migratory breeding season.	Stanley et al. 2021
... age-sex class	The scale of woodcock habitat selection will differ by sex during the post-migratory breeding season	Slezak et al. 2024
<i>Habitat selection coefficients will differ by...</i>		
... season	Woodcock will become more generalist with their habitat selection during migration.	Stanley et al. 2021
... age-sex class	Competitive exclusion will shift subordinate age-sex classes into lower quality habitat, and reproductive roles will cause habitat selection in the post-migratory breeding season to differ by sex.	Marra et al. 1993, Phillips et al. 2004
... region	Woodcock will shift their habitat selection across their range due to functional responses.	Gillies and St. Clair 2010
<i>Individual variation in selection coefficients will differ by...</i>		
... season & age-sex class	Reproductive roles will cause reduced individual variability among females during the post-migratory breeding season.	Baert et al. 2021
... region	Individual variation in woodcock habitat selection will change across the range due to functional responses.	Newsome et al. 2015

## 3.2 Methods

### 3.2.1 Data collection and preprocessing

In coordination with the Eastern Woodcock Migration Research Cooperative (Clements et al. 2024), we captured woodcock throughout eastern North America in 2017–2023 using spotlighting and mist nets (McAuley et al. 1993) and used a rump-mounted leg loop harness (Fish et al. 2024) to attach 4–7 g PinPoint transmitters (Lotek Wireless Inc., Newmarket, Ontario, CA) to captured birds. All capture and handling was conducted in accordance with protocols approved by the University of Maine Institutional Animal Care and Use Committee (Protocols A2017-05-02 and A2020-07-01) as well as permits from the USGS Bird Banding Laboratory and Canadian Bird Banding Office. Transmitters collected GPS location data, which were preprocessed using hidden Markov models to delineate migration from periods of residency (full methods available in Chapter 2). We removed long-distance movements that occurred outside of spring and fall migration from further consideration, and classified the remaining locations as summering, wintering, spring migration, or fall migration based on the initiation and termination dates of each individual’s spring and fall migratory movements. We further categorized summering points as post-migratory breeding (before July 25<sup>th</sup>) or post-breeding (on or after July 25<sup>th</sup>), based on prior research using this dataset which indicates that 95% of nesting attempts have concluded by this date (Slezak et al. 2024a). The term “post-migratory breeding” was chosen due to woodcocks’ itinerant breeding strategy, in which nesting attempts frequently cooccur with migratory movements, which might make the use of the traditional term “breeding season” to describe the post-migratory period misleading. We removed repeated locations from known nesting attempts (Slezak et al. 2024a), as well as mortality locations (Chapter 2), migratory flight locations (nocturnal locations with a recorded altitude >107 m; Chapter 4), and individuals with fewer than 5 locations before further analysis.

To examine how woodcock habitat relationships varied among regions within the species' range, we classified all points according to the Bird Conservation Region (hereinafter BCR; Sauer et al. 2003) in which they were located. Bird Conservation Regions are a set of ecological units delineated by the North American Bird Conservation Initiative based on the similarity of bird communities, ecosystems, and conservation issues within each region (Fig. 3.1). These designations were used for the BCR suite of habitat selection models (see section 3.2.6 below).

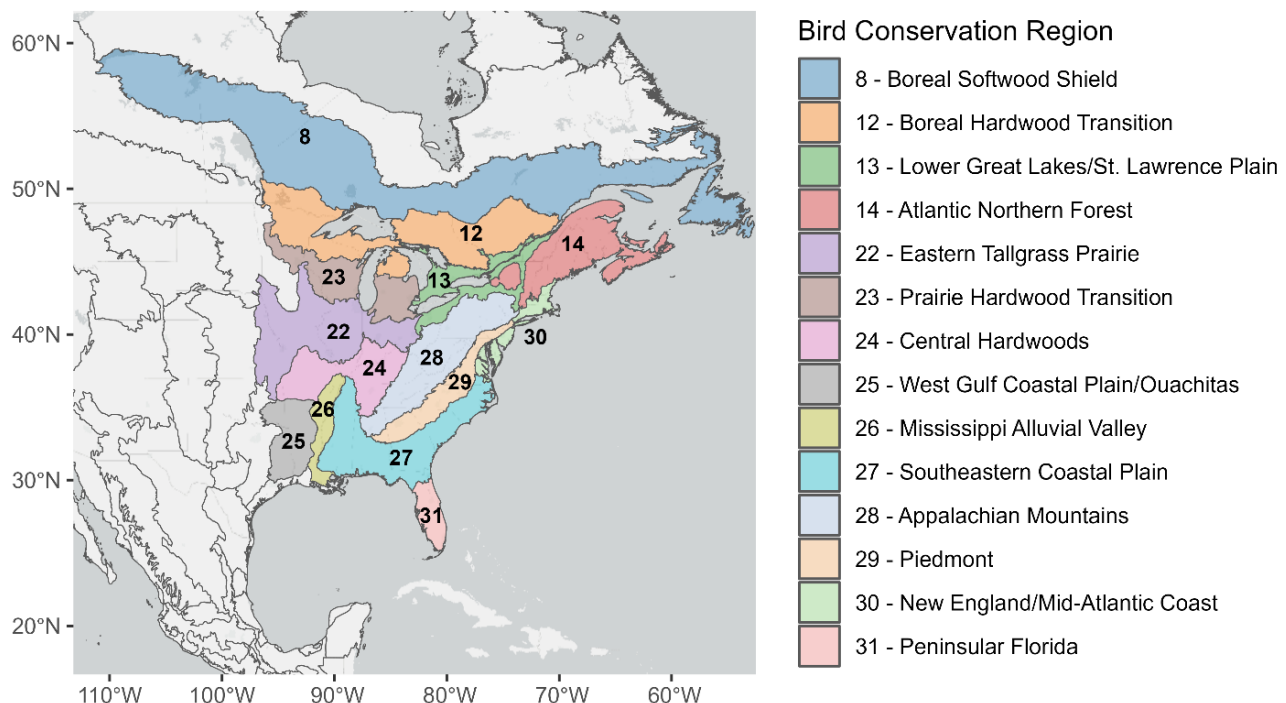


Figure 3.1. Map of Bird Conservation Regions (BCRs; Sauer et al. 2003) in eastern North America. Only BCRs that had a large enough sample size of woodcock locations to be included in the BCR suite of habitat selection models are illustrated here.

### *3.2.2 Delineating levels of habitat selection*

Habitat selection is a multi-level process, involving hierarchical decisions to choose a suitable geographic range, home range, and areas within the home range (Johnson 1980). Examining the habitat selection of migratory birds has some parallels to Johnson (1980)'s orders of selection, as birds migrate between sites (among-site selection; analogous to 2<sup>nd</sup> order selection of home ranges) and then select habitat resources within sites (within-site selection; analogous to 3<sup>rd</sup> order selection of areas within the home range). Among-site selection encompasses both a) the selection of new stopover sites following migratory flights and b) the selection of a summering or wintering site at the conclusion of migration. Within-site selection encompasses selection occurring within a given stopover site, summering home range, or wintering home range. As migratory flights consist of movements  $\geq 16.1$  km (Blomberg et al. 2023), among-site selection occurs whenever a bird makes a  $\geq 16.1$  km movement to a migratory stopover site or a post-migratory breeding/wintering home range. Within-site selection occurs when woodcock make movements  $< 16.1$  km, either within unique stopover sites, or within their summer or winter home ranges. For the purposes of this dissertation chapter, we will focus solely on the habitat relationships observed in within-site selection.

### *3.2.3 Delineating availability*

We calculated available habitat for each  $< 16.1$  km step under a step selection framework, which compares collected GPS locations (simplified into steps between successive locations) with hypothetical paired steps generated based on the distribution of all step lengths and turn angles in the dataset (Fortin et al. 2005). Step selection functions typically assume a regular interval of sampling to ensure that step lengths and turn angles are comparable throughout the dataset (Thurfjell et al. 2014). Our transmitters were constrained by battery life and were programmed to collect data at irregular time intervals to meet varied study objectives, which violates assumptions of regular sampling. We

compensated for irregular time intervals between points by creating step length and turn angle distributions that were dependent on the duration of the step. We rounded these durations into 8-hour blocks, up to 72 hours. For example, a step of 36 hours would have available steps generated from the distribution of all step lengths and turn angles from steps with durations of 32–40 hours. We used these time difference-specific distributions to generate available steps for each used step that were realistically accessible given observed step lengths and turn angles from steps with similar time differences. We simulated 50 available steps for each used step using the *amt* package in R (Signer et al. 2019, R Core Team 2024). We chose 50 available steps to ensure that infrequent, long steps were reflected in our delineation of availability, while keeping the number of steps low enough to be computationally tractable (Thurfjell et al. 2014). We removed any available steps which intersected open water, as these could not plausibly be used by a non-flying woodcock.

### 3.2.4 Extracting habitat covariates

We classified habitat characteristics using broad-scale covariates reflecting land cover composition and configuration. We used a 2020 landcover layer at continental-scale and 30m resolution produced by the North American Land Change Monitoring System (NALCMS; Brown et al. 2020), which provides 19 land cover classes specific to tropical, temperate, sub-polar, or polar biomes. To ensure land cover classes were comparable among seasons, relevant to woodcock biology, and represented within our dataset, we aggregated classes into 8 categories: needleleaf forest, broadleaf forest, mixed forest, shrubland, grassland, wetland, cropland, and urban. We used this reclassified layer to calculate percent composition within buffers around the endpoint of each step, which were defined by radii of varying distances (50m, 100 m, 200 m, 500 m, and 1 km) chosen for their relevance to woodcock habitat selection during the post-migratory breeding and migratory seasons (Chapter 1). We calculated all landscape metrics in R using general functionality provided by the sf and terra

packages, as well as the landscape composition functions provided by the landscapemetrics package (Pebesma 2018, Hesselbarth et al. 2019, Hijmans 2023).

We calculated landscape configuration metrics to determine how woodcock would select for differing levels of forest edge habitat and connectivity. For use in this analysis, we reclassified the NALCMS layer into two categories: forest and non-forest. We cropped this raster to only include those cells which fell within a buffer around the endpoint of each step, using the same radii as we did for the landcover composition analysis. We then calculated edge density (representing the total length of forest/non-forest edges) and cohesion (representing the connectivity between forest patches) around each buffered point using the landscapemetrics package in R (Hesselbarth et al. 2019).

### *3.2.5 Scale of habitat selection*

#### *3.2.5.1 Model design and implementation*

To examine questions of variation in scale among seasons and age-sex classes and ensure that the most relevant scale was included in subsequent habitat analyses, we used a Bayesian latent indicator scale selection (BLISS; Stuber et al. 2017) analysis to examine comparative support for several scales of habitat selection. BLISS offers a computationally efficient method of scale optimization while reflecting uncertainty in estimation and can be implemented using a conditional logistic regression framework similar to a resource selection function (Manly et al. 2007), with a latent indicator selecting the scale at which a covariate is most appropriately measured. The model is structured as

#### **Equation 3.1**

$$\Pr(S_z = y) = p_{y,z} / \sum_{y=1}^{51} p_{y,z}$$

#### **Equation 3.2**

$$p_{y,z} = \exp(\alpha + \beta * X_{y,z,v})$$

where Equation 3.1 illustrates the matched case-control portion of the conditional logistic model and Equation 3.2 describes the regression equation.  $\mathbf{S}$  is the binomial case status (0 or 1) of the used or available step and  $\mathbf{p}$  is the likelihood of using step index  $\mathbf{y}$  within strata  $\mathbf{z}$ , with strata representing one used step and 50 available steps generated from the same starting location.  $\alpha$  is the intercept value,  $\beta$  is the covariate slope, and  $\mathbf{X}$  is the covariate value at used or available step  $\mathbf{y}$  within strata  $\mathbf{z}$ , assuming scale of selection  $v$ . When estimated in a Bayesian framework using Markov Chain Monte Carlo (MCMC), BLISS will estimate not just the  $\alpha$  and  $\beta$  values, but also the latent indicator  $v$ , which is expressed as a categorical variable with a uniform prior. The scale of selection which received the most support in the posterior of  $v$  was designated the best supported scale and used to measure each covariate for subsequent habitat analyses. The full posterior of  $v$ , including scales besides the best supported scale, was used to analyze how habitat selection varied by season and age-sex class.

We implemented our BLISS models in the Bayesian MCMC program JAGS (Plummer 2003), testing scales of selection for each covariate and season individually. We used uninformative normal priors (mean = 0, variance = 1000) for  $\alpha$  and  $\beta$  values, and a uniform categorical prior for  $v$ , with possible values representing 50m, 100 m, 200 m, 500 m, and 1 km scales of selection. We conducted scale optimization for the full dataset and for each age-sex class individually. We used age-sex specific scale optimization in any models exploring differences in selection among age or sex classes, and otherwise used optimization based on the full dataset. One covariate in the age-sex models (grassland for juvenile males in the post-migratory breeding season) did not converge and was thus removed from further analyses.

### *3.2.5.2 Synthesizing scale optimization results*

We summarized the posterior of  $v$  by season (using the full models) and age-sex class (using the age-sex models) to evaluate our hypotheses that the scale of habitat selection would vary by season, age,

and sex. This produced estimates of the proportional importance of selection at each scale in that season and age-sex class, respectively. We also examined the unmodified posteriors of the full BLISS models to evaluate how selection for specific covariates changed between seasons.

### 3.2.6 Habitat selection

#### 3.2.6.1 Model design and implementation

Our step selection models used the most likely scales of selection for each covariate, determined using BLISS, to estimate habitat selection coefficients and individual variation in habitat selection. We used a conditional logistic regression (Equation 3.1), and modified Equation 3.2 as follows

**Equation 3.3**

$$p_{y,z} = \exp(\alpha + \sum_{i=1}^n \gamma_i + \sum_{T=1}^m \sum_{i=1}^n (\beta_T + \delta_{T,i}) * X_{T,y,z,v})$$

which allows inclusion of multiple covariates and incorporates individually-varying intercepts ( $\gamma$ ) and slopes ( $\delta$ ). In addition to the variable definitions in Equations 3.1 and 3.2,  $i$  represents the index of an individual woodcock with levels  $n$ , and  $T$  represents the index of a covariate with levels  $m$ . Unlike Equation 3.2,  $v$  is treated here as a known variable based on the most likely scale for each covariate. We set  $\gamma$  and each value of  $\delta_T$  to a mean of zero while sharing variance among individuals, which is equivalent to setting these variables as random intercepts and slopes in a frequentist framework. We used uninformative normal priors (mean = 0, variance = 1000) for all  $\alpha$  and  $\beta$  variables, and uninformative half-normal priors (mean = 0, variance = 1000) for the variance of  $\gamma$  and  $\delta$  variables.

We ran separate models for each age-sex class to explored differences in selection between males and females as well as adult and juvenile woodcock. We further explored spatial variation in selection by running different models for each BCR, but in this case we aggregated age-sex classes

because we lacked sufficient replication within each BCR. We removed a covariate from two age-sex models due to convergence issues (grassland for adult males in fall migration, and shrubland for juvenile males in the post-migratory breeding season). For the BCR models, we only included season/BCR combinations which had >20 steps and >5 individuals (37 of 60 season/BCR combinations), due to issues in model convergence below that sample size. We removed all covariates from BCR models in which the covariate was observed less than 5 times due to issues in estimation below this sample size (19 covariates removed), and an additional 26 covariates due to convergence issues. This resulted in removal of 45 of 370 covariate-season-BCR combinations from consideration in the BCR model suite.

#### *3.2.6.2 Evaluating habitat selection and individual variability*

We evaluated general trends in habitat selection using  $\beta$  coefficients, for which we calculated 95% credible intervals using the built-in functionality in the R package jagsUI (Kellner 2015). We evaluated individual variability in habitat selection by summarizing the variance of  $\delta$  across several levels. We summed the posteriors of the variance of  $\delta$  by covariate, season, and age-sex class using the age-sex suite of habitat selection models and summed the posteriors of the variance of  $\delta$  by BCR using the BCR suite of habitat selection models. The resulting summed  $\delta$  metric represents the degree of individual variation in selection, indicative of the importance of individual heterogeneity for driving habitat relationships during that season. We used these summaries to test hypotheses regarding how individual variation in habitat selection might differ by season, age-sex class, or BCR.

### **3.3 Results**

#### *3.3.1 Scale of habitat selection*

We deployed GPS transmitters on 572 woodcock, with 530 of these woodcock providing enough data to delineate seasonal movements (Chapter 2). This yielded 1,015,886 GPS locations for analysis of woodcock habitat relationships. Woodcock selected habitat at smaller scales (50 and 100m; 69% of samples) during migration than during non-migratory seasons (Fig. 3.2; 30% of samples). This effect seemed to be driven primarily by three covariates, cropland, edge density, and cohesion, all of which were selected for at a smaller scale during migration than during other parts of the year (Fig. 3.3). However, there was little variation among age-sex classes in the scale of habitat selection (Fig. 3.4), and no consistent pattern in scale of selection among individual covariates, such as wetland and forest with best supported scales varying among seasons. Selection for wetland occurs at larger scales in post-breeding and wintering and smaller scales in other seasons (Fig. 3.3). Selection for forest covariates occurred primarily at smaller scales for needleleaf and broadleaf forests, and at larger scales for mixed forest. Selection for urban areas occurred at small scales in all seasons but post-migratory breeding and post-breeding, in which there was support for moderate scales.

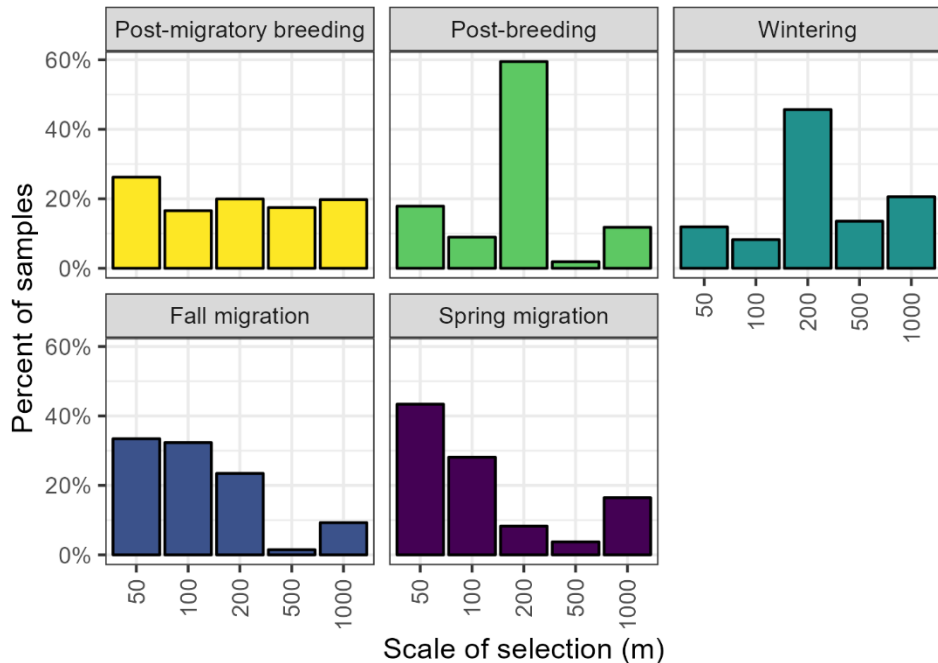


Figure 3.2. Scales at which American Woodcock (*Scolopax minor*) selected habitat covariates throughout their full annual cycle, derived from GPS locations collected throughout eastern North America. Scales of selection are summed across covariates to display seasonal relationships. Percent of samples represents the probability of support for a given scale of selection in comparison to tested alternatives. Estimates are derived from the base suite of BLISS models (Stuber et al. 2017).

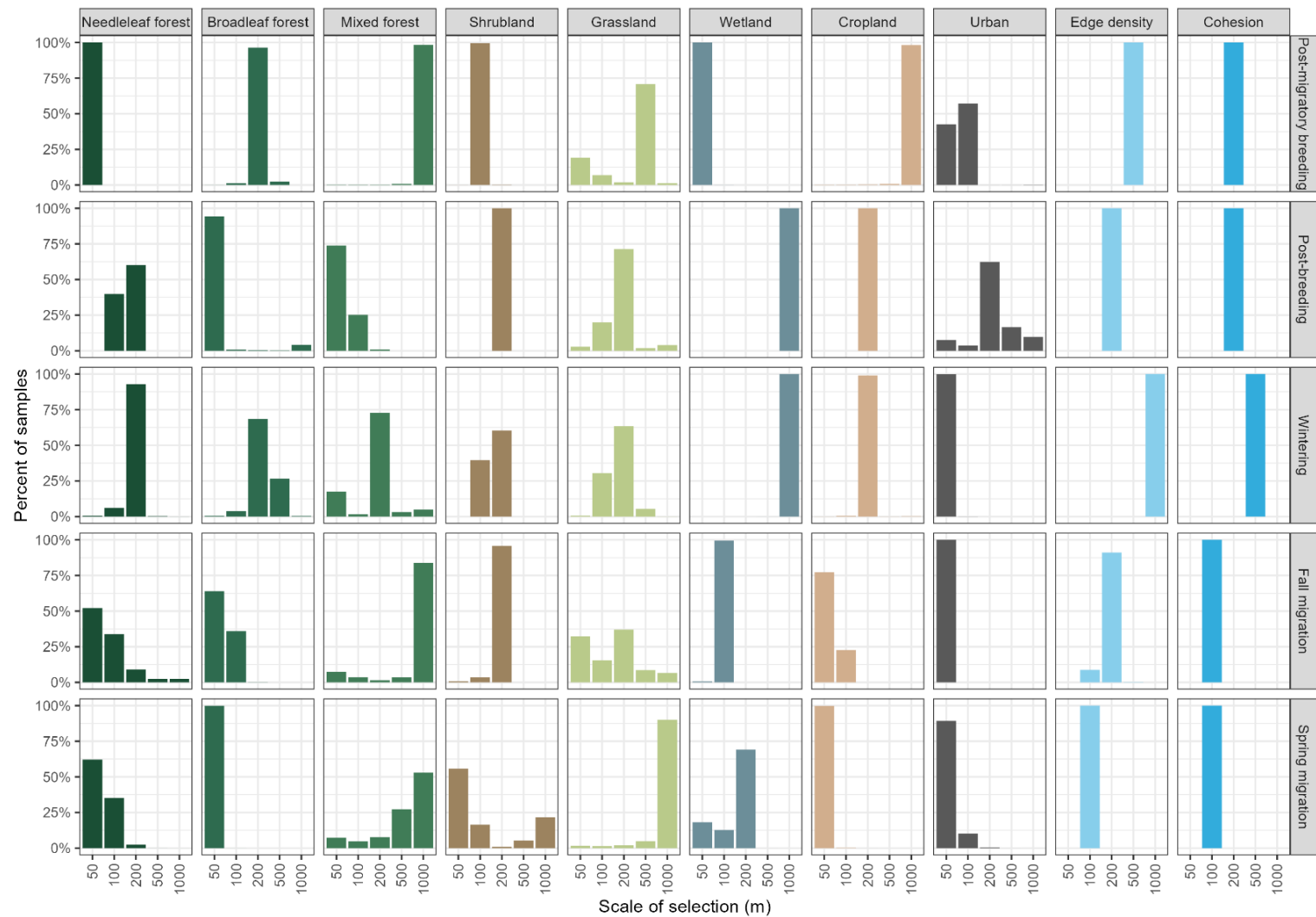


Figure 3.3. Scales of American Woodcock (*Scolopax minor*) habitat selection among seasons and habitat covariates, derived from GPS locations collected throughout eastern North America. Percent of samples represents the probability of support for a given scale of selection in comparison to tested alternatives. Estimates are derived from the base suite of BLISS models (Stuber et al. 2017).

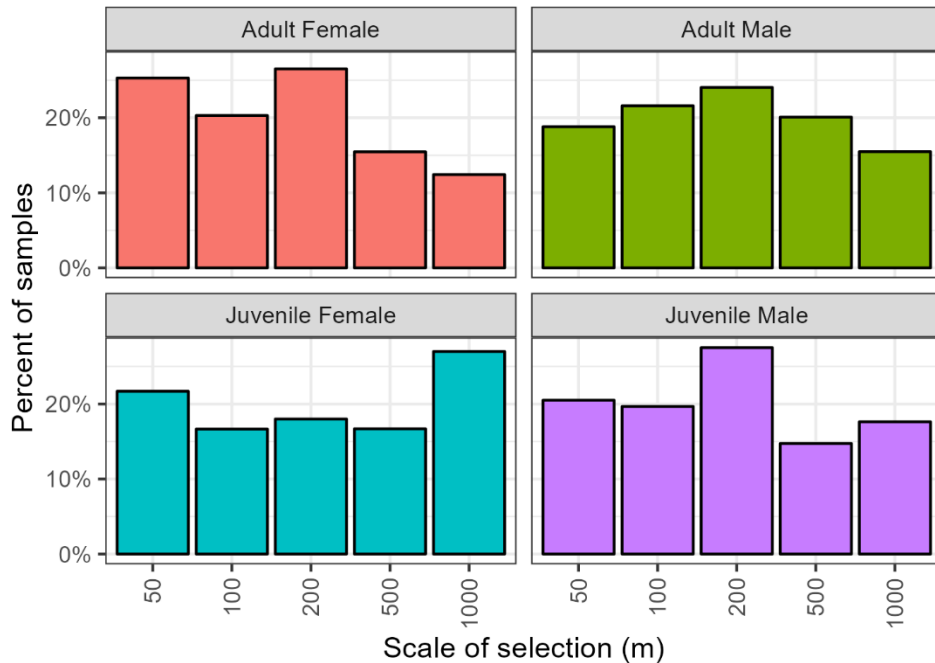


Figure 3.4. Scales at which American Woodcock (*Scolopax minor*) select habitat covariates among age-sex classes, derived from GPS locations collected throughout eastern North America. Chosen scales of selection are summed across covariates and seasons to display relationships among age-sex classes. Percent of samples represents the probability of support for each scale of selection. Estimates are derived from the age-sex suite of BLISS models (Stuber et al. 2017).

### *3.3.2 Habitat selection coefficients*

Across all model suites, woodcock generally selected for wetland and edge density and against needleleaf forest, cohesion, and urban (Fig. 3.5). Selection for habitat covariates generally did not vary extensively by age-sex class, with a few exceptions. Juvenile males selected for needleleaf forest during the wintering season, in contrast with other age-sex classes and their habitat use during other seasons. Females and males differed in their selection for broadleaf forest during the post-migratory breeding season, with females selecting for the covariate and males selecting against it. There was substantially more intra-season variation in habitat selection among BCRs than among age-sex classes (Figs. 3.5 & 3.6). This frequently resulted in contrasting coefficient relationships among BCRs. During the post-breeding season, for example, woodcock selected for wetlands in BCRs 13, 14, 28, and 30 and against wetland in BCRs 8 and 12. During the wintering season, woodcock selected for edge density in BCRs 25 and 27–31 and against edge density in BCR 26.

Three covariates (needleleaf forest, wetland, and urban) displayed differences in the intensity of their habitat selection during the post-migratory breeding and post-breeding seasons compared to other seasons (Fig. 3.7). This relationship was clearest for needleleaf forest, with woodcock selecting against needleleaf forest more strongly during post-migratory breeding and post-breeding than during other seasons. Woodcock selected for wetland more strongly during post-breeding than during post-migratory breeding or other seasons. While there was less of a difference in selection for urban areas, woodcock generally selected against urban areas more strongly during post-migratory breeding and post-breeding than during other seasons.

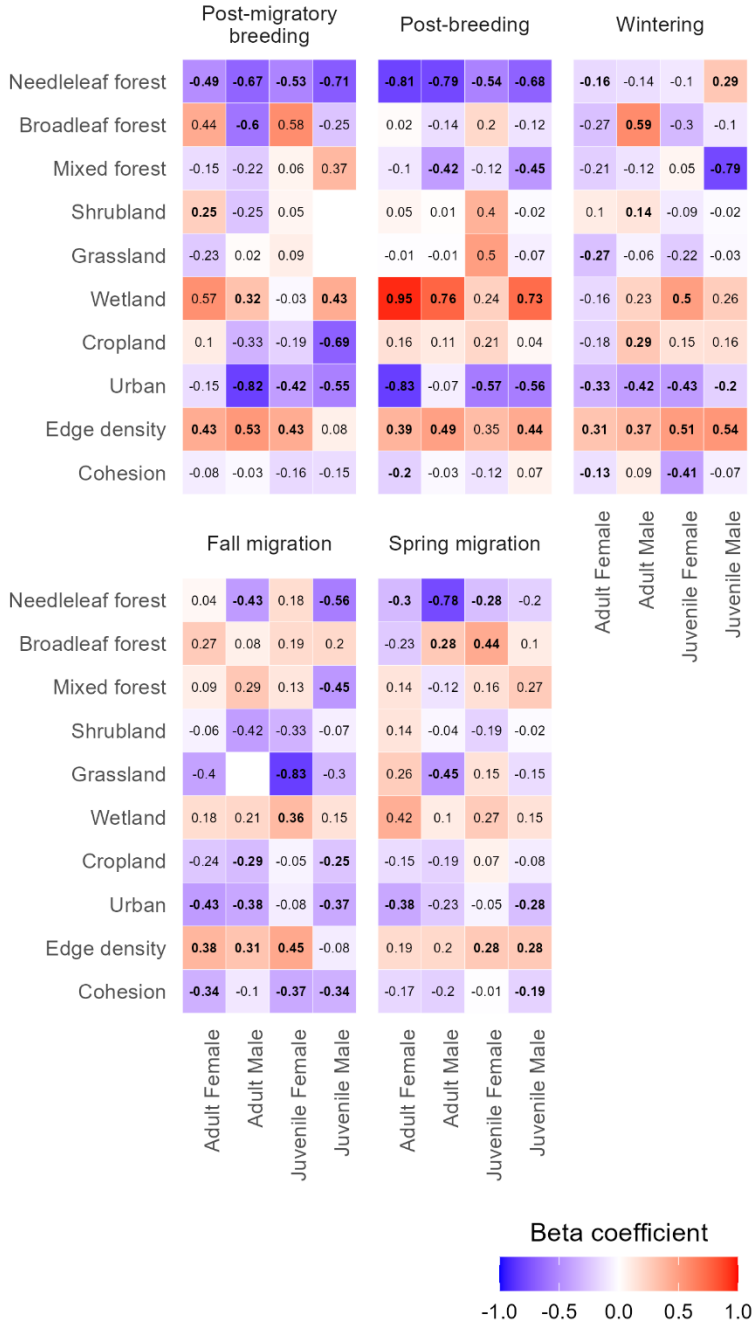


Figure 3.5. Mean habitat selection coefficients for covariates from the age-sex suite of habitat selection models. Numbers in bold indicate coefficients for which the 95% credible interval did not overlap with zero. Empty boxes indicate that the covariate was not included in the model due to convergence issues.

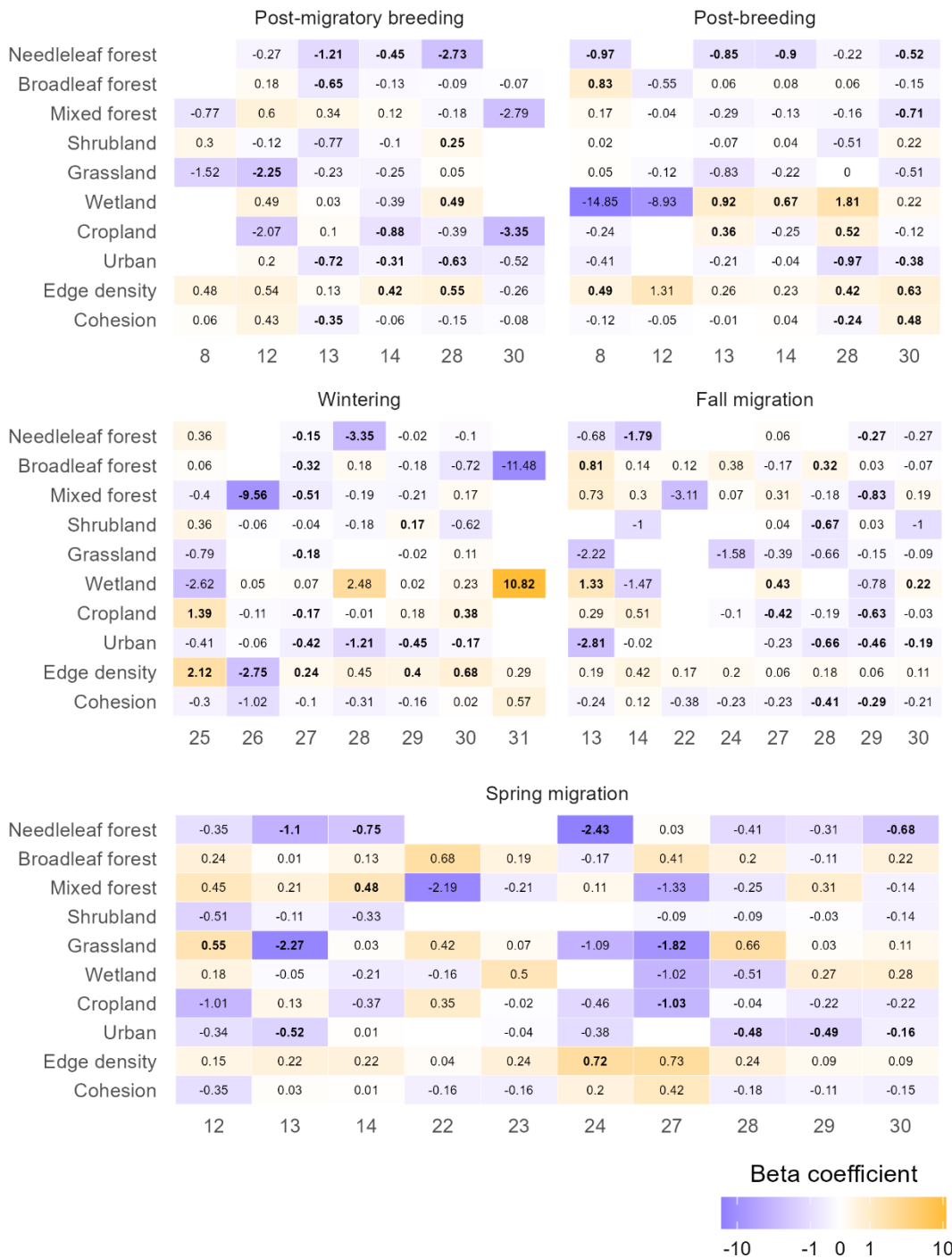


Figure 3.6. Mean habitat selection coefficients for covariates from the Bird Conservation Region (BCR) suite of habitat selection models. Numbers in bold indicate coefficients for which the 95% credible interval did not overlap with zero. Empty boxes indicate that the covariate was not included in the model due to low sample size or convergence issues.

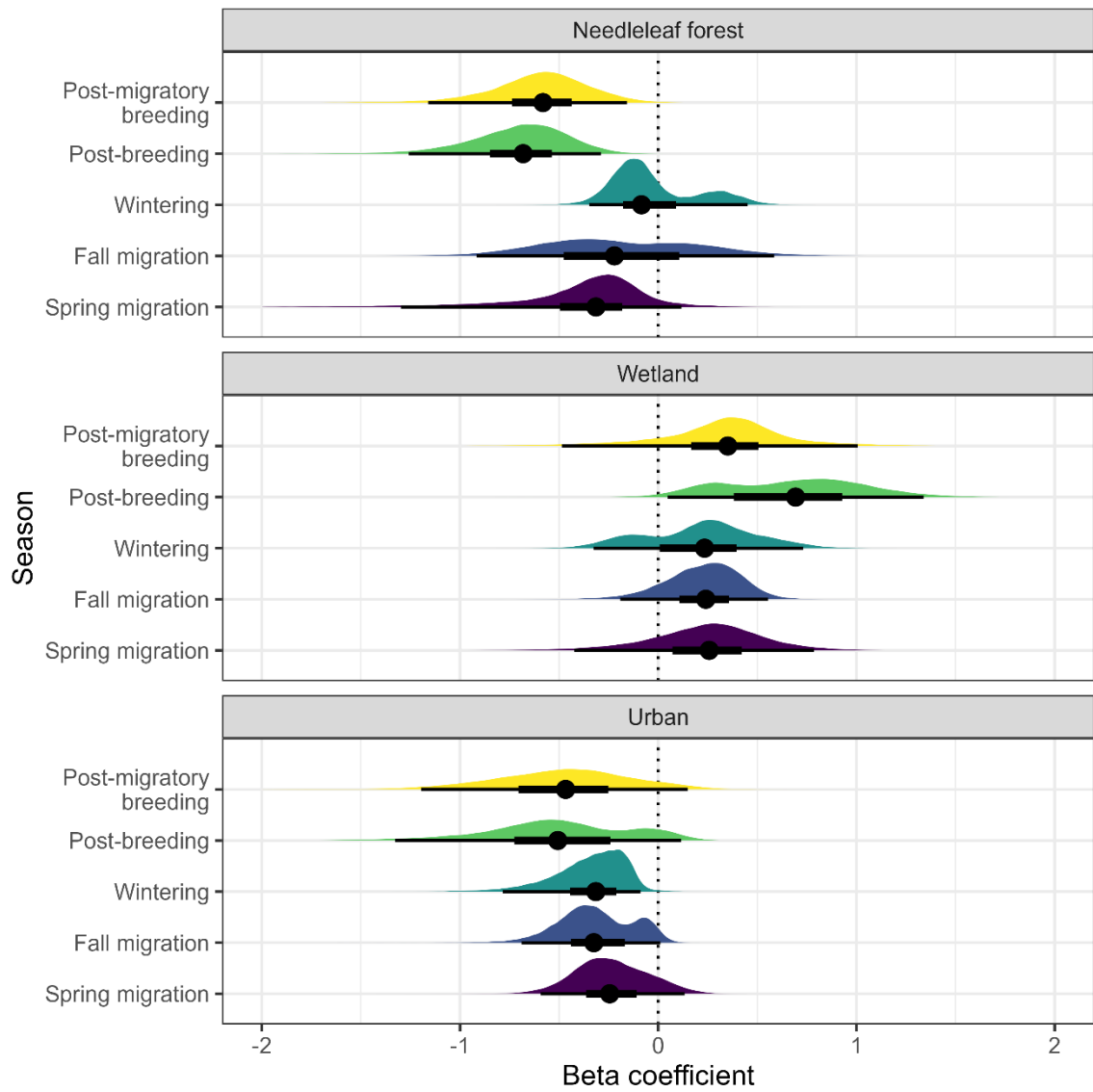


Figure 3.7. Selection preferences of American Woodcock (*Scolopax minor*) for needleleaf forests, wetland, and urban areas among seasons, derived from GPS locations collected throughout eastern North America. Beta coefficients are drawn from the age-sex suite of habitat selection models. Points represent median coefficient values, thick lines represent 50% credible intervals, and thin lines represent 95% credible intervals. Curves illustrate the distributions of the posterior samples.

### *3.3.3 Individual variation in habitat selection*

We found that individual random effects generally did not vary by covariate, season, and age-sex class (Fig. 3.8). One BCR (31, Peninsular Florida), which contained elements of both coastal plain and sub-tropical biomes (NABCI 2021), displayed more individual variation than other BCRs. Otherwise, individual variation was relatively uniform among BCRs.

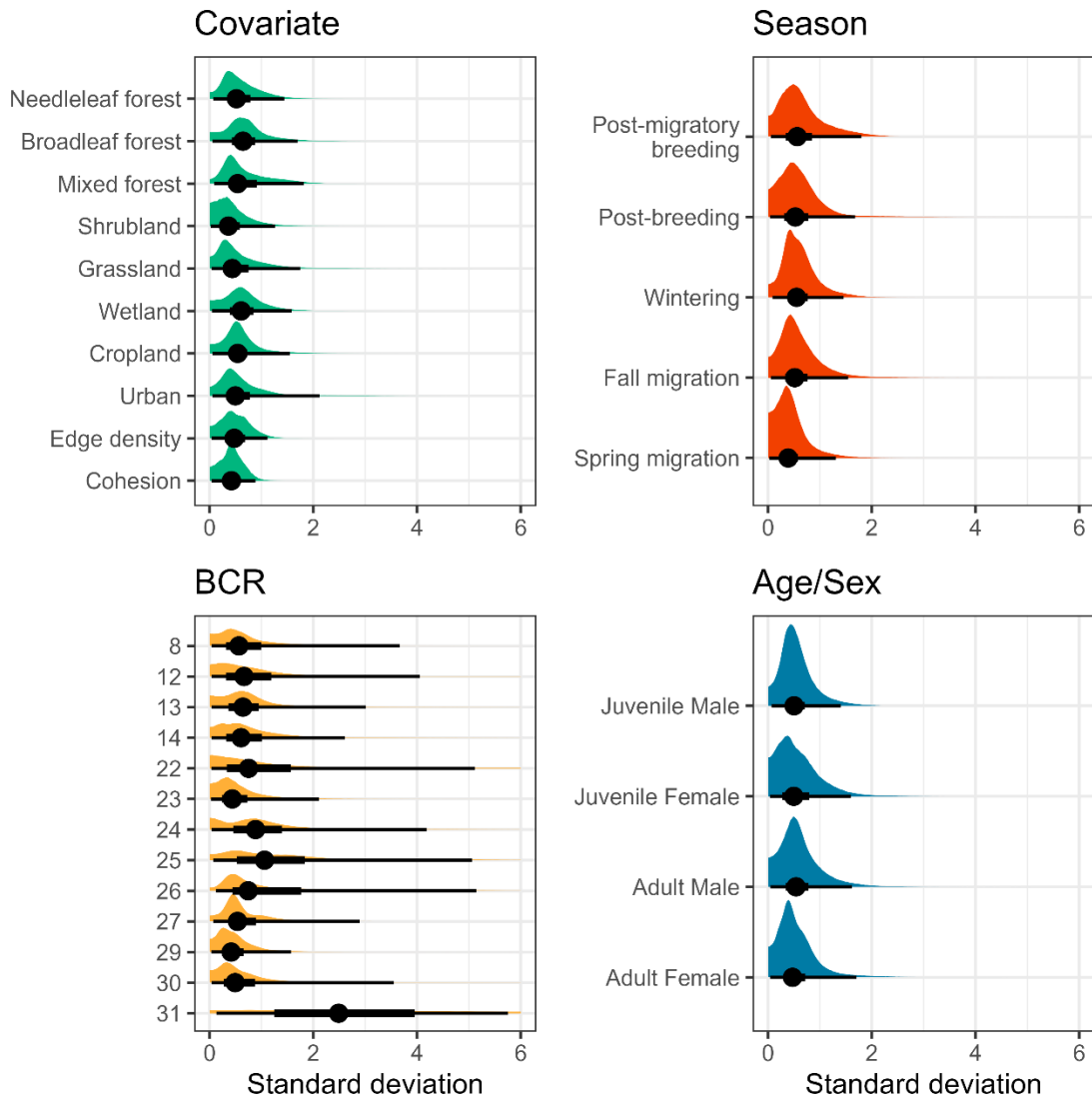


Figure 3.8. Individual variation in habitat selection (standard deviation of  $\delta$  in Equation 3.2), summed by covariate, season, Bird Conservation Region (BCR), and age-sex class. Points represent median coefficient values, thick lines represent 50% credible intervals, and thin lines represent 95% credible intervals. Curves illustrate the distributions of the posterior samples.

### **3.4 Discussion**

We found that variation in woodcock habitat use among seasons reflected less pronounced habitat selection outside of the post-migratory breeding and post-breeding seasons, while the strength of habitat selection often varied or even contrasted among BCRs. Differing habitat selection among seasons or regions could be due to several ecological factors. Niche partitioning may lead to differing habitat use in regions where interspecific competitors are present (Jablonski et al. 2020), although woodcocks' fairly stable and unique niche as an earthworm forager in early successional habitat (McAuley et al. 2020) makes this hypothesis less likely in this circumstance. Another potential factor could be ecological differences in cover types among regions and seasons, either due to resources, predators, or the configuration of habitat. For example, needleleaf forests are hypothesized to be more amenable to woodcock occupancy in the wintering range than the breeding range due to increased earthworm densities, which would explain their decreased avoidance of this cover type outside of the breeding range (Kelley et al. 2008). Another factor might be differences in biological requirements between seasons, with birds maintaining more strict resource requirements during the breeding season than they do during other portions of the year. Many birds require high protein diets to raise their young (Johnston 1993), and additional breeding season requirements might include avoidance of nest or brood predation (Fontaine and Martin 2006) and presence of conspecifics to facilitate mate choice (Ward 1987). The final potential factor that might explain differing habitat selection among seasons and regions is a functional response to habitat availability. Woodcock experience gradients in habitat availability throughout their range, with cover types such as needleleaf forest being more abundant in the breeding range than the wintering range (Brown et al. 2020). Shifts in the strength of selection for these cover types may be due in part to their prevalence on the landscape. In circumstances where a preferred cover type is less available (e.g. lower wetland availability in the wintering range), woodcock may shift their habitat selection to a more abundant cover type which

provides adequate resources and is easier to find on the landscape. Similarly, avoidance of cover types such as needleleaf forest may be less influential in the wintering range simply because it is less prominent on the landscape.

Typically, three hypotheses (reproductive roles, competitive exclusion, and niche divergence; Phillips et al. 2004, Orgeret et al. 2021) are used to explain potential differences in habitat selection by age-sex class. We found some support for the reproductive roles hypothesis, as woodcock females, but not males, selected for broadleaf forest during the post-migratory breeding season. Broadleaf forest is noted to be important for woodcock reproduction, particularly nesting and brooding, while needleleaf forest is avoided due to a lack of earthworm abundance (Kelley et al. 2008). The competitive exclusion hypothesis found less support in our data, with only one age-sex class that might presumably be forced into substandard habitat (juvenile males in needleleaf forest). However, this pattern only held during winter, when woodcock are generally more flexible with their habitat selection, and did not carry through the rest of the year. The niche divergence hypothesis also found little support in our data, with no clear differences in male and female habitat use throughout the year at the scales we examined. This may be due in part to the similar morphology of males and females; males are slightly smaller (92% of female mass) and have shorter bills than females (89% of female bill length; Keppie and Redmond 1988), but otherwise there are few morphological differences that might cause niches to differ by sex.

Although woodcock maintain similar habitat relationships throughout the year, these relationships are often scale-specific. The scale at which woodcock select habitat varies seasonally, with woodcock primarily selecting habitat at smaller scales (50–100m) during migration and larger scales (200–1000m) throughout the rest of the year. This has similarities to the selection behavior of Wood Thrush (*Hylocichla mustelina*), which select habitat at larger scales only during the breeding season (Stanley et al. 2021). The reasons for this difference in scale of selection among seasons may

come down largely to the mechanisms used to select stopover, breeding, and wintering habitat.

Selection of stopover habitat is a function of a bird's ability to detect habitat after a migratory flight, which, in the case of a nocturnal migrant such as a woodcock, may also occur during a portion of the day in which light is restricted (Chernetsov 2006). Selection of a breeding or wintering site, however, occurs over a much longer period, during which a bird might examine several potential sites before settling into a home range. Having more time to explore an area may result in birds considering habitat characteristics at larger spatial scales during their selection of breeding or wintering home ranges. In comparison to season, there was little variation in the scale of habitat selection by age-sex class, matching observations of minimal sex-based scale variation in other taxa during reproductive periods (Oehlers et al. 2011). While females have different reproductive needs than males during breeding, scale of selection seems to be unimportant for selecting habitat that meets those needs.

Unlike habitat selection coefficients, we found that the extent of individual variation in habitat selection generally did not vary by covariate, season, age-sex class, and region. This lack of structured individual variation in habitat selection matches the lack of structure in woodcock migratory strategies, for which individual variation was not well explained by age-sex class or region (Clements et al. 2024). Other taxa have demonstrated more of a tendency for individual variation to shift based on differing foraging strategies in different sexes or seasons (Baert et al. 2021). One reason for the lack of patterns in individual variation for this species might be its specialist ecological role, particularly regarding diet. Individual variation in other species have been driven largely by foraging preferences (Newsome et al. 2015, Baert et al. 2021), while woodcock are restricted to a diet of primarily earthworms in a limited number of habitat types (Miller and Causey 1985). This might cause most variation in habitat selection for this species to emerge at a population rather than an individual level, due to differing resource requirements or habitat availability between seasons or regions.

Despite woodcocks' atypical role as an early successional habitat and earthworm specialist with an itinerant breeding system (McAuley et al. 2020, Slezak et al. 2024a), we found that several patterns observed in other forest-dwelling birds also hold true for this species. Like the Wood Thrush, woodcock seem to select at smaller scales during the migratory season than the breeding season and hold stronger relationships with habitat covariates during the breeding season (Stanley et al. 2021). Woodcock also exhibit changes in their habitat selection throughout the year, in response to differing seasons and regions. We believe that this shift is due in part to a functional response to habitat availability, a pattern which likely holds true for other migratory birds. Further research, focusing on the role of ecological differences between these cover types versus changes in availability between regions, may allow us to better understand the extent to which functional responses drive shifts in habitat selection throughout the full annual cycle.

## **CHAPTER 4: LOW MIGRATORY FLIGHT ALTITUDES EXPLAIN INCREASED COLLISION RISK FOR AMERICAN WOODCOCK**

Understanding bird migration at low altitudes is critical to evaluating risk of collision with obstacles; however, quantifying flight at low altitudes is often complicated by difficulty measuring low altitude flight using weather radar, and the tendency of some species to fly at lower altitudes than others. Studies using transmitters and dataloggers can quantify use of low altitudes by nocturnal migrants, allowing species-level inference into potential collision risk based on use of risky altitudes. The American Woodcock (*Scolopax minor*) has long been considered a low altitude migrant due to its frequent collisions with buildings, and mortality during migration may be contributing to population declines. We investigated migratory flight altitudes using satellite transmitters deployed on woodcock in 2020–2024 and examined how flight altitudes compare to the heights of common airspace obstacles. Transmitters recorded nocturnal GPS locations with altitude readings at 1200–0100 hours Eastern Time during fall and spring migrations. We implemented a model using Bayesian Markov Chain Monte Carlo to identify whether locations were recorded on the ground or during flight and describe the distribution of flight altitudes. We found that woodcock fly at mean altitudes of 364m (95% credible interval: 300–432m), flying higher during spring (428m, 95% CRI: 326–539m) than fall (312m, 95% CRI: 239–398m). Mean flight altitudes were slightly higher for adults (400m, 95% CRI: 301–516m) than juveniles (344m, 95% CRI: 270–430m). Woodcock flight altitudes were frequently lower than could be observed using weather radar (33% of observations), and 47% of observations fell within the altitude range of at least one airspace obstacle. Our results suggest that woodcock fly at altitudes lower than reported for most nocturnal avian migrants, which likely contributes to their vulnerability to obstacle collisions. Further study on low altitude flights, especially among species known for disproportionate collisions with obstacles, may allow us to better

understand the circumstances that result in obstacle collisions and can inform mitigation strategies to reduce bird mortality.

#### **4.1 Introduction**

Avian migratory flights can be studied using a wide range of techniques, including GPS and satellite telemetry, altimeters, imaging, and radar (Thaxter et al. 2016). These tools can be used to describe the altitudinal distributions of nocturnal avian migrants and examine how those altitudes shift in response to wind, weather, and artificial light during migration (Bauer et al. 2019). Research has focused on how these factors influence the risk of bird collision with obstacles (Lao et al. 2020), although there are still knowledge gaps regarding low altitude flights which put birds within range of airspace obstacles (<200m above ground level, hereinafter AGL). Obstacles present at these altitudes include buildings (365–988 million bird collisions per year, Loss et al. 2014), wind turbines (234 thousand bird collisions per year, Loss et al. 2013), and communication towers (4–5 million bird collisions per year, Gehring et al. 2011). Flights at obstacle height can be difficult to study due to blind spots in weather radar at low altitudes (Rogers et al. 2020), although some radar studies have had success in quantifying their prevalence. Cohen et al. (2022) estimated that 35% of birds migrating along the Great Lakes shorelines passed through the rotor sweep of a wind turbine at some point during their migratory flight, and White et al. (2020) found that migrating bird densities remained highest below 400m, even during peak migratory periods. Despite the utility of these studies, radar is generally limited to making inferences about overall patterns in bird migration and cannot provide insights into susceptibility to obstacle collisions at a species level. Species level insight is particularly important as not all birds are equally susceptible to obstacle collisions; Nichols et al. (2018) has identified 13 species and 7 genera as “supercolliders”, or birds which are found more often after obstacle collisions than expected given their population size. Gathering species-level data regarding use of low altitudes,

at which building collisions occur, is therefore important for understanding and mitigating these collisions.

Gaining species-level insight into bird flight altitudes requires the use of bird-borne telemetry equipment, usually either altimeters or satellite GPS transmitters (Thaxter et al. 2016). Transmitters come with their own set of drawbacks; they are frequently expensive to deploy, collect far less data than other techniques, and are usually limited to birds above a specific size. However, telemetry equipment can be used to make inferences about species-specific flight altitudes, including both high and low altitudes, and in the case of GPS transmitters, can often do so with a very high level of precision. Several studies have described low altitude flights using GPS transmitters, including Bowlin et al. (2015), which found that of 13 tracked Swainson's Thrush (*Catharus ustulatus*) migratory flights, one bird spent over an hour flying at altitudes <100m before rising to altitudes of 300–500m. A second thrush spent the entirety of its ~2 hour migratory flight at an altitude of ~40 m. Galtbalt et al. (2021) found that Whimbrel (*Numenius phaeopus*) and Far Eastern Curlew (*Numenius madagascariensis*) have overwater median flight altitudes of 132m and 156m above sea level, respectively, although those altitudes increase by 382m and 586m when flying over land. Further transmitter studies focusing specifically on birds with high susceptibility of collision to airspace obstacles may allow us to better understand the prevalence of low altitude flights among these species, and how those flights influence collision risk.

The American Woodcock (*Scolopax minor*, hereinafter woodcock) has long been thought to migrate at low altitudes. Even before tracking data were available, Mendall and Aldous (1943) estimated that woodcock migrate at altitudes 12–15m based on the high rate of woodcock collisions with power, telephone, and telegraph lines. Woodcock are among the most frequently found species due to building collisions in major US cities such as Minneapolis (Loss et al. 2019) and Chicago (Van Doren et al. 2021), and mass building collision events occurred when woodcock were caught in

snowstorms during their early spring migration (Loss et al. 2020). Woodcock morphology is believed to play a role in their susceptibility to building collisions; the species is comparatively rotund with shorter wings than many other nocturnal migrants, which may make woodcock less maneuverable during migratory flight (Loss et al. 2020). The comparative positioning of woodcock eyes further back on the head than most other birds provides greater peripheral vision but also substantially reduces their binocular vision, which may impede their ability to avoid airspace obstacles (Cobb 1959, Martin 1994). Woodcock have declined at a rate of 0.8% per year since surveys began in the 1960s, and migratory mortality has been identified as a potential causal factor (Cooper and Rau 2012, Loss et al. 2020). No studies to date have quantified woodcock flight altitudes, or examined how those altitudes might impact their vulnerability to collision with airspace obstacles.

Here we investigate the propensity for the American Woodcock to fly at low altitudes during migratory flights and examine how flight altitudes compare to the altitudinal distributions of common airspace obstacles. We also quantify the proportion of woodcock flight locations which fall below a threshold detectable by weather radar to provide some context for comparing our estimates to other studies. We hypothesized that woodcock flight altitudes would fall below mean estimates for nocturnal migrants (418–459m AGL; Horton et al. 2016) and would frequently fall within altitudinal ranges corresponding with obstacles such as buildings, air turbines, and communication towers, based on high rates of collisions for this species (Mendall and Aldous 1943, Loss et al. 2020). We also hypothesized that woodcock flight altitudes will be lower in fall than spring, in accordance with general trends in nocturnal migrants (Horton et al. 2016), and that flight altitudes will be similar among age and sex classes due to minimal differences in morphological characteristics among these classes (McAuley et al. 2020, Agostini et al. 2023). Our analysis sheds light on the vulnerability of woodcock and other nocturnal migrants to airspace collisions during their migratory flights, and the necessity for further study of low altitude movements of birds in general.

## 4.2 Methods

### 4.2.1 Data collection and preprocessing

We collected woodcock locations with altitude readings from 2020–2024 using GPS transmitters as a part of a larger collaborative effort by the Eastern Woodcock Migration Research Cooperative (Blomberg et al. 2023, Clements et al. 2024, Fish et al. 2024). We captured woodcock across the eastern portion of their range using spotlighting and mist nets (McAuley et al. 1993) and attached 4–7 g PinPoint transmitters with altimeters (Lotek Wireless Inc., Newmarket, Ontario, CA) using a rump-mounted leg loop harness (Fish et al. 2024). We aged and sexed birds upon capture, where juveniles were birds undertaking their first fall and spring migrations, after which they were considered adults. All capture and handling was conducted in accordance with protocols approved by the University of Maine Institutional Animal Care and Use Committee (Protocols A2017-05-02 and A2020-07-01) as well as permits from the USGS Bird Banding Laboratory and Canadian Bird Banding Office.

We programmed transmitters to collect locations every 1–3 days during migration, with locations alternating between diurnal (1300–1500 hours Eastern Time) and nocturnal (0000–0100 hours) locations. We subset these readings to include only locations in which birds had a known migratory or non-migratory state (Chp. 2). We used ArcGIS Pro 3.2.1 (ESRI 2024) to calculate the difference between the recorded altitude and orthometric elevation for each location (ESRI 2023b), providing a measurement of height above ground level for each point. To ensure computational tractability, we divided all observed altitudes by the maximum altitude in the dataset (2183m), allowing estimated flight altitudes to scale between 0 and 1. As woodcock are nocturnal migrants, we assumed all diurnal and non-migratory points were known ground locations, while the flight status of nocturnal migratory points was unknown.

#### 4.2.2 Modeling altitude distributions

Our model of woodcock flight altitudes included both potential flight locations and known ground locations, with each class of data informing a different aspect of the model. Known ground locations were assumed to always have a true altitude of 0m, making their recorded altitudes  $A_r$  solely attributable to measurement error  $E$  ( $A_r = E$ ; importance of accommodating for measurement error is reviewed in Poessel et al. 2018, Péron et al. 2020). As such, we used known ground locations to estimate the error terms of the model. Potential flight locations had either a true altitude of 0m, in which case  $A_r = E$ , or a flight altitude  $A_f$ , in which case  $A_r = A_f + E$ . Thus, potential flight locations could be used to estimate a latent flight state which we represented as binomial variable  $I$ , with  $I=0$  indicating a ground location and  $I=1$  indicating a flight location. We derived  $A_f$  from locations where  $I=1$ ,

**Equation 4.1**

$$A_r = I * A_f + E$$

$$E \sim Normal(\mu_{bias}, \sigma_{error})$$

$$A_f \sim Gamma(\alpha, \beta)$$

with  $I$  fixed to 0 for all known ground locations and as an estimable parameter for all potential flight locations. When  $I$  was not known, we provided an informed prior of  $p = 0.33$ , which we based on pre-existing knowledge of the ratio of stopovers to migratory flights during a typical woodcock migration (Fish et al. 2024). Measurement bias in the data,  $\mu_{bias}$ , was given an uninformative normal prior with mean 0 and standard deviation 1, while the standard deviation of the measurement error,  $\sigma_{error}$ , was given a half-normal prior with standard deviation 1. We modelled the distribution of  $A_f$  using a gamma distribution with shape parameter  $\alpha$  and rate parameter  $\beta$ . We gave  $\alpha$  and  $\beta$  semi-informative priors to restrict their possible values to those that might sensibly describe a distribution

scaled between 0 and 1 (McElreath 2018). After simulating possible distributions, we chose to give  $\alpha$  a half-normal prior with standard derivation 5 and  $\beta$  a half-normal prior with standard derivation 10.

Season and age models both received a similar formulation to the base model, with the only difference being the use of group-specific ( $g$ )  $\alpha$  and  $\beta$  parameters

**Equation 4.2**

$$A_{f,g} \sim \text{Gamma}(\alpha_g, \beta_g)$$

where the  $\alpha_g$  and  $\beta_g$  parameters were dependent on the season or age class associated with any given altitude observation. This model structure allowed the distribution of flight altitudes to be estimated for each season and age class separately, but with shared inference of error terms  $\mu_{bias}$  and  $\sigma_{error}$ .

We implemented these models using Bayesian Markov Chain Monte Carlo in program JAGS (Plummer 2003) running 4 chains at 200,000 iterations with 10,000 iterations burn-in and no sample thinning. We checked all models for convergence using trace plots and ensured that R-hat values were  $<1.1$ . A model with sex as the grouping variable did not converge, so we did not consider its results further. We ran models using the transformed height above ground level estimates for  $A_r$ , and back-transformed all parameter estimates into meters AGL for evaluation. We derived the posteriors of parameters describing flight altitude distributions by simulating a gamma distribution for each posterior value of  $\alpha$  and  $\beta$ , and sampling the mean, median, and standard deviation of each simulated distribution. We estimated the number of flight locations from the base, season, and age models by summing estimated  $I$  values. We summarized posteriors for all parameters using median values and highest density credible intervals following the guidelines outlined in Makowski et al. (2019). We also calculate the probability of superiority, or the likelihood of one group having a higher parameter value than another group, for age and sex models following Ruscio (2008).

#### 4.2.3 Comparison of flight altitudes to other metrics

We evaluated how often woodcock flight altitudes occurred in the altitude range typically detected by ground-based radar and how they coincided with height intervals associated with common airspace obstacles that pose collision risk. We compared woodcock flight altitudes to the minimum altitude (120m) detected by Horton et al. (2016) using the Next Generation Weather Radar (NEXRAD) system, a weather radar system in the United States frequently used to study bird migration (DeMott et al. 2022, Horton et al. 2023). We quantified the proportion of woodcock flight locations (represented by the posterior of  $\text{Gamma}(\alpha, \beta)$ ) which fell below a 120m threshold, which we used to represent the proportion of locations would not be detectable by weather radar. As low-rise buildings (defined as residential buildings 4–11 stories and non-residential buildings  $\leq$ 11 stories) result in the majority of window collision mortalities in the United States (Loss et al. 2014), we also quantified the proportion of locations at an altitude below that of an 11-story low-rise building (47m). We also estimated the proportion of woodcock flight locations which fell within the rotor sweep of the average land-based wind turbine installed in 2022 (32–164m; Wiser et al. 2023). Finally, we measured the proportion of woodcock flight locations which fell below the height of a 305m communication tower, as these towers are responsible for 5–70x as many collisions as shorter towers (Gehring et al. 2011).

### 4.3 Results

We collected 12,558 GPS locations with altitude recordings, of which 428 could potentially be flight locations based on time of day and migratory classification. The base model predicted that 144 of these locations were most likely recorded when the bird was in flight (95% CRI: 131–161). The season model identified 78 flight locations in the fall (95% CRI: 67–90) and 65 in the spring (95% CRI: 58–74), while the age model identified 58 flight locations among adults (95% CRI: 51–67) and

80 locations among juveniles (95% CRI: 71–93). Woodcock estimated median flight altitude was 262m, and mean flight altitude was 363m (Table 4.1). Woodcock flew at mean altitudes of 310m in fall and 427m in spring, with 96% probability that mean flight altitudes are higher in fall than spring (Fig. 4.1). Adult woodcock flew at mean altitudes of 397m while juveniles flew at altitudes of 343m, with 79% probability that mean flight altitudes are higher for adults than juveniles (Fig. 4.2).

Over half of woodcock flight locations were at altitudes <305m, posing potential risks for collisions with low-rise buildings, wind turbines, and communications towers (Table 4.2, Fig. 4.3). Woodcock were more likely to fly within range of obstacles in fall, with 5% more locations occurring at low-rise building altitude, 8% more at wind turbine altitude, and 14% more at communication tower altitude. 33% of woodcock locations were below the minimum flight altitude reported in Horton et al. (2016) and likely would not have been detectable using NEXRAD weather radar.

Table 4.1. Characteristics of American Woodcock (*Scolopax minor*) altitudes above ground level during migratory flights, measured using a base model (bold) as well as season and age models. Estimates indicate the median value of the posterior distribution, while credible intervals reflect highest density intervals.

Metric	Estimate	50% Credible Interval	95% Credible Interval
<b>Median Flight Altitude</b>	<b>262m</b>	<b>240–286m</b>	<b>194–331m</b>
<i>Fall</i>	224m	193–249m	145–308m
<i>Spring</i>	320m	283–356m	215–426m
<i>Adult</i>	294m	256–334m	181–403m
<i>Juvenile</i>	260m	229–287m	179–342m
<b>Mean Flight Altitude</b>	<b>363m</b>	<b>339–385m</b>	<b>299–430m</b>
<i>Fall</i>	310m	279–334m	235–393m
<i>Spring</i>	427m	392–463m	324–536m
<i>Adult</i>	397m	355–431m	295–509m
<i>Juvenile</i>	343m	313–367m	266–425m

Table 4.2. Proportion of American Woodcock (*Scolopax minor*) migratory flight altitudes within height intervals related to weather radar and airspace obstacles. Metrics are measured using a base model (bold) as well as season and age models. Estimates indicate the median value of the posterior distribution, while credible intervals reflect highest density intervals.

Metric	Estimate	50% Credible Interval	95% Credible Interval
<b>Below NEXRAD detection altitude (120m)<sup>1</sup></b>	<b>32%</b>	<b>29–36%</b>	<b>22–43%</b>
<i>Fall</i>	37%	32–42%	23–51%
<i>Spring</i>	26%	21–30%	13–40%
<i>Adult</i>	28%	22–33%	14–45%
<i>Juvenile</i>	31%	26–36%	18–45%
<b>Below height of low-rise buildings (47m)<sup>2</sup></b>	<b>10%</b>	<b>7–12%</b>	<b>4–18%</b>
<i>Fall</i>	12%	7–15%	3–23%
<i>Spring</i>	7%	3–8%	1–16%
<i>Adult</i>	8%	4–10%	1–20%
<i>Juvenile</i>	8%	4–10%	2–18%
<b>Within sweep of land-based wind turbines (32–164m)<sup>3</sup></b>	<b>27%</b>	<b>26–29%</b>	<b>22–32%</b>
<i>Fall</i>	31%	29–33%	23–37%
<i>Spring</i>	23%	20–26%	15–30%
<i>Adult</i>	25%	23–28%	16–32%
<i>Juvenile</i>	28%	26–31%	19–35%
<b>Below height of large communication towers (305m)<sup>4</sup></b>	<b>56%</b>	<b>53–59%</b>	<b>47–65%</b>
<i>Fall</i>	62%	58–66%	50–73%
<i>Spring</i>	48%	44–53%	35–62%
<i>Adult</i>	51%	46–56%	38–66%
<i>Juvenile</i>	57%	53–61%	45–68%

Table 4.2 Continued.

<sup>1</sup> Minimum NEXRAD detection height is based on the lowest altitude detected by Horton et al. (2016).

<sup>2</sup> Height of low-rise buildings is determined based on that of an 11-story building, based on Loss et al. (2014).

<sup>3</sup> Sweep of wind turbines is based on the average land-based turbine constructed in 2022 (Wiser et al. 2023).

<sup>4</sup> Height of large communication towers based on Gehring et al. (2011).

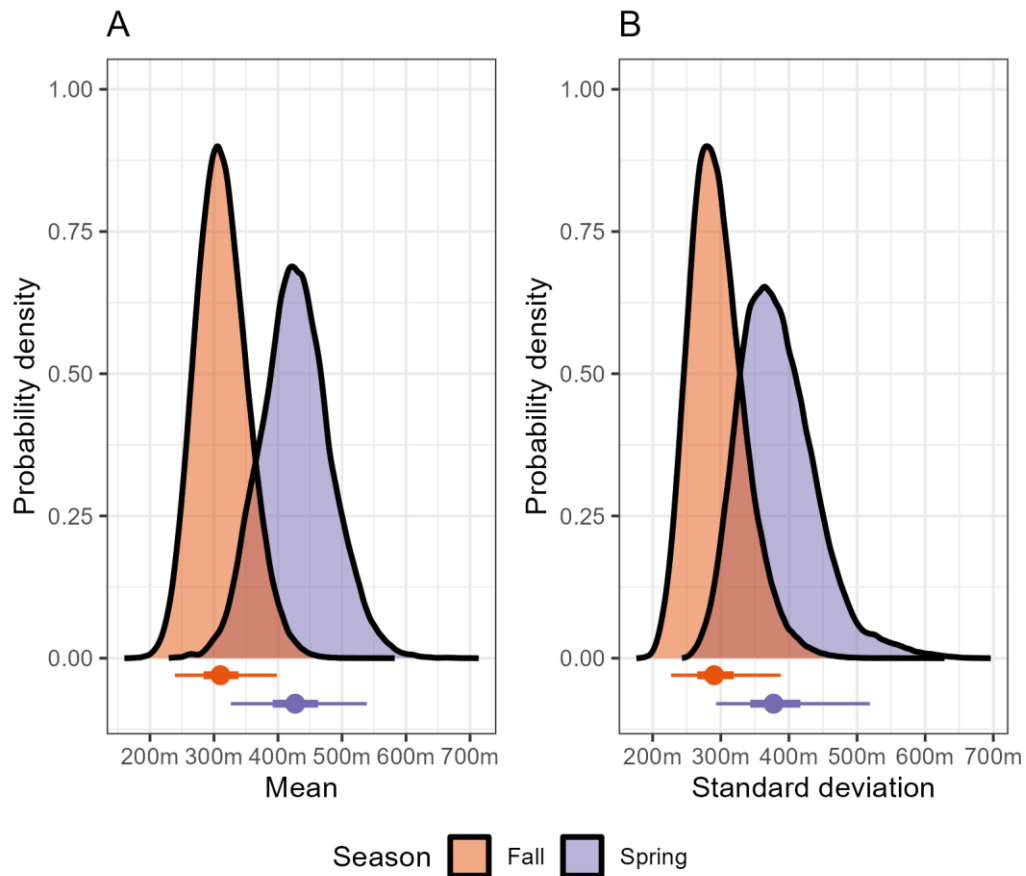


Figure 4.1. Means and standard deviations of American Woodcock (*Scolopax minor*) flight altitudes above ground level during fall and spring migration. Density plots represent posterior distributions of parameters, while point intervals represent the medians (points), 50% highest density credible intervals (thick lines), and 95% highest density credible intervals (thin lines) of the posteriors.

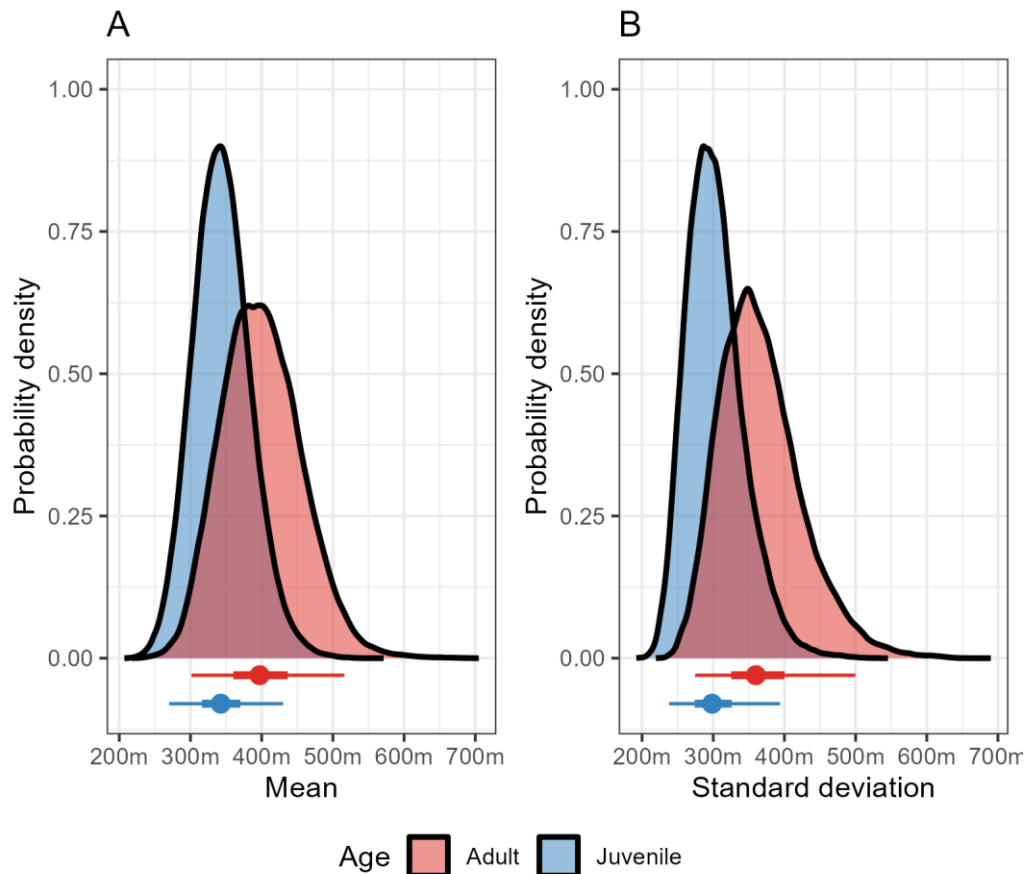


Figure 4.2. Means and standard deviations of American Woodcock (*Scolopax minor*) flight altitudes above ground level for adult and juvenile individuals. Density plots represent posterior distributions of parameters, while point intervals represent the medians (points), 50% highest density credible intervals (thick lines), and 95% highest density credible intervals (thin lines) of the posteriors.

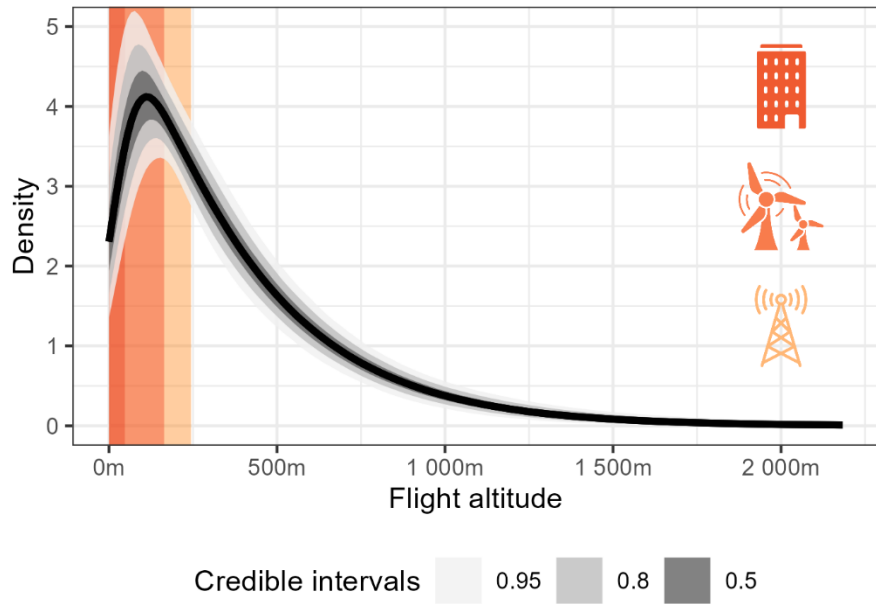


Figure 4.3. Distribution of woodcock flight altitudes above ground level compared to the heights of low-rise buildings (red; 47m), land-based wind turbines (orange; 32–164m), and large communications towers (yellow; 244m). The dark line represents the median flight altitude distribution calculated using the base model, while ribbons represent 50%, 80%, and 95% highest density credible intervals for the distribution.

#### 4.4 Discussion

We found that mean woodcock flight altitudes fell below those typical of most migrating birds during fall (woodcock: 310m; all birds: 418–491m) and spring (woodcock: 427m; all birds: 438–559m; Horton et al. 2016). This result may be due, in part, to the greater representation of lower altitude flight locations in our data, as 33% of woodcock flight locations fell below the minimum altitude normally observed via weather radar (120m; Horton et al. 2016). However, given preexisting information about woodcock's high susceptibility to collisions with anthropogenic structures (Mendall and Aldous 1943, Loss et al. 2020) we believe that some portion of this effect is due to a biological difference between the flight altitudes of woodcock and other nocturnal migrants.

Woodcock use of lower altitudes than other birds may be related to morphology, as they have a greater wing loading than 79% of species sampled by Poole (1938), and their wing loading appears to be considerably higher than other birds of comparable size. Birds with a higher wing loading than woodcock were generally non-migratory gamebirds or ducks, and the most similar species in terms of wing loading and mass is the non-migratory Rock Pigeon (*Columba livia*). As high wing loading is speculated to be associated with migratory inefficiency (Bowlin et al. 2015), woodcock may be inefficient fliers and choose lower altitudes as a result (Galtbalt et al. 2021).

As anticipated, we found little support for an age difference in woodcock flight altitudes but considerable support for a seasonal difference, with woodcock flight altitudes being higher during spring (mean: 427m, 95% CRI: 324–536m) than fall (mean: 310m, 95% CRI: 235–393m). This matches seasonal variation in flight altitudes observed via radar (Horton et al. 2016), presumably due to migrants utilizing southerly jet streams present at higher altitudes in the spring (La Sorte et al. 2014). As a result of these seasonal differences, woodcock are more likely to fly at altitudes like to intersect airspace obstacles during fall, with 5% more locations occurring at low-rise building altitude, 8% more at wind turbine altitude, and 14% more at communication tower altitude.

Woodcock collisions with buildings are generally observed during the spring rather than fall (Loss et al. 2019), which is interesting given that flight altitudes are generally higher during spring. This may be due to the short migratory durations of woodcock in the fall (Fish et al. 2024) or a mismatch between the data collection windows for bird collision studies and the fall migratory periods of woodcock (Loss et al. 2020).

Despite a mean flight altitude of 364m, we found that more than half of woodcock flight altitudes occurred below 305m. The occurrence of so many flight locations within the range of anthropogenic obstacles during peak times for migratory flight (12–1am Eastern Time) suggests that woodcock are not solely vulnerable to collision with these obstacles during takeoff and landing, but throughout their migratory flights. While all three types of structures examined here are responsible for substantial migratory bird mortality, collisions with these structures are likely caused by different mechanisms. Low-rise buildings, for example, are responsible for more collisions than any other structure examined in this study (est. 339 million per annum, Loss et al. 2014) despite having the lowest height (47m). The exceptional rate of mortality associated with low rise buildings is likely the joint function of their prevalence (est. 15.1 million low rise buildings in the United States, Loss et al. 2014) and a higher rate of mortality associated with birds undergoing stopovers, which can be lengthy and expose birds to mortality risk through the diurnal hours in addition to nocturnal migratory flights (Cusa et al. 2015). In comparison, communication towers kill fewer birds (4–5 million per annum) and are less prevalent on the landscape (>26 thousand in the United States) but are more likely to result in collisions during migratory flights, especially if guy lines are present (Gehring et al. 2011). Understanding these differing risk profiles is an important facet of interpreting the relative risk of low altitude flights and drawing connections between low altitude flights and increased rates of bird collisions.

It is unclear whether woodcock are the only species with such substantial use of low flight altitudes. Woodcock appear to fly at altitudes lower than most other nocturnal migrants, but many other bird species have disproportionate representation among bird collision victims, including White-throated Sparrows (*Zonotrichia albicollis*), Tennessee Warblers (*Leiothlypis peregrina*) and Mourning Doves (*Zenaida macroura*, Nichols et al. 2018). These species may benefit from further study on whether their increased vulnerability is also due to low migratory flight altitudes or other factors. Future work might also focus on individual variability in flight altitudes, which suggests that individual migratory strategies (e.g., short migratory flights) might increase the prevalence of low altitude flights (Bowlin et al. 2015). Further research on species- and individual-specific variation in flight altitudes may allow us to better understand how use of low altitudes impacts bird collision risk and devise strategies for its mitigation.

## BIBLIOGRAPHY

- Agafonkin, V. (2022). Leaflet.js. [Online.] Available at <https://leafletjs.com/>.
- Agostini, N., M. Gustin, M. Cento, J. Von Hardenberg, and G. Chiatante (2023). Differential Flight Strategies of Western Marsh Harrier *Circus aeruginosus* in Relation to Sex and Age Class during Spring Migration in the Central Mediterranean. *Acta Ornithologica* 58:41–53.
- Allen, B. B., D. G. McAuley, and E. J. Blomberg (2020). Migratory status determines resource selection by American Woodcock at an important fall stopover, Cape May, New Jersey. *The Condor* 122:duaa046.
- Baert, J. M., E. W. M. Stienen, F. Verbruggen, N. Van De Weghe, L. Lens, and W. Müller (2021). Context-dependent specialisation drives temporal dynamics in intra- and inter-individual variation in foraging behaviour within a generalist bird population. *Oikos* 130:1272–1283.
- Battley, P. F., N. Warnock, T. L. Tibbitts, R. E. Gill, T. Piersma, C. J. Hassell, D. C. Douglas, D. M. Mulcahy, B. D. Gartrell, R. Schuckard, D. S. Melville, and A. C. Riegen (2012). Contrasting extreme long-distance migration patterns in bar-tailed godwits *Limosa lapponica*. *Journal of Avian Biology* 43:21–32.
- Bauer, S., J. Shamoun-Baranes, C. Nilsson, A. Farnsworth, J. F. Kelly, D. R. Reynolds, A. M. Dokter, J. F. Krauel, L. B. Petterson, K. G. Horton, and J. W. Chapman (2019). The grand challenges of migration ecology that radar aeroecology can help answer. *Ecography* 42:861–875.
- Berger-Tal, O., and S. Bar-David (2015). Recursive movement patterns: review and synthesis across species. *Ecosphere* 6:art149.
- Berigan, L. A., C. S. H. Aulicky, E. C. Teige, D. S. Sullins, K. A. Fricke, J. H. Reitz, L. G. Rossi, K. A. Schultz, M. B. Rice, E. Tanner, S. D. Fuhlendorf, and D. A. Haukos (2024). Lesser prairie-chicken dispersal after translocation: Implications for restoration and population connectivity. *Ecology and Evolution* 14:e10871.
- Blomberg, E. J., A. C. Fish, L. A. Berigan, A. M. Roth, R. Rau, S. J. Clements, G. Balkcom, B. Carpenter, G. Costanzo, J. Duguay, C. L. Graham, et al. (2023). The American Woodcock Singing Ground Survey largely conforms to the phenology of male woodcock migration. *The Journal of Wildlife Management* 87:e22488.
- Bohonak, A. J. (1999). Dispersal, Gene Flow, and Population Structure. *The Quarterly Review of Biology* 74:21–45.
- Bonter, D. N., and E. I. Greig (2021). Over 30 years of standardized bird counts at supplementary feeding stations in North America: a citizen science data report for Project FeederWatch. *Frontiers in Ecology and Evolution* 9:619682.
- Botecetti, C. I., D. M. Donner, and H. F. Mayfield (2020). Kirtland's Warbler (*Setophaga kirtlandii*), version 1.0. In *Birds of the World* (A. F. Poole, Editor). Cornell Lab of Ornithology, Ithaca, NY, USA.

- Bowlin, M. S., D. A. Enstrom, B. J. Murphy, E. Plaza, P. Jurich, and J. Cochran (2015). Unexplained altitude changes in a migrating thrush: long-flight altitude data from radio-telemetry. *The Auk: Ornithological Advances* 132:808–816.
- Boyce, M. S. (1991). Migratory behavior and management of elk (*Cervus elaphus*). *Applied Animal Behaviour Science* 29:239–250.
- Breiman, L. (2001). Random forests. *Machine learning* 45:5–32.
- Bridge, E. S., K. Thorup, M. S. Bowlin, P. B. Chilson, R. H. Diehl, R. W. Fléron, P. Hartl, R. Kays, J. F. Kelly, and W. D. Robinson (2011). Technology on the move: recent and forthcoming innovations for tracking migratory birds. *BioScience* 61:689–698.
- Brown, J. F., H. J. Tollerud, C. P. Barber, Q. Zhou, J. L. Dwyer, J. E. Vogelmann, T. R. Loveland, C. E. Woodcock, S. V. Stehman, and Z. Zhu (2020). Lessons learned implementing an operational continuous United States national land change monitoring capability: The Land Change Monitoring, Assessment, and Projection (LCMAP) approach. *Remote sensing of environment* 238:111356.
- Buler, J. J., and D. K. Dawson (2014). Radar analysis of fall bird migration stopover sites in the northeastern US. *The Condor: Ornithological Applications* 116:357–370.
- Buler, J. J., F. R. Moore, and S. Woltmann (2007). A multi-scale examination of stopover habitat use by birds. *Ecology* 88:1789–1802.
- Burnside, R. J., N. J. Collar, and P. M. Dolman (2017). Comparative migration strategies of wild and captive-bred Asian Houbara *Chlamydotis macqueenii*. *Ibis* 159:374–389.
- Cerra, J. F. (2017). Emerging strategies for voluntary urban ecological stewardship on private property. *Landscape and Urban Planning* 157:586–597.
- Chang, W., J. Cheng, J. J. Allaire, C. Sievert, B. Schloerke, Y. Xie, J. Allen, J. McPherson, A. Dipert, and B. Borges (2022). shiny: Web Application Framework for R. [Online.] Available at <https://CRAN.R-project.org/package=shiny>.
- Chapman, B. B., C. Brönmark, J.-Å. Nilsson, and L.-A. Hansson (2011). The ecology and evolution of partial migration. *Oikos* 120:1764–1775.
- Chernetsov, N. (2006). Habitat selection by nocturnal passerine migrants en route: mechanisms and results. *Journal of Ornithology* 147:185–191.
- Clark, E. R. (1970). Woodcock status report, 1969. U.S. Fish and Wildlife Service.
- Clements, S. J., L. A. Berigan, A. C. Fish, R. L. Darling, A. M. Roth, G. Balkcom, B. Carpenter, G. Costanzo, J. Duguay, and K. Filkins (2024). Satellite tracking of American Woodcock reveals a gradient of migration strategies. *Ornithology*:ukae008.
- Cobb, S. (1959). On the angle of the cerebral axis in the American woodcock. *The Auk* 76:55–59.

- Cohen, E. B., J. J. Buler, K. G. Horton, S. R. Loss, S. A. Cabrera-Cruz, J. A. Smolinsky, and P. P. Marra (2022). Using weather radar to help minimize wind energy impacts on nocturnally migrating birds. *Conservation Letters* 15:e12887.
- Cohen, I., Y. Huang, J. Chen, J. Benesty, J. Benesty, J. Chen, Y. Huang, and I. Cohen (2009). Pearson correlation coefficient. *Noise reduction in speech processing*:1–4.
- Colwell, M. A. (2010). Shorebird ecology, conservation, and management. Univ of California Press.
- Combreaud, O., S. Riou, J. Judas, M. Lawrence, and F. Launay (2011). Migratory pathways and connectivity in Asian houbara bustards: evidence from 15 years of satellite tracking. *PloS one* 6:e20570.
- Cooper, N. W., and P. P. Marra (2020). Hidden long-distance movements by a migratory bird. *Current Biology* 30:4056-4062.e3.
- Cooper, T. R., and R. D. Rau (2012). American Woodcock: Population Status, 2012. U.S. Fish and Wildlife Service.
- Cusa, M., D. A. Jackson, and M. Mesure (2015). Window collisions by migratory bird species: urban geographical patterns and habitat associations. *Urban Ecosystems* 18:1427–1446.
- Dawson, W. R. (2020). Pine Siskin (*Spinus pinus*), version 1.0. In *Birds of the World* (A. F. Poole, Editor). Cornell Lab of Ornithology, Ithaca, NY, USA.
- Dean, B., R. Freeman, H. Kirk, K. Leonard, R. A. Phillips, C. M. Perrins, and T. Guilford (2013). Behavioural mapping of a pelagic seabird: combining multiple sensors and a hidden Markov model reveals the distribution of at-sea behaviour. *Journal of The Royal Society Interface* 10:20120570.
- DeMott, W. G., A. N. Stillman, J. B. Kolb, and C. S. Elphick (2022). NEXRAD highlights the effects of wind and date at a Tree Swallow (*Tachycineta bicolor*) roost during fall migration. *The Wilson Journal of Ornithology* 134:623–632.
- Dingle, H. (2014). *Migration: the biology of life on the move*. Oxford University Press, USA.
- Dobrowski, S. Z., J. H. Thorne, J. A. Greenberg, H. D. Safford, A. R. Mynsberge, S. M. Crimmins, and A. K. Swanson (2011). Modeling plant ranges over 75 years of climate change in California, USA: temporal transferability and species traits. *Ecological Monographs* 81:241–257.
- Duerr, A. E., and B. D. Watts (2012). Waterbirds of the Chesapeake Bay: Status, ecological requirements, and threats. Center for Conservation Biology, College of William and Mary/Virginia Commonwealth University.
- Earl, J. E., S. D. Fuhlendorf, D. Haukos, A. M. Tanner, D. Elmore, and S. A. Carleton (2016). Characteristics of lesser prairie-chicken (*Tympanuchus pallidicinctus*) long-distance movements across their distribution. *Ecosphere* 7:e01441.

- Elith, J., J. R. Leathwick, and T. Hastie (2008). A working guide to boosted regression trees. *Journal of animal ecology* 77:802–813.
- ESRI (2023a). ArcGIS Online. [Online.] Available at <https://www.arcgis.com/>.
- ESRI (2023b). Terrain. [Online.] Available at <https://www.arcgis.com/home/item.html?id=58a541efc59545e6b7137f961d7de883>.
- ESRI (2024). ArcGIS Pro. Environmental Systems Research Institute.
- Fattorini, N., S. Lovari, P. Watson, and R. Putman (2020). The scale-dependent effectiveness of wildlife management: A case study on British deer. *Journal of Environmental Management* 276:111303.
- Fielding, A. H., and J. F. Bell (1997). A review of methods for the assessment of prediction errors in conservation presence/absence models. *Environmental conservation* 24:38–49.
- Fink, C. M. (2013). Dynamic soil property change in response to natural gas development in Pennsylvania. Thesis. Pennsylvania State University.
- Fink, D., T. Auer, A. Johnston, M. Strimas-Mackey, S. Ligocki, O. Robinson, W. Hochachka, L. Jaromczyk, A. Rodewald, C. Wood, I. Davies, and A. Spencer (2022). eBird Status and Trends. [Online.] Available at <https://doi.org/10.2173/ebirdst.2021>.
- Fish, A. C., A. M. Roth, G. Balkcom, L. Berigan, K. Brunette, S. Clements, G. Costanzo, C. L. Graham, W. F. Harvey, M. Hook, D. L. Howell, et al. (2024). American woodcock migration phenology in eastern North America: implications for hunting season timing. *The Journal of Wildlife Management* e22565.
- Flack, A., E. O. Aikens, A. Kölzsch, E. Nourani, K. R. S. Snell, W. Fiedler, N. Linek, H.-G. Bauer, K. Thorup, J. Partecke, M. Wikelski, and H. J. Williams (2022). New frontiers in bird migration research. *Current Biology* 32:R1187–R1199.
- Fontaine, J. J., and T. E. Martin (2006). Habitat Selection Responses of Parents to Offspring Predation Risk: An Experimental Test. *The American Naturalist* 168:811–818.
- Fortin, D., H. L. Beyer, M. S. Boyce, D. W. Smith, T. Duchesne, and J. S. Mao (2005). Wolves influence elk movements: behavior shapes a trophic cascade in Yellowstone National Park. *Ecology* 86:1320–1330.
- Fuentes, M., B. M. Van Doren, D. Fink, and D. Sheldon (2023). BirdFlow: Learning seasonal bird movements from eBird data. *Methods in Ecology and Evolution* 14:923–938.
- Galtbalt, B., A. Lilleyman, J. T. Coleman, C. Cheng, Z. Ma, D. I. Rogers, B. K. Woodworth, R. A. Fuller, S. T. Garnett, and M. Klaassen (2021). Far eastern curlew and whimbrel prefer flying low - wind support and good visibility appear only secondary factors in determining migratory flight altitude. *Movement Ecology* 9:32.

- Gehring, J., P. Kerlinger, and A. M. Manville (2011). The role of tower height and guy wires on avian collisions with communication towers. *The Journal of Wildlife Management* 75:848–855.
- Genuer, R., J.-M. Poggi, and C. Tuleau-Malot (2015). VSURF: an R package for variable selection using random forests. *The R Journal* 7:19–33.
- Genuer, R., J.-M. Poggi, and C. Tuleau-Malot (2022). VSURF: Variable Selection Using Random Forests. [Online.] Available at <https://CRAN.R-project.org/package=VSURF>.
- Gillies, C. S., and C. C. St. Clair (2010). Functional responses in habitat selection by tropical birds moving through fragmented forest. *Journal of Applied Ecology* 47:182–190.
- Glasgow, L. L. (1958). Contributions to the knowledge of the ecology of the American woodcock, *Philohela minor* (Gmelin), on the wintering range in Louisiana. Dissertation. Texas A&M University.
- Goudie, R. I., G. J. Robertson, A. Reed, and S. M. Billerman (2020). Common Eider (*Somateria mollissima*), version 1.0. In Birds of the World. Cornell Lab of Ornithology, Ithaca, NY, USA.
- Harper, E. (2006). Open-source technologies in web-based GIS and mapping. Thesis. Northwest Missouri State University.
- Hesselbarth, M. H. K., M. Scaini, K. A. With, K. Wiegand, and J. Nowosad (2019). landscapemetrics: an open-source R tool to calculate landscape metrics. *Ecography* 42:1648–1657.
- Hijmans, R. J. (2023). terra: Spatial Data Analysis. [Online.] Available at <https://rspatial.org/>.
- Hoepfner, S. A. (2023). High-Frequency GPS Transmitters Allow Understanding of Breeding Shorebird Movements and Nest Survival Without Human Disturbance. Thesis. Iowa State University.
- Holbrook, J. D., L. E. Olson, N. J. DeCesare, M. Hebblewhite, J. R. Squires, and R. Steenweg (2019). Functional responses in habitat selection: clarifying hypotheses and interpretations. *Ecological Applications* 29:e01852.
- Hopkins, L. D., and M. P. Armstrong (1985). Analytic and cartographic data storage: a two-tiered approach to spatial decision support systems. Proceedings of seventh international symposium on computer-assisted cartography. Washington, DC: American Congress on Surveying and Mapping.
- Horton, K. G., J. J. Buler, S. J. Anderson, C. S. Burt, A. C. Collins, A. M. Dokter, F. Guo, D. Sheldon, M. A. Tomaszewska, and G. M. Henebry (2023). Artificial light at night is a top predictor of bird migration stopover density. *Nature Communications* 14:7446.
- Horton, K. G., B. M. Van Doren, P. M. Stepanian, A. Farnsworth, and J. F. Kelly (2016). Where in the air? Aerial habitat use of nocturnally migrating birds. *Biology Letters* 12:20160591.

- Iverson, A. R., D. L. Humple, R. L. Cormier, and J. Hull (2023a). Land cover and NDVI are important predictors in habitat selection along migration for the Golden-crowned Sparrow, a temperate-zone migrating songbird. *Movement Ecology* 11:2.
- Iverson, A. R., J. L. Schaefer, S. M. Skalos, and C. E. Hawkins (2023b). Global positioning system (GPS) and platform transmitter terminal (PTT) tags reveal fine-scale migratory movements of small birds: A review highlights further opportunities for hypothesis-driven research. *Ornithological Applications* 125:duad014.
- Jablonski, P. G., M. Borowiec, J. J. Nowakowski, and T. Stawarczyk (2020). Ecological niche partitioning in a fragmented landscape between two highly specialized avian flush-pursuit foragers in the Andean zone of sympatry. *Scientific Reports* 10:22024.
- Jehl Jr., J. R., J. Klima, and H. F. Harris (2020). Short-billed Dowitcher (*Limnodromus griseus*), version 1.0. In *Birds of the World* (A. F. Poole, Editor). Cornell Lab of Ornithology, Ithaca, NY, USA.
- Jin, S., C. Homer, L. Yang, P. Danielson, J. Dewitz, C. Li, Z. Zhu, G. Xian, and D. Howard (2019). Overall methodology design for the United States national land cover database 2016 products. *Remote Sensing* 11:2971.
- Johnson, D. H. (1980). The comparison of usage and availability measurements for evaluating resource preference. *Ecology* 61:65–71.
- Johnson, D. S., and J. M. London (2018). crawl: an R package for fitting continuous-time correlated random walk models to animal movement data. [Online.] Available at <https://doi.org/10.5281/zenodo.596464>.
- Johnston, R. D. (1993). Effects of diet quality on the nestling growth of a wild insectivorous passerine, the house martin *Delichon urbica*. *Functional Ecology*:255–266.
- Kareiva, P. M., and N. Shigesada (1983). Analyzing insect movement as a correlated random walk. *Oecologia* 56:234–238.
- Kelley, J. R., S. Williamson, and T. R. Cooper (2008). American Woodcock Conservation Plan: a summary of and recommendations for woodcock conservation in North America. US Fish & Wildlife Publications 430.
- Kellner, K. (2015). jagsUI: a wrapper around rjags to streamline JAGS analyses. [Online.] Available at <https://cran.r-project.org/web/packages/jagsUI/index.html>.
- Kent, J. T., and D. E. Tyler (1988). Maximum likelihood estimation for the wrapped Cauchy distribution. *Journal of Applied Statistics* 15:247–254.
- Keppie, D. M., and G. W. Redmond (1988). A review of possible explanations for reverse size dimorphism of American woodcock. *Canadian Journal of Zoology* 66:2390–2397.

- Klaassen, R. H. G., M. Hake, R. Strandberg, B. J. Koks, C. Trierweiler, K. Exo, F. Bairlein, and T. Alerstam (2014). When and where does mortality occur in migratory birds? Direct evidence from long-term satellite tracking of raptors. *Journal of Animal Ecology* 83:176–184.
- Krementz, D. G., J. T. Seginak, and G. W. Pendleton (1995). Habitat use at night by wintering American woodcock in coastal Georgia and Virginia. *The Wilson Bulletin*:686–697.
- La Sorte, F. A., D. Fink, W. M. Hochachka, A. Farnsworth, A. D. Rodewald, K. V. Rosenberg, B. L. Sullivan, D. W. Winkler, C. Wood, and S. Kelling (2014). The role of atmospheric conditions in the seasonal dynamics of North American migration flyways. *Journal of Biogeography* 41:1685–1696.
- Langrock, R., R. King, J. Matthiopoulos, L. Thomas, D. Fortin, and J. M. Morales (2012). Flexible and practical modeling of animal telemetry data: hidden Markov models and extensions. *Ecology* 93:2336–2342.
- Lao, S., B. A. Robertson, A. W. Anderson, R. B. Blair, J. W. Eckles, R. J. Turner, and S. R. Loss (2020). The influence of artificial light at night and polarized light on bird-building collisions. *Biological Conservation* 241:108358.
- Leclerc, M., E. Vander Wal, A. Zedrosser, J. E. Swenson, J. Kindberg, and F. Pelletier (2016). Quantifying consistent individual differences in habitat selection. *Oecologia* 180:697–705.
- Liaw, A., and M. Wiener (2002). Classification and Regression by randomForest. *R News* 2:18–22.
- Linscott, J. A., J. G. Navedo, S. J. Clements, J. P. Loghry, J. Ruiz, B. M. Ballard, M. D. Weegman, and N. R. Senner (2022). Compensation for wind drift prevails for a shorebird on a long-distance, transoceanic flight. *Movement Ecology* 10:11.
- Loss, S. R., S. Lao, A. W. Anderson, R. B. Blair, J. W. Eckles, and R. J. Turner (2020). Inclement weather and American woodcock building collisions during spring migration. *Wildlife Biology* 2020.
- Loss, S. R., S. Lao, J. W. Eckles, A. W. Anderson, R. B. Blair, and R. J. Turner (2019). Factors influencing bird-building collisions in the downtown area of a major North American city. *PLOS ONE* 14:e0224164.
- Loss, S. R., T. Will, S. S. Loss, and P. P. Marra (2014). Bird–building collisions in the United States: Estimates of annual mortality and species vulnerability. *The Condor* 116:8–23.
- Loss, S. R., T. Will, and P. P. Marra (2013). Estimates of bird collision mortality at wind facilities in the contiguous United States. *Biological Conservation* 168:201–209.
- Makowski, D., M. Ben-Shachar, and D. Lüdecke (2019). bayestestR: Describing Effects and their Uncertainty, Existence and Significance within the Bayesian Framework. *Journal of Open Source Software* 4:1541.

- Mander, L., I. Nicholson, R. M. W. Green, S. G. Dodd, R. M. Forster, and N. H. K. Burton (2022). Individual, sexual and temporal variation in the winter home range sizes of GPS-tagged Eurasian Curlews *Numenius arquata*. *Bird Study* 69:39–52.
- Manly, B. F. L., L. McDonald, D. L. Thomas, T. L. McDonald, and W. P. Erickson (2007). Resource selection by animals: statistical design and analysis for field studies. Springer Science & Business Media.
- Marra, P. P., E. B. Cohen, S. R. Loss, J. E. Rutter, and C. M. Tonra (2015). A call for full annual cycle research in animal ecology. *Biology letters* 11:20150552.
- Marra, P. P., T. W. Sherry, and R. T. Holmes (1993). Territorial exclusion by a long-distance migrant warbler in Jamaica: a removal experiment with American Redstarts (*Setophaga ruticilla*). *The Auk* 110:565–572.
- Martin, G. R. (1994). Visual fields in woodcocks *Scolopax rusticola* (Scolopacidae; Charadriiformes). *Journal of Comparative Physiology A* 174.
- Masse, R. J., B. C. Tefft, and S. R. McWilliams (2014). Multiscale habitat selection by a forest-dwelling shorebird, the American woodcock: Implications for forest management in southern New England, USA. *Forest Ecology and Management* 325:37–48.
- Mauer, F. J. (1998). Moose migration: northeastern Alaska to northwestern Yukon territory, Canada. *Alces: A Journal Devoted to the Biology and Management of Moose* 34:75–81.
- McAuley, D. G., D. M. Keppie, and R. M. Whiting Jr. (2020). American Woodcock (*Scolopax minor*), version 1.0. In *Birds of the World* (A. F. Poole, Editor). Cornell Lab of Ornithology, Ithaca, NY, USA.
- McAuley, D. G., J. R. Longcore, and G. F. Sepik (1993). Techniques for Research into Woodcocks: Experiences and Recommendations. Proceedings of the eighth American woodcock symposium. U.S. Fish and Wildlife Service, p. 5.
- McCance, E. C., D. J. Decker, A. M. Colturi, R. K. Baydack, W. F. Siemer, P. D. Curtis, and T. Eason (2017). Importance of urban wildlife management in the United States and Canada. *Mammal Study* 42:1–16.
- McClintock, B. T., and T. Michelot (2018). momentuHMM: R package for generalized hidden Markov models of animal movement. *Methods in Ecology and Evolution* 9:1518–1530.
- McConnell, M., and L. W. Burger (2011). Precision conservation: a geospatial decision support tool for optimizing conservation and profitability in agricultural landscapes. *Journal of Soil and Water Conservation* 66:347–354.
- McElreath, R. (2018). Statistical rethinking: A Bayesian course with examples in R and Stan. Chapman and Hall/CRC.

- McLaren, J. D., J. J. Buler, T. Schreckengost, J. A. Smolinsky, M. Boone, E. Emiel van Loon, D. K. Dawson, and E. L. Walters (2018). Artificial light at night confounds broad-scale habitat use by migrating birds. *Ecology Letters* 21:356–364.
- Mehlman, D. W., S. E. Mabey, D. N. Ewert, C. Duncan, B. Abel, D. Cimprich, R. D. Sutter, and M. Woodrey (2005). Conserving stopover sites for forest-dwelling migratory landbirds. *The Auk* 122:1281–1290.
- Mendall, H. L., and C. M. Aldous (1943). The ecology and management of American woodcock. Maine Cooperative Wildlife Research Unit.
- Mettke-Hofmann, C., P. B. Hamel, G. Hofmann, T. J. Zenzal Jr, A. Pellegrini, J. Malpass, M. Garfinkel, N. Schiff, and R. Greenberg (2015). Competition and habitat quality influence age and sex distribution in wintering Rusty Blackbirds. *PLoS One* 10:e0123775.
- Miller, D. L., and M. K. Causey (1985). Food preferences of American woodcock wintering in Alabama. *The Journal of wildlife management* 49:492–496.
- Miller, J. (2010). Species distribution modeling. *Geography Compass* 4:490–509.
- Moore, J. D., D. E. Andersen, T. Cooper, J. P. Duguay, S. L. Oldenburger, C. A. Stewart, and D. G. Krementz (2021). Migration phenology and patterns of American woodcock in central North America derived using satellite telemetry. *Wildlife Biology* 2021.
- Moore, J. D., D. E. Andersen, T. R. Cooper, J. P. Duguay, S. L. Oldenburger, C. A. Stewart, and D. G. Krementz (2019). Migratory connectivity of American Woodcock derived using satellite telemetry. *The Journal of Wildlife Management* 83:1617–1627.
- Morales, J. M., P. R. Moorcroft, J. Matthiopoulos, J. L. Frair, J. G. Kie, R. A. Powell, E. H. Merrill, and D. T. Haydon (2010). Building the bridge between animal movement and population dynamics. *Philosophical Transactions of the Royal Society B: Biological Sciences* 365:2289–2301.
- Moskát, C., M. Bán, A. Fülöp, J. Bereczki, and M. E. Hauber (2019). Bimodal habitat use in brood parasitic Common Cuckoos (*Cuculus canorus*) revealed by GPS telemetry. *The Auk: Ornithological Advances* 136:uky019.
- Muff, S., J. Signer, and J. Fieberg (2020). Accounting for individual-specific variation in habitat-selection studies: Efficient estimation of mixed-effects models using Bayesian or frequentist computation. *Journal of Animal Ecology* 89:80–92.
- Myatt, N. A., and D. G. Krementz (2007). Fall migration and habitat use of American woodcock in the central United States. *The Journal of wildlife management* 71:1197–1205.
- Mysterud, A., and R. A. Ims (1998). Functional Responses in Habitat Use: Availability Influences Relative Use in Trade-Off Situations. *Ecology* 79:1435–1441.
- NABCI (2021). Bird Conservation Regions Map. *North American Bird Conservation Initiative*. [Online.] Available at <https://nabci-us.org/resources/bird-conservation-regions-map/>.

- Newsome, S. D., M. T. Tinker, V. A. Gill, Z. N. Hoyt, A. Doroff, L. Nichol, and J. L. Bodkin (2015). The interaction of intraspecific competition and habitat on individual diet specialization: a near range-wide examination of sea otters. *Oecologia* 178:45–59.
- Nichols, K. S., T. Homayoun, J. Eckles, and R. B. Blair (2018). Bird-building collision risk: An assessment of the collision risk of birds with buildings by phylogeny and behavior using two citizen-science datasets. *PLOS ONE* 13:e0201558.
- Nicol, S., M. Cros, N. Peyrard, R. Sabbadin, R. Trépos, R. A. Fuller, and B. K. Woodworth (2023). FlywayNet: A hidden semi-Markov model for inferring the structure of migratory bird networks from count data. *Methods in Ecology and Evolution* 14:265–279.
- Norris, D. R., and P. P. Marra (2007). Seasonal interactions, habitat quality, and population dynamics in migratory birds. *The Condor* 109:535–547.
- NRCS (2021). Web Soil Survey. [Online.] Available at <https://websoilsurvey.nrcs.usda.gov/>.
- Oehlers, S. A., R. T. Bowyer, F. Huettmann, D. K. Person, and W. B. Kessler (2011). Sex and scale: implications for habitat selection by Alaskan moose *Alces alces gigas*. *Wildlife Biology* 17:67–84.
- Omernik, J. M., and G. E. Griffith (2014). Ecoregions of the conterminous United States: evolution of a hierarchical spatial framework. *Environmental Management* 54:1249–1266.
- OpenStreetMap contributors (2023). OpenStreetMap. [Online.] Available at [www.openstreetmap.org](http://www.openstreetmap.org).
- Orgeret, F., R. R. Reisinger, T. Carpenter-Kling, D. Z. Keys, A. Corbeau, C. Bost, H. Weimerskirch, and P. A. Pistorius (2021). Spatial segregation in a sexually dimorphic central place forager: Competitive exclusion or niche divergence? *Journal of Animal Ecology* 90:2404–2420.
- Pebesma, E. (2018). Simple Features for R: Standardized Support for Spatial Vector Data. *The R Journal* 10:439–446.
- Pennsylvania Game Commission (2023). Pennsylvania State Game Lands. [Online.] Available at <https://www.pgc.pa.gov/HuntTrap/StateGameLands/Pages/default.aspx>.
- Péron, G., J. M. Calabrese, O. Duriez, C. H. Fleming, R. García-Jiménez, A. Johnston, S. A. Lambertucci, K. Safi, and E. L. C. Shepard (2020). The challenges of estimating the distribution of flight heights from telemetry or altimetry data. *Animal Biotelemetry* 8:5.
- Phillips, R. A., J. R. D. Silk, B. Phalan, P. Catry, and J. P. Croxall (2004). Seasonal sexual segregation in two *Thalassarche* albatross species: competitive exclusion, reproductive role specialization or foraging niche divergence? *Proceedings of the Royal Society of London. Series B: Biological Sciences* 271:1283–1291.
- Phillips, S. J., R. P. Anderson, and R. E. Schapire (2006). Maximum entropy modeling of species geographic distributions. *Ecological modelling* 190:231–259.

- Picardi, S., P. Coates, J. Kolar, S. O’Neil, S. Mathews, and D. Dahlgren (2022). Behavioural state-dependent habitat selection and implications for animal translocations. *Journal of Applied Ecology* 59:624–635.
- Plummer, M. (2003). JAGS: A program for analysis of Bayesian graphical models using Gibbs sampling. Proceedings of the 3rd international workshop on distributed statistical computing. Vienna, Austria, pp. 1–10.
- Poessel, S. A., A. E. Duerr, J. C. Hall, M. A. Braham, and T. E. Katzner (2018). Improving estimation of flight altitude in wildlife telemetry studies. *Journal of Applied Ecology* 55:2064–2070.
- Poole, E. L. (1938). Weights and Wing Areas in North American Birds. *The Auk* 55:511–517.
- Pribil, S., and J. Picman (1997). The importance of using the proper methodology and spatial scale in the study of habitat selection by birds. *Canadian Journal of Zoology* 75:1835–1844.
- R Core Team (2024). R: A Language and Environment for Statistical Computing. R Foundation for Statistical Computing, Vienna, Austria.
- Randin, C. F., T. Dirnböck, S. Dullinger, N. E. Zimmermann, M. Zappa, and A. Guisan (2006). Are niche-based species distribution models transferable in space? *Journal of Biogeography* 33:1689–1703.
- Rappole, J. H. (2013). The avian migrant: the biology of bird migration. Columbia University Press.
- Rice, J., B. W. Anderson, and R. D. Ohmart (1980). Seasonal Habitat Selection by Birds in the Lower Colorado River Valley. *Ecology* 61:1402–1411.
- Rieffenberger, J. C., and R. C. Kletzly (1966). Woodcock night-lighting techniques and equipment. WH Goudy, compiler. *Woodcock research and management*:33–35.
- Robbins, C. S., D. Bystrak, and P. H. Geissler (1986). The Breeding Bird Survey: its first fifteen years, 1965–1979. Patuxent Wildlife Research Center.
- Rogers, R. M., J. J. Buler, C. E. Wainwright, and H. A. Campbell (2020). Opportunities and challenges in using weather radar for detecting and monitoring flying animals in the Southern Hemisphere. *Austral Ecology* 45:127–136.
- Ronce, O. (2007). How Does It Feel to Be Like a Rolling Stone? Ten Questions About Dispersal Evolution. *Annual Review of Ecology, Evolution, and Systematics* 38:231–253.
- Ruscio, J. (2008). A probability-based measure of effect size: robustness to base rates and other factors. *Psychological methods* 13:19.
- Sauer, J. R., J. E. Fallon, and R. Johnson (2003). Use of North American Breeding Bird Survey data to estimate population change for bird conservation regions. *The Journal of wildlife management*:372–389.

- Seamans, M. E., and R. D. Rau (2020). American Woodcock Population Status, 2020. U.S. Fish and Wildlife Service.
- Sheldon, W. G. (1960). A method of mist netting woodcocks in summer. *Bird-banding* 31:130–135.
- Signer, J., J. Fieberg, and T. Avgar (2019). Animal movement tools (amt): R package for managing tracking data and conducting habitat selection analyses. *Ecology and Evolution* 9:880–890.
- Slezak, C. R., E. J. Blomberg, L. A. Berigan, R. Darling, A. C. Fish, S. J. Clements, A. M. Roth, R. D. Rau, G. Balkcom, B. Carpenter, G. Costanzo, et al. (2024a). Unconventional life-history in a migratory shorebird: desegregating reproduction and migration. *Proceedings of the Royal Society B*:20240021.
- Slezak, C. R., R. J. Masse, and S. R. McWilliams (2024b). Sex-specific differences and long-term trends in habitat selection of American woodcock. *The Journal of Wildlife Management* 88:e22518.
- Stafford, J. D., A. K. Janke, M. J. Anteau, A. T. Pearse, A. D. Fox, J. Elmberg, J. N. Straub, M. W. Eichholz, and C. Arzel (2014). Spring migration of waterfowl in the northern hemisphere: a conservation perspective. *Wildfowl*:70–85.
- Stanley, C. Q., M. R. Dudash, T. B. Ryder, W. G. Shriver, K. Serno, S. Adalsteinsson, and P. P. Marra (2021). Seasonal variation in habitat selection for a Neotropical migratory songbird using high-resolution GPS tracking. *Ecosphere* 12:e03421.
- Stuber, E. F., L. F. Gruber, and J. J. Fontaine (2017). A Bayesian method for assessing multi-scale species-habitat relationships. *Landscape Ecology* 32:2365–2381.
- Sugumaran, R., and J. Degroote (2010). Components of SDSS II. In Spatial decision support systems: principles and practices. CRC Press, Boca Raton, FL, USA, pp. 145–190.
- Sugumaran, V., and R. Sugumaran (2007). Web-based Spatial Decision Support Systems (WebSDSS): evolution, architecture, examples and challenges. *Communications of the Association for Information Systems* 19:40.
- Sullivan, B. L., C. L. Wood, M. J. Iliff, R. E. Bonney, D. Fink, and S. Kelling (2009). eBird: A citizen-based bird observation network in the biological sciences. *Biological conservation* 142:2282–2292.
- Thaxter, C. B., V. H. Ross-Smith, and A. Cook (2016). How high do Birds fly?: A review of current datasets and an appraisal of current methodologies for collecting flight height data; literature review. British Trust for Ornithology.
- Thurfjell, H., S. Ciuti, and M. S. Boyce (2014). Applications of step-selection functions in ecology and conservation. *Movement ecology* 2:1–12.
- U.S. Census Bureau (2021). 2020 Decennial Census. [Online.] Available at [data.census.gov](http://data.census.gov).
- U.S. Fish and Wildlife Service (1996). U.S. Fish and Wildlife Service Service Manual. 870 FW 1.

- USFWS (2023). Urban Wildlife Conservation Program. *FWS.gov*. [Online.] Available at <https://www.fws.gov/program/urban-wildlife-conservation>.
- USGS (2000). 7.5 minute digital elevation models (DEM) for Pennsylvania (30 meter). [Online.] Available at <http://www.pasda.psu.edu/>.
- USGS and USDA (2020). LANDFIRE 2.0.0 Successional Class Layer. [Online.] Available at <http://landfire.cr.usgs.gov/viewer/>.
- Van Doren, B. M., D. E. Willard, M. Hennen, K. G. Horton, E. F. Stuber, D. Sheldon, A. H. Sivakumar, J. Wang, A. Farnsworth, and B. M. Winger (2021). Drivers of fatal bird collisions in an urban center. *Proceedings of the National Academy of Sciences* 118:e2101666118.
- Vanderhoff, N., P. Pyle, M. A. Patten, R. Sallabanks, and F. C. James (2020). American Robin (*Turdus migratorius*), version 1.0. In *Birds of the World* (P. G. Rodewald, Editor). Cornell Lab of Ornithology, Ithaca, NY, USA.
- Vignali, S., A. G. Barras, R. Arlettaz, and V. Braunisch (2020). SDMtune: An R package to tune and evaluate species distribution models. *Ecology and Evolution* 10:11488–11506.
- Wang, J., and L. S. Chen (2016). MixRF: A Random-Forest-Based Approach for Imputing Clustered Incomplete Data. [Online.] Available at <https://github.com/randel/MixRF>.
- Ward, S. A. (1987). Optimal Habitat Selection in Time-Limited Dispersers. *The American Naturalist* 129:568–579.
- White, J. D., K. W. Heist, and M. T. Wells (2020). Great Lakes Avian Radar Technical Report Lake Erie Lakeshore: Macomb and Wayne County, MI, Fall 2018. U.S. Fish and Wildlife Service.
- Wiser, R., M. Bolinger, B. Hoen, D. Millstein, J. Rand, G. Barbose, N. Darghouth, W. Gorman, S. Jeong, and E. O'Shaughnessy (2023). Land-based wind market report: 2023 edition. Lawrence Berkeley National Laboratory (LBNL), Berkeley, CA (United States).
- Wright, J. R., J. A. Johnson, E. Bayne, L. L. Powell, C. R. Foss, J. C. Kennedy, and P. P. Marra (2021). Migratory connectivity and annual cycle phenology of Rusty Blackbirds (*Euphagus carolinus*) revealed through archival GPS tags. *Avian Conservation & Ecology* 16.
- Zhang, J., M. Rayner, S. Vickers, T. Landers, R. Sagar, J. Stewart, and B. Dunphy (2019). GPS telemetry for small seabirds: using hidden Markov models to infer foraging behaviour of Common Diving Petrels (*Pelecanoides urinatrix urinatrix*). *Emu - Austral Ornithology* 119:126–137.
- Zucchini, W., I. L. MacDonald, and R. Langrock (2017). Hidden Markov models for time series: an introduction using R. CRC Press.
- Zucchini, W., D. Raubenheimer, and I. L. MacDonald (2008). Modeling time series of animal behavior by means of a latent-state model with feedback. *Biometrics* 64:807–815.



## APPENDICES

### A. APPENDIX A

Table A.1. Area-under-the-curve (AUC; Fielding and Bell 1997) scores for three different modeling techniques evaluated for use in creating species distribution models. Models were evaluated using the migratory dataset, with 113 American woodcock (*Scolopax minor*) GPS locations to delineate use and 10,000 locations randomly distributed throughout Pennsylvania, USA to delineate pseudoabsence. Predictive variables included all metrics listed for the migratory model in Table 1.2. The modeling technique with the greatest AUC during this testing process (random forest) was used for all further modeling of the migratory and breeding datasets.

<b>Modeling Technique</b>	<b>AUC</b>
MaxEnt (Phillips et al. 2006)	0.68
Random forest (Breiman 2001)	0.70
Boosted regression trees (Elith et al. 2008)	0.63

## B. APPENDIX B

### B.1 *Individual exceptions*

Throughout the study, we encountered 45 of 522 (9%) classified migratory tracks that failed to fit the parameters of the full model due to erratic behavior. These exceptions were broadly categorized as misclassification errors due to the presence of foray loops ( $n = 19$  misclassification errors), dispersals (3), and summer migrations (2), as well as errors caused by continued migration after the end of the HMM's consideration period (14) and transmissions beginning after the start of migration (3). We additionally edited the known state classification for 4 birds, two of which were captured on their nests late in spring migration, one which was recaptured at a suspected post-migratory site several months after its transmitter had prematurely died, and one which continued regular  $\geq 16.1$  km movements between sections of its wintering home range. We modified the HMM classification process for these individuals by removing locations or setting known movement states to ensure that these tracks were classified correctly by our HMMs (Table B1).

The base model required all the same individual exceptions as the full model, in addition to several additional fixes to pre-migratory state delineation ( $n = 11$ ). All eleven exceptions were made to individuals captured in New Jersey or Virginia for whom the initial state was erroneously estimated to be migratory, despite pre-existing knowledge that the bird was in a pre-migratory state (either due to capture at that site prior to the migratory season or migratory data from previous seasons). For all 11 exceptions we addressed the issue by setting a known pre-migration state for the first location in that individual's seasonal HMM.

Table B.1. Individual exceptions to the full model ruleset made in hidden Markov Model delineation to improve seasonal model fits for individual birds. <sup>1</sup> Year in which the issue occurred. <sup>2</sup> Seasonal HMM that encountered the issue. <sup>3</sup> Short description of why the edit was necessary. <sup>4</sup> Steps that were taken to alleviate the corresponding issue.

Bird ID	Year	Season <sup>2</sup>	Issue <sup>3</sup>	Edit <sup>4</sup>
RI-2020-31	2020	Fall	Foray loop caused early initiation of migration	Removed points on Aug. 29 <sup>th</sup> and Nov. 21 <sup>st</sup> from the HMM
NY-2018-04	2018	Fall	Foray loop caused late termination of migration	Removed points on Nov. 21 <sup>st</sup> –23 <sup>rd</sup> from the HMM
NJ-2018-03	2018	Fall	Foray loop caused an apparent migration	Removed points on Jan. 10 <sup>th</sup> and 18 <sup>th</sup> from the HMM
PA-2018-01	2018	Fall	Foray loop caused late termination of migration	Removed points on Dec. 18 <sup>th</sup> –20 <sup>th</sup> from the HMM
ME-2018-08	2018	Fall	Foray loop caused late termination of migration	Removed points on Dec. 23 <sup>rd</sup> –25 <sup>th</sup> from the HMM
PA-2019-15	2019	Fall	Foray loop caused late termination of migration	Removed points on Dec. 10 <sup>th</sup> –13 <sup>th</sup> from the HMM
VA-2021-92	2021	Fall	Foray loop caused early initiation of migration	Removed points on Sep. 20 <sup>th</sup> –October 6 <sup>th</sup> from the HMM
RI-2021-46	2021	Fall	Foray loop caused late termination of migration	Removed points on Feb. 10 <sup>th</sup> –14 <sup>th</sup> from the HMM

Table B.1 Continued.

RI-2021-59	2021	Fall	No locations prior to the start of migration due to transmitter glitch	Set a known stopover state for the first location in the HMM
VA-2019-48	2019	Fall	Bird settles after Feb. 25th	Set a known post-migration state for the final location in the HMM
RI-2021-58	2021	Fall	Bird settles after Feb. 25th	Set a known post-migration state for the final location in the HMM
RI-2019-29	2019	Fall	Series of dispersal movements caused an apparent migration	Removed bird from HMM classification
SC-2020-13	2020	Fall	Summer migration erroneously classified as a fall migration	Removed from HMM classification
GA-2021-18	2021	Fall	Foray loop caused an apparent migration	Removed from HMM classification
NY-2018-06	2018	Fall	Foray loops caused late termination of migration	Removed points on Nov. 17 <sup>th</sup> –18 <sup>th</sup> and Dec. 25 <sup>th</sup> –27 <sup>th</sup> from the HMM
PA-2021-37	2021	Fall	Foray loops caused late termination of migration	Removed points on Dec. 8 <sup>th</sup> from the HMM
NY-2018-03	2018	Fall	Foray loops caused early initiation of migration	Removed points on Oct. 6 <sup>th</sup> –15 <sup>th</sup> from the model

Table B.1 Continued.

PA-2021-34	2021	Fall	Regular movements $\geq 16.1$ km between two sections of the wintering home range caused late termination of migration.	Set a known post-migratory state on Nov. 7 <sup>th</sup> .
VA-2020-52	2020	Spring (male)	Dispersal movement caused late termination of migration	Removed points on Jun. 18 <sup>th</sup> –28 <sup>th</sup> from the HMM
NJ-2018-03	2019	Spring (male)	Foray loop caused early initiation of migration	Removed points on Jan. 10 <sup>th</sup> –17 <sup>th</sup> from the HMM
RI-2019-21	2020	Spring (male)	Late termination of fall migration, never initiated spring migration	Removed from HMM classification
RI-2019-29	2020	Spring (male)	Dispersal movement caused an apparent migration	Removed from HMM classification
VA-2018-03	2018	Spring (male)	Foray loop caused an apparent migration	Removed from HMM classification
FL-2021-01	2021	Spring (male)	Foray loop caused an apparent migration	Removed from HMM classification
NJ-2018-08	2019	Spring (female)	Late termination of fall migration	Removed points prior to Jan. 12 <sup>th</sup> from the HMM
NJ-2018-15	2019	Spring (female)	Late termination of fall migration	Removed points prior to Jan. 14 <sup>th</sup> from the HMM

Table B.1 Continued.

NJ-2018-13	2019	Spring (female)	Late termination of fall migration	Removed points prior to Feb. 5 <sup>th</sup> from the HMM
RI-2020-31	2021	Spring (female)	Late termination of fall migration	Removed points prior to Mar. 2 <sup>nd</sup> from the HMM
ME-2018-13	2019	Spring (female)	Late termination of fall migration	Removed points prior to Jan. 8 <sup>th</sup> from the HMM
RI-2021-46	2022	Spring (female)	Foray loop caused early initiation of migration	Removed points on Feb. 10 <sup>th</sup> –14 <sup>th</sup> from the HMM
NY-2018-07	2019	Spring (female)	Foray loop caused early initiation of migration	Removed points on Dec. 2 <sup>nd</sup> –Dec. 9 <sup>th</sup> from the HMM
RI-2020-44	2021	Spring (female)	Foray loop caused early initiation of migration	Removed points on Dec. 4 <sup>th</sup> –Dec. 18 <sup>th</sup> from the HMM
NJ-2018-13	2019	Spring (female)	Locations began later in the season than other New Jersey transmitters, creating issues with initial state estimation	Excluded from initial state estimation
NJ-2018-15	2019	Spring (female)	Locations began later in the season than other New Jersey transmitters, creating issues with initial state estimation	Excluded from initial state estimation
NY-2022-40	2022	Spring (female)	Bird captured on the nest in late spring that continued migration after nest failure	Set a known stopover state for the first location in the HMM

Table B.1 Continued.

RI-2018-11	2019	Spring (female)	Bird recaptured at the terminal site the next fall, so it is known to have settled	Set a known post-migration state for the final location in the HMM
NS-2019-02	2020	Spring (female)	Late termination of fall migration	Removed points prior to Jan. 28 <sup>th</sup> from the HMM
RI-2020-42	2021	Spring (female)	Late termination of fall migration	Removed points prior to Jan. 23 <sup>rd</sup> from the HMM
RI-2021-47	2022	Spring (female)	Fall migration does not terminate	Removed from spring HMM classification
RI-2021-52	2022	Spring (female)	Fall migration does not terminate	Removed from spring HMM classification
SC-2019-03	2019	Spring (female)	Late termination of spring migration	Used Jul. 30 <sup>th</sup> , instead of Jun. 30 <sup>th</sup> , as the last date of consideration for the HMM
VA-2019-36	2020	Spring (female)	Late termination of spring migration	Used Jul. 30 <sup>th</sup> , instead of Jun. 30 <sup>th</sup> , as the last date of consideration for the HMM
VA-2020-66	2021	Spring (female)	Foray loop caused early initiation of migration	Removed points on January 24th - 29th from the HMM
NY-2022-42	2022	Spring (female)	Bird captured on the nest in late spring that continued migration after nest failure	Set a known stopover state for the first location in the HMM

## B.2 *HMM ruleset bug fixes*

Each seasonal HMM was set to follow certain rules regarding possible state designations based on step length. For example, the only state in any HMM that was allowed to have step lengths  $\geq 16.1$  km was migration. The pre-migration state could only occur before the first  $\geq 16.1$  km step was observed, and the post-migration state could only occur after the last  $\geq 16.1$  km step was observed. These rules were enforced within the HMMs using 2 mechanisms. The first was a fixed, large negative value for certain state transition coefficients, which effectively acted to prohibit movements between states that would not correspond to the diagram shown in Fig. 1 in the main text (e.g. a bird could move from pre-migration into migration, but not from migration into pre-migration). The second was a fixed probability of  $\sim 0$  that birds in any state other than migration would have a step length  $\geq 16.1$  km, and a fixed probability of  $\sim 1$  that birds in the migration state would have a step length  $\geq 16.1$  km. These fixed parameters effectively prohibited most state assignments that fell outside of our ruleset, but in 2 circumstances the HMM failed to enforce these rules. The first occurred when birds that stayed in the pre-migration state later into the year than expected by the HMM, which would sometimes result in the HMM classifying later pre-migratory movements as stopover locations, despite the lack of a  $\geq 16.1$  km step between the interpolated pre-migration and stopover states. The second occurred when birds entered the post-migration state earlier in the year than expected by the HMM, which occasionally resulted in the HMM classifying earlier post-migration locations as stopover locations despite the lack of an intervening  $\geq 16.1$  km movement. These two issues were both fixed after HMM classification using code to identify transitions between pre-migration and stopover, as well as stopover and post-migration, without an intervening  $\geq 16.1$  km step, and manually assigning pre-migration or post-migration states to the erroneously classified locations. This resulted in reclassifications for 35 seasonal migratory tracks, including 8 changes to pre-migratory classifications and 27 changes to post-migratory classifications.

### B.3 *Modeling bird mortality*

The Pinpoint GPS transmitters used during this study usually stopped transmitting upon bird mortality due to attenuation of the signal when the antenna touched the ground. However, there were some circumstances in which transmitters continued to transmit when antennae remained upright after the bird's death. To recognize and filter out these occurrences, we designed a two-stage process for recognizing and removing the locations of deceased birds from our dataset. The first step was an automated process, which used a hidden Markov Model (HMM) to recognize locations from birds that had ceased making normal movements. We trained this HMM using a subset of 413 training locations gathered during transmitter testing, when 10 transmitters were left on the ground to gather 1 location per minute for ~40 minutes. During this test, we placed 2 transmitters under negligible vegetation cover (short grass, height: ~10 cm), 3 transmitters under low cover (tall grass, height: ~100 cm), 2 transmitters under medium cover (early successional aspen stand, canopy height: ~8 m), and 3 transmitters under high cover (mature deciduous forest, canopy height: ~15 m). We collected these data to provide a balanced sample size from each cover type and demonstrate the likely patterns of locations produced by stationary transmitters on deceased birds under a variety of vegetative cover circumstances.

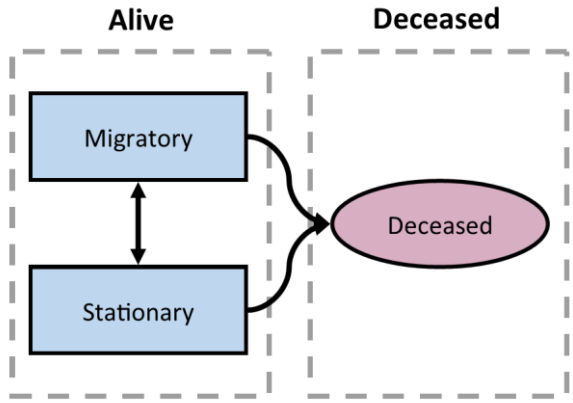


Figure B.1. Movement state transition diagram for the hidden Markov Model used to identify potential mortalities among tagged American Woodcock (*Scolopax minor*). Woodcock were allowed to begin their track in any state, and transition freely between either of the two living states (migratory and stationary). Birds that entered the deceased state, however, were forced to remain in this state for the remainder of their track.

The HMM trained on these data used step length, turn angle, and mean distance to the nearest 15 points in a 3-state model to determine whether a bird was likely deceased when locations were recorded. The mean distance to the nearest 15 points metric was decided based on an exploratory analysis of the training dataset, where we determined that the mean distance to the nearest 15 points metric was more consistent between individuals than alternative metrics (mean distance to the nearest 5 and 10 points). The HMM was trained to identify 3 states in the data: migratory, stationary, and deceased. The migratory and stationary states were both living states, and birds were allowed to transition between them freely. Deceased was a terminal state, which birds could enter from either of the two living states (Fig. A1). Among 512 birds in our dataset, the HMM identified 137 individuals that had potentially experienced mortality and continued transmitting. We confirmed these mortalities during a second step, in which we manually checked and adjusted the dates for all potential

mortalities identified by the HMM. We only confirmed a mortality during the second step if the following 2 criteria were met:

The bird had  $\geq 15$  mortality locations

At least half of mortality points fell within a threshold distance of the centroid, with the threshold distance varying based on the dominant land cover type as shown in Table B.2.

Table B.2. 50% threshold values for 4 land cover types, demonstrating the distance (m) from the centroid within which at least half of GPS points fall when a GPS transmitter is taking locations while stationary. The 50% threshold values are represented by the variable X in the criterion “At least half of mortality points fell within X m of the centroid, with X varying based on the dominant land cover type”.

<b>Dominant land cover</b>	<b>50% threshold distance (m)</b>
Young forest	4.93
Mature forest	10.85
Short grass	5.33
Tall grass	3.93

The threshold distance ensured that we had enough locations to determine that the bird was indeed stationary, and the distance to centroid threshold allowed us to ensure that the bird's movements occurred within a distance consistent with the GPS error associated with the locations' land cover type. We required that 50% of all mortality points fell within the distance to centroid threshold, with the 50% value chosen based on consistency between individuals in the training dataset. Distance to centroid thresholds were set based on the mean values observed among all

individuals in that cover type in the training dataset. Dominant land cover type was assessed via publicly available satellite imagery (OpenStreetMap contributors 2023) for both the test and training datasets.

We manually classified a mortality event when both criteria were met. In certain circumstances where mortalities met one threshold but came just shy on the other, we made the final determination regarding whether a mortality had indeed occurred. Of 137 potential mortalities, we determined 20 to be true mortality events. The code used in this delineation is publicly available at [github.com/EWMRC/mortality-detection](https://github.com/EWMRC/mortality-detection).

#### B.4 *Simplified movement state designations for Movebank*

Prior to use in other studies, we simplified our hidden Markov model (HMM) classification states to 3 classes: stationary, migration (fall), and migration (spring). The stationary class included all pre-migration and post-migration locations, while the fall and spring migration classes included migration and stopover locations. We added 3 additional classification states to represent long-distance movements outside of spring and fall migration: migration (summer), foray loop, and dispersal (described in section 2.2.4 of this dissertation). This class structure provided a simplified framework for delineating woodcock migratory phenology and long-distance movements throughout the full annual cycle, which could be applied to habitat use or survival analyses (Fig. B.2). These classes were uploaded to Movebank (repository 351564596) to facilitate collaborator access to data.

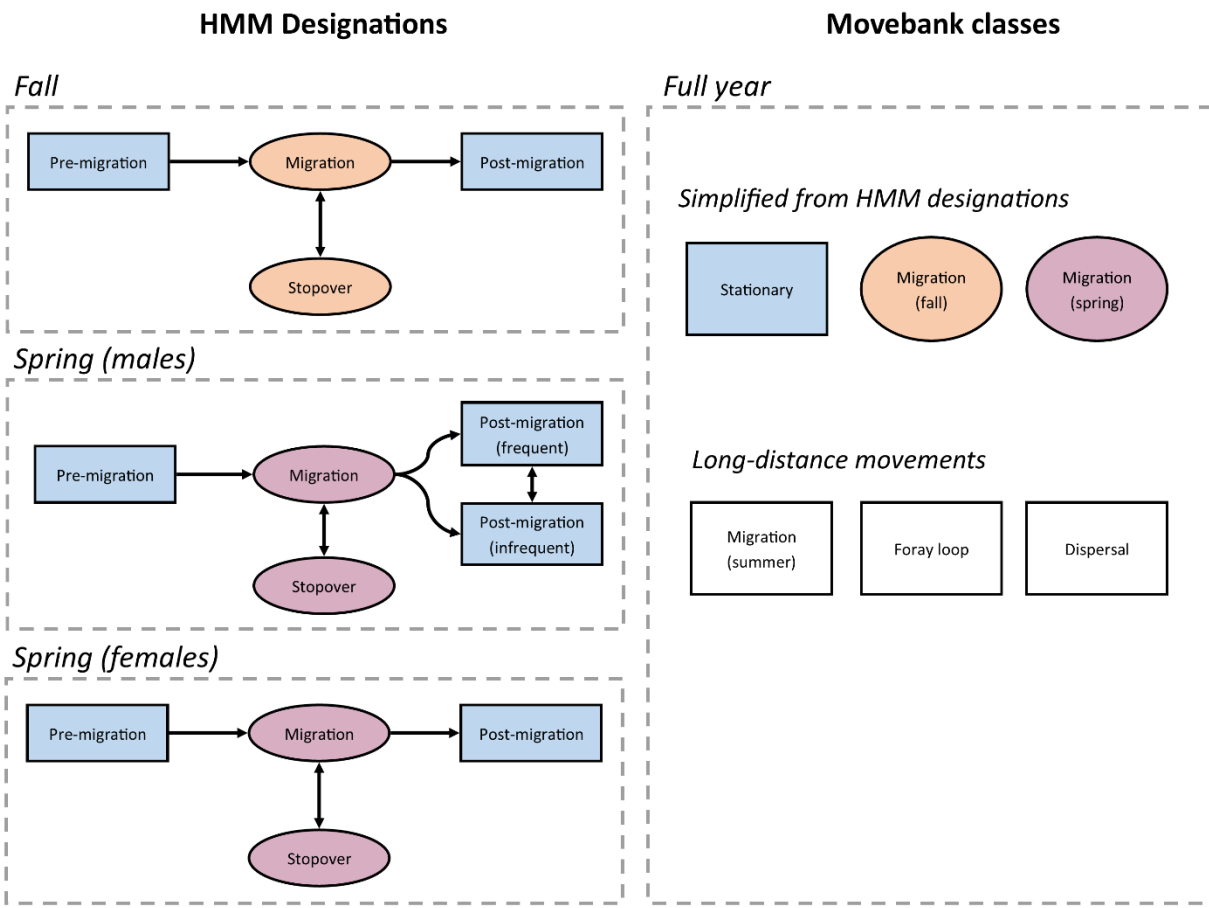


Figure B.2. Movement state transition diagram for each hidden Markov Model (HMM), and corresponding classes uploaded to the Movebank repository.

## **BIOGRAPHY OF THE AUTHOR**

Liam Berigan was born in Monterey, California just before Christmas in 1994. He graduated from Robinson Secondary School in Fairfax, Virginia in 2013, and obtained a Bachelor of Science degree with Distinction in Research from Cornell University in 2017, majoring in biology. He obtained a master's degree in biology from Kansas State University in 2019, where he was involved in a study on the response of lesser prairie-chickens (*Tympanuchus pallidicinctus*) to translocation. He is a candidate for a Doctor of Philosophy degree in Wildlife Ecology from the University of Maine in May 2024.